University of Cincinnati

Date: 5/27/2015

I, Smrithi Rajagopal , hereby submit this original work as part of the requirements for the degree of Master of Science in Chemical Engineering.

It is entitled:

Optimization of Polyethelenimine(PEI) Impregnated Adsorbents for Capturing CO2 From Ambient Air

Student's name: **Smrithi Rajagopal**

This work and its defense approved by:

Committee chair: Vadim Guliants, Ph.D.

Committee member: Junhang Dong, Ph.D.

Committee member: Joo Youp Lee, Ph.D.

UNIVERSITY OF Cincinnati

16233

Optimization of Polyethelenimine(PEI) Impregnated Adsorbents for Capturing CO_2 From Ambient Air

A thesis submitted to the

Graduate School

of the University of Cincinnati

in partial fulfillment of the

requirements for the degree of

Master of Science

in the Department of Biomedical, Chemical, and Environmental Engineering

of the College of Engineering and Applied Science

by

Smrithi Rajagopal

May 27, 2015

Committee Members

Dr. Vadim V. Guliants (Chair)

Dr. Junhang Dong

Dr. Joo-Youp Lee

Abstract

Silica and carbonaceous supports were impregnated with varying quantities of polyethylenimine(PEI) to study the CO_2 adsorption capacities of the resulting adsorbents. The adsorbents were initially subjected to adsorption testing in a thermogravimetric analyzer (TGA) at atmospheric pressure under controlled and dilute CO_2 concentrations (400 ppm CO_2 balanced in helium) at 25^{o}C to evaluate performance of the adsorbents for CO_2 capture in ambient air. The adsorbents were further investigated for their regenerative capacities to determine their stability over multiple cycles of adsorption. The silica adsorbents showed promising results for adsorption capacities and were determined to be the most stable.

A small-scale adsorber system was employed to test the performance of these adsorbents under practical conditions, by allowing ambient air in lab conditions to flow through a fixed bed of adsorbents. Using TSA (Temperature Swing Adsorption) cycles, CO_2 adsorption was measured in a volumetric adsorption system, where liberated CO_2 was allowed to expand into a previously evacuated calibrated cylinder and the ideal gas equation applied to calculate the amount of CO_2 desorbed. The results of the adsorber experiment and the factors affecting the adsorption capacities were further investigated.

Introduction

Emissions of green house gases, particularly rising levels of atmospheric CO_2, have been building up in the atmosphere over decades and centuries and warming the climate, leading to many other changes around the world—in the atmosphere, on land, and in the oceans (Meehl et al. 2007, Azar et al. 1997). The present global energy demand is primarily met by heavy consumption of fossil fuels, producing ever-increasing levels of atmospheric CO_2 (Pachauri et al. 2007, Siriwardane et al. 2001).

As of March 2015, the average CO_2 level in atmosphere measured at Mauna Loa Observatory, Hawaii by the National Oceanic and Atmospheric Administration was 400 ppm (Tans, Keeling). The average global CO_2 level is expected to reach 400 ppm in 2016 (Conway et al.). The rising concentrations of CO_2 are expected to have the following effects on the earth's climate: increase in average temperature, changes in patterns and amounts of precipitation, reduction of ice and snow cover, rise of sea levels and increase in the acidity level of oceans. The Intergovernmental Panel on Climate Change (IPCC) released a report in 2014, discussing the effects of climate change on food crops, global species, water supplies and human health. The following are a few of the striking conclusions made in the report (IPCC 2014).

- "A large fraction of both terrestrial and freshwater species faces increased extinction risk under projected climate change during and beyond the 21st century, especially as climate change interacts with other stressors, such as habitat modification, over-exploitation, pollution, and invasive species."
- "Climate change over the 21st century is projected to reduce renewable surface water and groundwater resources significantly in most dry subtropical regions (robust evidence, high agreement), intensifying competition for water among sectors."

- "Due to sea level rise projected throughout the 21st century and beyond, coastal systems and low-lying areas will increasingly experience adverse impacts such as submergence, coastal flooding, and coastal erosion."
- "Throughout the 21st century, climate change is expected to lead to increases in ill-health in many regions and especially in developing countries with low income, as compared to a baseline without climate change."
- Throughout the 21st century, climate-change impacts are projected to slow down economic growth, make poverty reduction more difficult, further erode food security, and prolong existing and create new poverty traps."

To curb rising levels of atmospheric CO_2, efforts have been directed towards its capture at source (Herzog et al. 2001, Lackner et al. 2000, Lund et al. 2012) and at the replacement of fossil fuels with a renewable alternative (Atabani et al. 2012, Mazloomi et al. 2012 , Pandey et al. 2012, Erdinc et al. 2012).

Captured CO_2 can be used in CO_2 mineralization (Geerlings et al. 2013), enhanced oil recovery (Melzer 2012), for the synthesis of urea, methanol, cyclic carbonates, lactone and salicylic acid to name a few chemicals (Behr et al. 2011, Sakakura et al. 2007) and production of plastics (Darensbourg 2007), although the global supply by far outstrips its demand requiring the captured carbon dioxide to be sequestered in agricultural soils (Lal, R. 2004).

Background

I. Rising atmospheric CO_2 concentration and its cause

The concentration of CO_2 in the atmosphere steeply increased since the onset of the industrial age, when the concentration of atmospheric CO_2 was 280 ppm. Studies suggest that the safe limit of atmospheric CO_2 should be a maximum of 350 ppm (Hansen et al. 2008), a level

that was crossed two decades ago (Fig 1.). About 40% of the worldwide greenhouse gas emissions is estimated to be contributed by fossil fuel-fired industries while 26% is from vehicular emissions alone (Chapman 2007). As of 2002, the statistics at the International Energy Association claim that 80% of the global energy demand is met by consumption of fossil fuels (IEA). Concerns about the future of this planet has driven efforts towards not just mitigating such emissions at the point of source (Roddy 2007, Berggren et al. 2012) but also to bring down the atmospheric concentration within the safe limit.

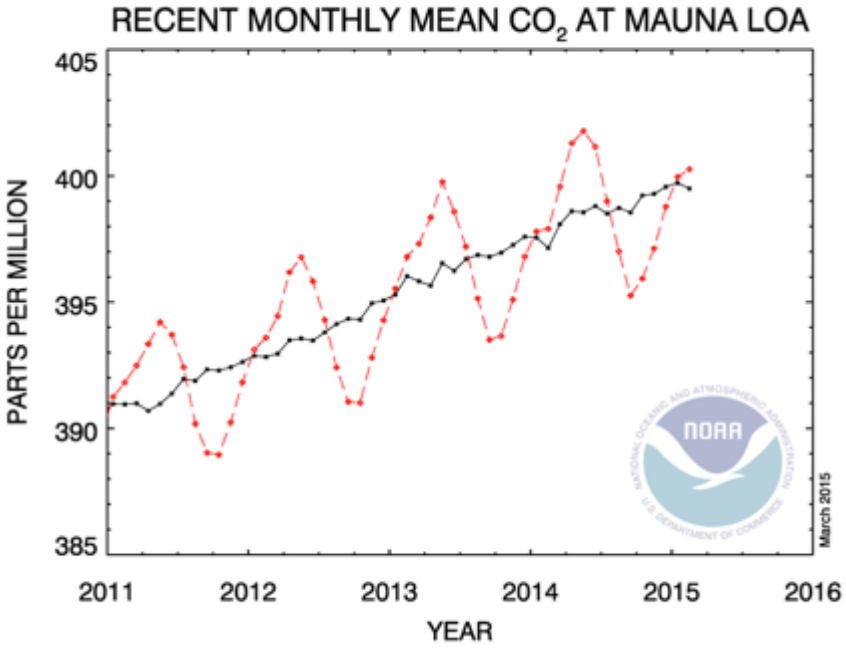

Fig 1. Atmospheric CO_2 (monthly average) as measured in air samples collected at Mauna Loa, Hawaii from 2011 to 2015. Units are parts per million by volume (Tans, Keeling).

II. Efforts towards CO_2 abatement

Hydrocarbons are primary fuels used in the transport sector like aviation and roadways while coal and natural gas have been energy providers for production of electricity. As the planet's population is growing and increasing number of societies are entering industrial age, the demand for energy continues to grow. Although the demand at present is being met, it must be

noted that the fossil fuels reserves will only last a couple more centuries and there is a need for an extremely reliant yet environmentally friendly source of energy to replace them.

Search for new sources of energy without the GHG emissions has yielded a range of promising alternatives like hydrogen fuel cells, biofuels and solar energy. Recent trends in biofuels include bio-ethanol, bio-methanol, fuels from Fischer-Tropsch synthesis and bio-hydrogen. The advantages are that they can be produced from common biomass sources like everyday household waste or wood. They are sustainable, biodegradable and are clean combustion fuels. The transition to cleaner energy will provide significant economic and fiscal benefits by generating increased economic output, jobs, and tax revenues to local governments.

III. Advancements in Carbon Capture

There are a variety of options available for post combustion carbon dioxide capture. The current commercial process for removing CO_2 from a flue gas stream is liquid amine scrubbing. Mono-ethanolamine (MEA) is a type of amine that has been extensively used for CO_2 capture, along with some other commonly used amines such as methyldiethanolamine (MDEA), 2-Amino-2- methylpropanol (AMP), Piperazine (PIPA), diglycolamine (DGA), diethanolamine (DEA), and di-isopropanolamine (DIPA). The process of scrubbing has the ability to achieve CO_2 recovery rates of 98% with high product purity (~99%). However, some constraints to this capture are that the capacity is limited by equilibrium and the fact that they are energy intensive when applied to a dilute stream, such as flue gas. The solvent being corrosive especially in the presence of residual oxygen in flue gas requires use of excessive water. The other gas impurities might react with amine, to form stable salts, which can accumulate. Improvements in this field are directed towards modifying tower packing to reduce pressure drop, optimize heat distribution for economic concerns, enhance contacting, develop efficient regeneration process and lastly minimize corrosion (Figueroa et al. 2008).

Membranes have been at the center of attention of various separation processes and studied extensively for their carbon dioxide capture properties. One of the applications of membranes allows amine to flow through the shell side in a bundle of membranes, while the flue gas is passed through the tube side. The CO_2 diffuses through, into the amine solution. The amine solution is regenerated once it leaves the bundle. Membranes cannot usually achieve high degrees of separation, so multiple stages and/or recycle of one of the streams is necessary. This leads to increased complexity, energy consumption and costs. Studies are being conducted to enhance the selectivity and permeability of the membranes for an efficient process (Falk Pederson et al. 2000).

IV. Solid CO_2 Adsorbents

Solid adsorbents can either trap carbon dioxide via physisorption or chemisorption at certain conditions and can be regenerated under a different set of operating conditions to liberate the captured carbon dioxide. Although they are promising for CO_2 capture, they have low adsorption capacities at low pressures and in presence of water vapor and other gases, and their application for a large-scale carbon dioxide adsorption has not been commercialized yet. According to Yu (Yu et al. 2012), an adsorbent can be classified suitable for carbon dioxide capture if it has high adsorption capacity, high thermal, mechanical and chemical stability over the course of successive cycles, regenerability, fast kinetics, high CO_2 selectivity, low heat capacity and low-cost raw materials.

Physical Adsorbents

Physical adsorbents like zeolites, MOFs (Millward et al. 2005) and activated carbon (Plaza et al. 2010) have been widely studied for their CO_2 capture capacities. MOFs have gained special attention in the recent years owing to their controllable pore structure, high surface area and pore surface properties that can be molded by re-arranging their organic ligands or metallic

clusters. Studies on MOFs, show remarkable CO_2 capture capacities at high pressures but fail to perform the same in presence of gas mixtures (Kuppler et al. 2009, Li et al. 2009, 2011). At present, there are very few studies on large-scale synthesis of MOFs and only very few are commercially available.

Zeolites are microporous aluminosilicates highly promising as adsorbents for gas separation applications, especially that of carbon dioxide from flue gases. According to Wang et al. (2011), the adsorption capacity of zeolites is dependent on the chemical composition of the cations in their microporous structure, their size and charge density. Recent studies by Sayari et al. (2011), claim that carbon dioxide/nitrogen selectivity and CO_2 adsorption capacity is comparatively low. Also the presence of moisture in flue gas greatly affects and decreases the adsorption capacity over successive cycles.

Recent studies are probing into mesoporous supports like silica and carbon, which by themselves have high adsorption capacities as well as high thermal and mechanical stability. Examples of recent mesoporous silica are families of M41S, Santa Barbara Amorphous type material (SBA-n) and anionic surfactant-templated mesoporous silica (AMS), have been reported (Liu et al. 2005, Sun et al. 2007, Chew et al. 2010).

Chemical Adsorbents

The recent adsorbents being investigated are high surface area, amine loaded supports. Their attraction over other conventional capture methods is that they require lower capital cost, can be used over a wider range of temperatures (up to 700^{o}C), consume lower energy for regeneration due to their low heat capacity, require lower pressure for gas recovery, produce less waste over cycles and are relatively easily disposable once spent (Harrison 2005, Khatri et al. 2006).

For optimization of amine loaded supports, there can be three major variables: amine content, nitrogen content in amine and procedures for loading the amines (Wang et al. 2011). Amines like monoethanolamine (MEA), diethanolamine (DEA), pentaethylenehexamine (PEHA), tetraethylenepentamine (TEPA) and polyethyleneimine (PEI) have been extensively researched. Several other amines were impregnated onto a polymeric material, polymethylmethacrylate (PMMA) by Filburn et al. (2005) and Lee et al. (2008). The highest capacity recorded of all adsorbents prepared was TEPA loaded PMMA, capturing 21.45 mmol CO_2 per g sorbent under flow of N_2 gas containing 15% CO_2 and 2.6% H_2O.

Plaza et al. (2007, 2008) worked with DETA, alkanolamines such as diisopropanolamine (DIPA), sterically hindered 2-amino-2-methyl-1,3-propanediol (AMPD), and triethanolamine (TEA) on alumina and carbon supports. The DETA-impregnated alumina sorbents exhibited the highest capacity.

According to Yue et al. (2006, 2008), TEPA impregnated adsorbents with a loading of 70 % TEPA showed a capacity of 3.93 mmol/g on original SBA-15, while 60% TEPA loaded on original MCM-41 showed a capacity of 5.39 mmol/g.

There have been speculations about the method of loading amines that assist in attaining maximum CO_2 capacity and according to Sayari et al. (2011) amine impregnated materials have weak interactions while amine-grafted materials have strong covalent bonds. Generally, amine grafted sorbents have comparatively higher stability and higher rate of adsorption than amine-impregnated sorbents in cyclic runs. There are possibilities of achieving lower amine loading with grafting when compared to impregnation, since the grafted amount depends on the surface silanol groups.

V. Polyethylenimine for CO_2 capture

CO_2-selective high-capacity adsorbents, which were developed using mesoporous support and a functional amine group, polyethelenimine (PEI) are called molecular baskets (Xu et al., 2005). These adsorbents have a higher adsorption capacity than the support or amine itself. The basic amine compounds on the adsorbent react with acidic carbon dioxide to form ammonium carbamates that bind to the surface. The heat of adsorption is higher, averaging at 75 kJ/mol due to bond formation. Nevertheless, desorption is reversible and pressure dependent (Chaffee et al. 2007). The stoichiometric limit for two moles of NH_2, is one mole CO_2 but it has been found that the presence of water in the gas mixture does not hamper adsorption capacity, but in fact promotes it towards one mole of CO_2 per mole of amine group because of formation of bicarbonates after proton exchange.

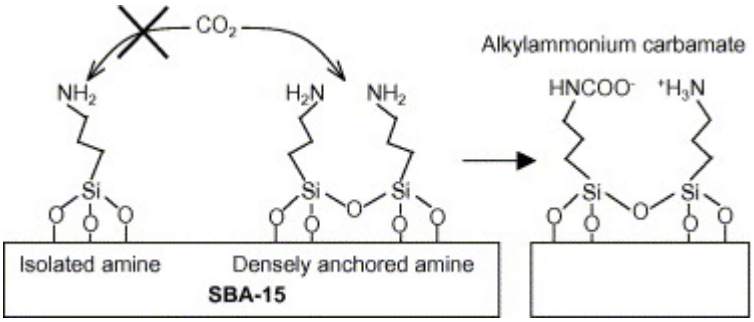

Fig 2. Adsorption of CO_2 on aminosilane-modified SBA-15 (Hiyoshi et al. 2005).

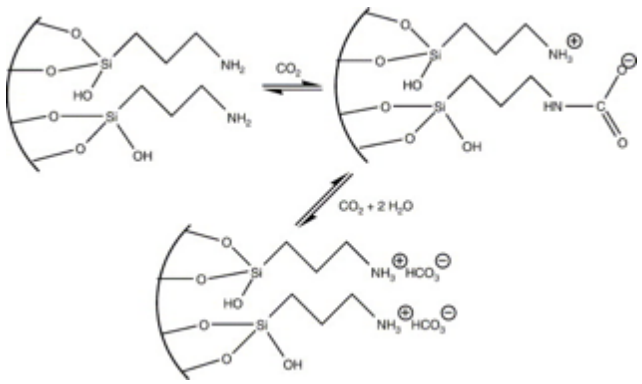

Fig 3. Surface reaction of tethered amine groups with CO_2 (Knowles et al. 2005).

It was observed by Sayari et al., (2010) that the presence of moisture could be considered an advantage only when the molar concentration of CO_2 is higher than that of moisture. Xu et al. (2005) studied the adsorption capacities of MCM-41 support with 50 wt% PEI in flue gas without moisture as well as containing 15% moisture. The moisture seemed to have a promoting effect on the adsorption and the capacity increased by 1.5 times when compared to dry conditions.

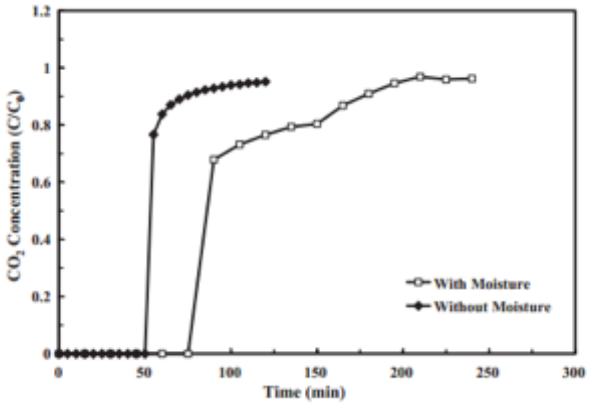

Fig 4. Comparison of CO_2 breakthrough curve without and with 15% moisture in the simulated flue gas (Xu et al. 2005).

Amine loading of an adsorbent is defined as mmoles of amine groups present in 1 g of adsorbent; in this case, only the primary and secondary amino groups of PEI were considered. The term amine loading cannot be related to the amine available for capture. The impregnated amine form aggregates on the support making some amine groups inaccessible to CO_2. At low temperatures, neat PEI exists in a bulk-like form making adsorption of CO_2 a diffusion limited process (Sayari et al. 2011, Qi et al. 2011). In this scenario, it can be speculated that a rise in temperature allows higher rate of adsorption and hence higher capacity. PEI decomposes at 230^{o}C, which allows subjecting it to temperatures around 120^{o}C to regenerate the adsorbent.

Studies by Song and his group (Xu et al. 2002, 2005, Ma et al. 2009, Wang et al. 2009, 2011) in the recent years have reported remarkable results for amine impregnated silica and

carbonaceous supports. Their work on MCM-41 has resulted in the highest CO_2 capacity of 3.02 mmol/g-sorbent at 75 wt. % PEI loading under flow of pure CO_2 at 75°C. However, they claimed that the capacity declined when the temperature was reduced to 25°C. In the presence of moisture, Song's group observed a capacity of 3.18 mmol/g-sorbent at 50 wt. % PEI loading on MCM-41 in 15 vol. % CO_2 in N_2 at 75°C.

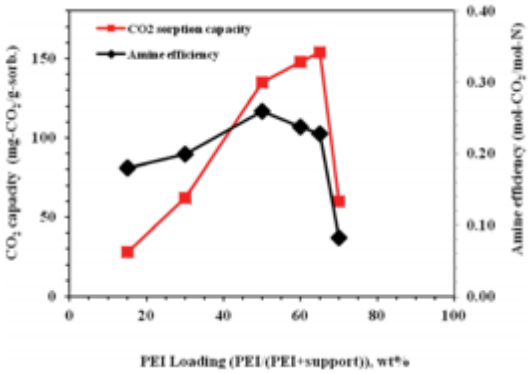

Fig 5. Effect of PEI loading on the CO_2 sorption capacity and the amine efficiency of PEI on BP2000 by Cabot. The capacity was measured by TGA at 75°C and ambient pressure under a pure CO_2 flow at a flow rate of 100 mL/min (Wang et al. 2012).

Wang et al. (2012) prepared a series of so-called "molecular baskets" using different carbon supports impregnated with different amounts of PEI and tested them under pure CO_2 at 75°C. The results showed that molecular basket containing 65 wt. % PEI on carbon black (BP 2000 from Cabot) yielded the highest CO_2 capacity of 3.5 mmol/g-sorbent. Higher loadings of PEI on the same support reduced the sorption capacities dramatically. They also studied the effects of PEI loading on adsorption capacity and amine effiency of PEI on carbon black supports. Amine efficiency can be defined as the number of CO_2 moles captured per mole of amine and as mentioned before, under anhydrous conditions, chemistry mandates the need of two amine groups to bind with a single CO_2 molecule to form carbamates. It can be thus concluded that the theoretical amine efficiency in this case would be 0.5 (Choi et al. 2009, Drese et al. 2009), assuming all the amine present in the adsorbent is available or accessible to CO_2. However, the amine efficiency reported in experiments is typically lower than its theoretical value and this can be attributed to certain defects in the adsorbent that render some of the amine

groups unavailable to CO_2. The amine groups in some cases form hydrogen bonds with the surface silanol groups and become deactivated. The amine efficiency of adsorbents reported from the experiments conducted in this study will be referred to as actual amine efficiency.

Similarly, Jones and his group impregnated a commercial porous silica support with PEI along with additives containing silicon and titanium, such as APTES ((3-aminopropyl) triethoxysilane) and titanium (IV) propoxide (tetrapropyl orthotitanate), to stabilize PEI. The adsorption capacities were tested under the flow of 400 ppm CO_2 balanced with Ar to simulate dry air. Their results showed a maximum adsorption capacity of 2.36 mmol/g-sorbent for the PEI loaded sorbent, 2.26 mmol/g-sorbent for the silane-modified sorbent and 2.19 mmol/g-sorbent for the titanium-modified sorbent (Choi et al. 2011).

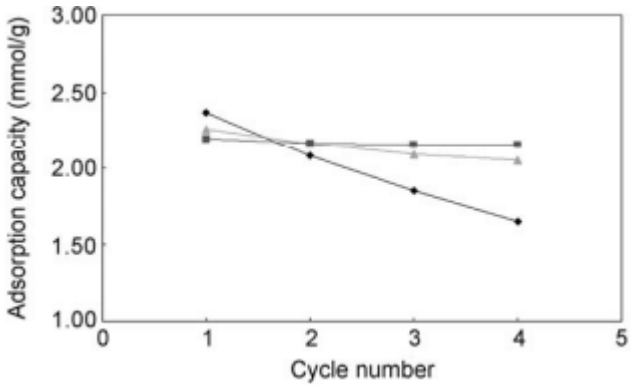

Fig 6. Changes of the adsorption capacities of different hybrid adsorbents as a function of the number of adsorption/desorption cycles: ●PEI/silica;▲A-PEI/silica; ■T-PEI/silica.

Limitations of previous studies

Most of the existing studies are tested under high CO_2 concentrations or for flue gas capture (Ma et al. 2009, Sayari et al. 2011, Su et al. 2009). The methodologies for CO_2 capture developed for flue gases cannot be implemented for ambient conditions. Capture from ambient air was studied by (Choi et al. 2011) and their adsorbents exhibited capacities in the order of 2.36

mmol/g-sorbents with 45 wt% PEI loading. Similar efforts were made by Belmabkhout et al. (2010) on tri-amine functionalized MCM-41, yielding adsorption capacities in the magnitude of 0.98 mmol/g-sorbent. It is to be noted that these adsorbents have not been tested for different amine content or in air, where in the real purpose of this research exists. Also, the studies of CO_2 adsorption to date have been performed only by TGA on minute samples, where the flow conditions are flow through, unlike real adsorption beds. Not only that, but the regeneration was done in a CO_2-free atmosphere resulting in very low CO_2 partial pressure during regeneration, which would negate the advantage of using these materials to capture CO_2 for sequestration, and unrealistically high extent of regeneration, recyclability and reproducibility. Considering the above-mentioned limitations, the results from TGA are clearly insufficient to determine the promise of these novel CO_2 adsorbents to remove CO_2 from dilute sources under realistic conditions.

Objectives

The major objective of this MS thesis research is to investigate the ability of several promising adsorbents to capture CO_2 from dilute sources and release it during regeneration at finite pressure. The adsorbents used in this project are silica and carbon supports impregnated with polyethylenimine (PEI), a liquid organic polymer with high amine content. To accomplish this objective, the following thrusts were pursued.

1. Investigate a series of PEI impregnated silica and PEI impregnated carbon supports with respect to their surface area, pore size, PEI loading and CO_2 sorption capacities.
2. Optimize the PEI loading on different supports to yield the highest possible adsorption capacity at low pressure in 400 ppm CO_2 in helium (mimicking ambient air) and 12 vol. % CO_2 in helium (mimicking flue gas) using TGA.
3. Investigate the regenerability of candidate adsorbents by TGA.
4. Verify conclusions of TGA experiments by testing candidate adsorbents in a small-scale adsorber system to capture CO_2 from ambient air.
5. Investigate reasons for low CO_2 capture capacities observed in adsorber experiments.

CHAPTER 2
CO_2 capture by Polyethylenimine (PEI) impregnated solid adsorbents

2.1 Introduction

As discussed above, PEI is a liquid organic polymer containing functional amine groups. The reasons for choosing PEI in this project over other amines, are due to its higher CO_2 capture capacities, higher amine content, comparatively lower molecular weight, lower heat requirement for regeneration and its economical.

In this project, PEI was applied at different loadings to four high surface area supports by several methods. The best method of PEI incorporation was identified after comparing the amine content in the resultant adsorbents. Depending on the loading procedure, loading amount and type of support used, an initial examination of PEI content in adsorbent was made using the thermogravimetric analyzer (TGA) to characterize the candidate adsorbents for further studies. The project focused on determining the optimum PEI loading on a particular support that results in maximum amine loading, amine efficiency to adsorb CO_2, chemical and thermal stability, and regenerability.

The supports containing varying amounts of PEI were assessed for sorption capacities (mmol/g-sorbent) of different concentrations of carbon dioxide, at 25^{o}C and 75^{o}C at atmospheric pressure using TGA. The best candidate adsorbent was later tested in a cyclic process employing a small scale adsorption system to remove CO_2 from ambient air at room temperature conditions as described below. Much lower CO_2 capacities were observed in a small-scale adsorption system as compared to TGA and their causes were investigated in a separate study described in detail below. The results of this study enabled identification and understanding of the various process parameters that affect practical capture of CO_2 directly from air.

2.2 Synthesis of adsorbents

2.2.1 Selection of suitable supports

The supports were chosen to be mesoporous in nature with large specific surface areas and averaging between 10 to 20 nm to enable both PEI incorporation and facile CO_2 diffusion. The supports chosen were commercial silica produced by Saint Gobain (SS 61138) and Grace Davison (SI 1101) with specific BET surface areas of 324 and 236 m^2/g, respectively, while the carbonaceous supports were activated carbon from Akzo Nobel (EC 600 JD) and carbon black from Cabot (BP 2000), both displaying the BET surface areas of 1400 m^2/g. The carbon supports are low-density materials with a particularly large surface area making them highly promising hosts for amine impregnation. The PEI used in this project (Aldrich) had a lower molecular weight, ~ 400 g/mol, as compared to that used in other studies, with an average diameter of ca. 1 nm. It was reported that PEI interacts strongly with silica (Choi et al. 2011) and carbon supports (Plaza et al. 2010) and is a good carbon dioxide adsorbent.

The BET data (surface area, micropore area) of these supports were used to determine the theoretical maximum amount of PEI that can be impregnated on to these supports. However, with higher amine loading, the formation of bulk-like PEI inside the pores at low temperature leads to CO_2 adsorption as a diffusion-limited process. To optimize the amount of PEI, another factor that needs to be examined is amine efficiency.

As mentioned before, the theoretical amine efficiency in this case would be 0.5 (Choi et al. 2009, Drese et al. 2009). Using this information, the optimal amount of PEI that would provide maximum CO_2 adsorption can be found only by impregnating different amounts of PEI to a support and then comparing their respective capacities.

2.2.2 Loading of PEI

The loading of PEI onto the support was calculated with respect to the number of monolayers of PEI to be impregnated into the pores of the support. Using the information of the diameter of a PEI molecule and the surface area of the support, the number of PEI molecules per g of support was established and consequently, the amount (in g) of PEI that would form a monolayer inside the pores of 1g of support was determined. The figure below explains the method of calculation. As discussed above, to optimize the amount of PEI, the supports were impregnated with three different quantities of PEI; the pores of the supports were impregnated with PEI to form (i) half a monolayer, (ii) a single monolayer and (iii) one and a half times a monolayer. The amounts to be loaded were calculated in the method described above and the following table shows the estimated PEI content for different supports and their respective loadings.

One monolayer calculation:

$$\text{Number of PEI molecules per g of support} = \frac{\text{Surface area of support's pore}}{\text{Cross-sectional area of a PEI molecule}}$$

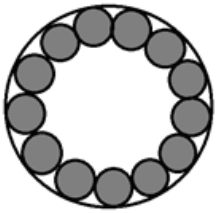

One monolayer PEI in a pore of support

$$\text{Number of PEI moles per g of support} = \frac{\text{Number of PEI molecules per 1 } g \text{ of support}}{\text{Avagadro's number}}$$

$$\text{Amount of PEI}(g)\text{ per } g \text{ of support} = \text{Number of PEI moles per } g \text{ of support} * \text{Molecular weight of PEI}$$

Fig.7 shows the method used for calculated amount of PEI to be impregnated to achieve desired loading.

Table 1 below shows the calculated amount of PEI for each support and Table A.1 in Appendix A shows the complete calculation.

Table 1. Calculation of amine content for different PEI loading.

			Grace Davison	**Saint Gobain**	**Akzo Nobel**	**Cabot**
			Silica	Silica	Carbon	Carbon
			SI 1101	SS 61138	EC 600JD	BP 2000
Weight of PEI per 1 g of support (g)	Monolayer		0.411	0.300	1.776	1.776
	Half Monolayer		0.206	0.150	0.888	0.888
	1.5 times Monolayer		0.617	0.450	2.664	2.664

In the course of this document, the supports will be referred to as mentioned below.

Saint Gobain Silica	SG Si	**Akzo Nobel Activated Carbon**	AN C
Grace Davison Silica	GD Si	**Cabot Carbon black**	Cabot C

1.5 times a monolayer of PEI	150M PEI
One monolayer of PEI	M PEI
Half a monolayer of PEI	50M PEI

Example: Saint Gobain support with one monolayer of PEI will be referred to as SG Si M PEI.

2.2.3 Preparation of PEI impregnated adsorbents

The preparation of adsorbents was performed by several techniques to maximize amine loading onto the support. The initial synthesis was performed following the procedure reported by Xu et al. 2002 to impregnate PEI on MCM-41 silica.

Method 1: Batch I adsorbents

The granular supports of Saint Gobain Silica (SS 61138) and Grace Davison Silica (SI 1101) were dried in a vacuum oven at 105^0C for a period of 24 hrs. The desired amount of PEI for a particular loading (Table 1) was mixed with 20 ml of methanol and stirred for several minutes using a glass rod to form a uniform solution. 1g of dried support was mixed with 15 ml of methanol in a plastic container to form a slurry, to which the PEI-methanol solution was added dropwise. The resultant slurry was dried in a vacuum oven at 40^0C for 72 hrs.

2.3 Results and Discussions

There have been several studies conducted on PEI impregnated amines on different supports with promising results. Dr. Song's group has published studies on CO_2 adsorption capacities on MCM-41 molecular sieves and SBA-15. The capacities of the adsorbents in these studies were tested under flue gas simulated environments (15 vol% CO_2) at 75^oC. The MCM-41 adsorbent exhibited its highest capacitiy of 133 mg/g-ads, with a PEI loading of 75 wt%, followed by 112 mg/g-ads when the PEI loading was 50 wt% (Xu et al. 2002). Their PEI loaded SBA-15 adsorbents performed better than the MCM-41, with the highest adsorption capacity recorded to be 140 mg/g-ads when PEI loading was 50 wt% (Wang et al 2013). A similar study performed by Wang, J. et al. (2013) on mesoporous carbon supports in 15 vol% CO_2 at 75^oC, yielded adsorption capacities of 212 mg/g-ads at 65 wt% PEI loading. Dr. Jones' group (Choi et al. 2011) has published studies concerning adsorption capacities from ambient air at STP conditions on MCM-48 Silica and the capacities were estimated in 400 ppm CO_2 to mimic ambient air. The adsorption capacities of the MCM-41 Silica with 45 wt% PEI were determined to be 104 mg/g-ads, which is a high capacity for a dilute CO_2 stream. Chen et al. (2013) also conducted experiments in ambient air, similar to Dr. Jones' group, but on a non-polar resin (HP20). The resin loaded with 50 wt% PEI, yielded adsorption capacities of 93.3 mg/g-ads at 25^oC. The synthesis and testing of these adsorbents are inspired by a few of these studies and will be discussed in the next section.

2.3.1 Method 1 Adsorbents:

The prepared adsorbents retained the color and shape of the original support and were non-sticky, although some PEI residue was found covering the walls of the container, where the slurry was dried. The adsorbents were crushed to micron-sized particles using a mortar and pestle.

PEI content in Batch I adsorbents

To calculate the amount of PEI that was successfully impregnated onto the support as compared to the amount added during preparation, the adsorbents were tested in TGA under the flow of air. Approximately 10 mg of adsorbent sample was placed in a TGA alumina pan and heated to 100^0C in nitrogen to remove adsorbed CO_2 and moisture. The temperature was increased to 700^0C at 10^0C/min under air flow (100 ml/min). The weight loss over the entire temperature range accounts for the loss of moisture, surface hydroxyl groups and PEI.

In order to account for amount of PEI impregnated, the moisture content as well as surface hydroxyl groups present on the original support were determined by running the same TGA experiment on an original support, which was crushed and dried prior to the experiment. Comparing the weight loss in these two experiments for an individual adsorbent, an estimate of PEI content for each adsorbent was made. Figure 8 shows the weight loss exhibited by samples of the original support (SG Si) and the SG Si 150M PEI sample over the same temperature range. The TGA curves of the remaining Batch I adsorbents can be found in Appendix B.1.

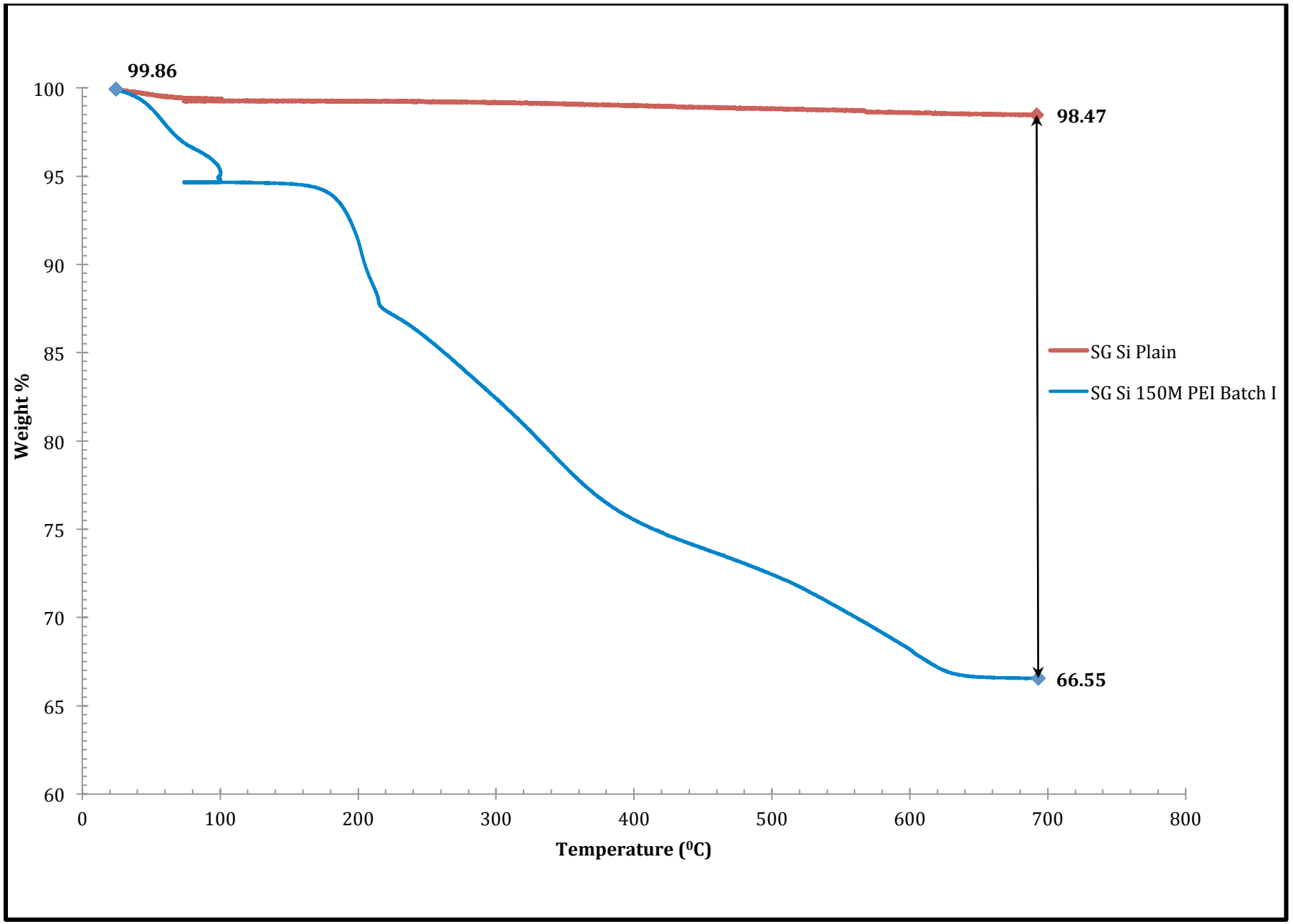

Fig 8. Determining PEI content in SG Si 150M PEI by comparing its TGA curve with that of original SG silica in air at 100 - 700^{0}C.

Table 2 shows the PEI content in Batch I adsorbents determined using the above-mentioned procedure; the calculations performed can found in Appendix A.3.

Table 2. PEI content in Batch I adsorbents

	Amount of PEI estimated using TGA (%)	Amount of PEI added during synthesis (%)	Difference in the amounts calculated (%)
SG Si 50M PEI	14.2	15.5	1.4
SG Si M PEI	28	31.4	3.4
SG Si 150M PEI	39.9	45.4	5.4
GD Si 50M PEI	42.3	23.6	-18.7
GD Si M PEI	19.3	45.9	26.6
GD Si 150M PEI	47.5	66.9	19.4

The information in the table above concludes that impregnations on the SG Si samples were more effective when compared to the GD Si samples. The data in the table above suggests that the adsorbent preparation procedure followed in this case did not provide efficient impregnation on the GD Si samples.

Carbon dioxide adsorption

In order to determine the CO_2 adsorption capacities of the candidate adsorbents, the samples were initially tested for CO_2 capture from flue gas. To perform this experiment on a laboratory scale, a gas mixture of 12 vol.% CO_2 balanced in helium was used to simulate flue gas. Our initial approach to test adsorption capacities involved running a TGA experiment on a small adsorbent sample under the flow of 12 vol. % CO_2 in He at 25 and 75^0C.

Adsorption capacities of Batch I adsorbents at 25^0C

Approximately 10 mg of adsorbent sample was placed in a TGA alumina pan under the flow of helium at 100 ml/min. The sample was heated to 110^0C at 10^0C/min and kept at that temperature for one hour to remove moisture and adsorbed gases. The temperature of the sample was brought down to 25^0C at 10^0C/min under He flow and kept at 25^0C for one hour. The gas flow was then switched to 12 vol. % CO_2 in He at 100 ml/min while maintaining the temperature at 25^0C for a period of six hours. Using the data from Fig 9, the amount of CO_2 adsorbed (mg/g-adsorbent) was calculated. A detailed table with calculations can be found in Appendix A.4.

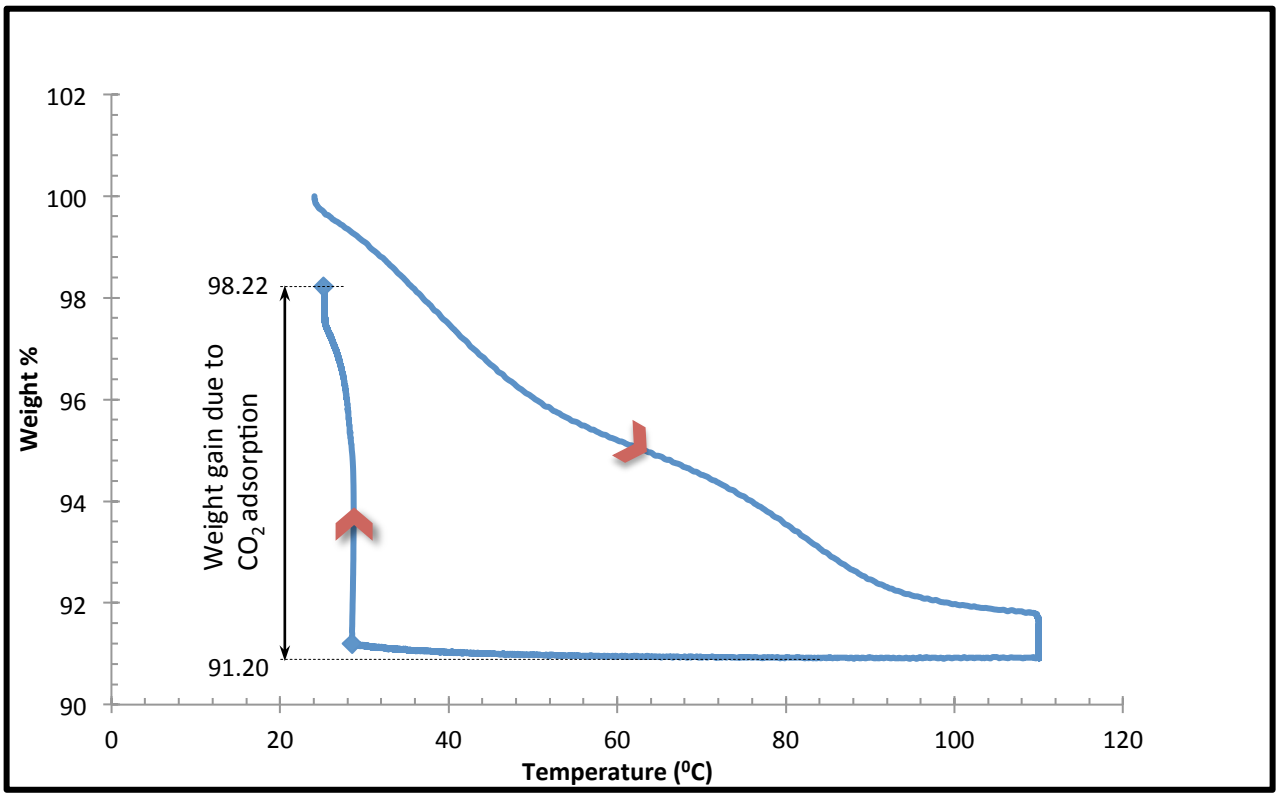

Fig 9. TGA curves for CO_2 adsorption on GD Si 150M PEI (Batch I) sample from 12 vol. % CO_2 in He at 25^0C.

Amine Loading and Amine Efficiency of Batch –I adsorbents

In order to calculate the amine efficiency of the adsorbents, the amine loading of each adsorbent was determined using the information acquired from TGA experiments for PEI estimation. The PEI content per g-ads was estimated from Table 2 and since only primary and secondary amines contribute to adsorption, and the ratio of primary, secondary and tertiary amines in PEI is 1:2:1, the amine content per gram adsorbent was estimated acoordingly.

The data obtained from CO_2 adsorption experiments on the TGA was used to calculate the amount of CO_2 captured per gram of the adsorbent. Since amine efficiency is described as the moles of CO_2 captured per mole of amine, dividing the CO_2 adsorption capacity/g-ads by amine content/g-ads, yielded the actual amine efficiency of each adsorbent. Table 3 presents the CO_2 capture capacity and comparisons between theoretical and actual amine efficiencies of each adsorbent.

Table 3. CO_2 adsorption capacity and amine efficiency of Batch I adsorbents in 12 vol. % CO_2 at 25^0C.

		Based on TGA estimate of PEI loading		**Based on PEI used in synthesis**		**Stoichiometry**
SAMPLES	**mmol CO_2 / g-ads**	**Amine Loading**	**Amine Efficiency**	**Theoretical Amine Loading**	**Theoretical Maximum Efficiency**	**Maximum Efficiency**
SG Si 50M PEI	0.32	2.105	0.15	2.124	0.150	0.5
SG Si M PEI	1.05	3.559	0.30	5.420	0.194	0.5
SG Si 150M PEI	1.27	4.705	0.27	7.823	0.163	0.5
GD Si 50 M PEI	0.90	4.918	0.18	3.864	0.23	0.5
GD Si M PEI	1.44	2.682	0.54	7.525	0.19	0.5
GD Si 150 M PEI	1.60	5.104	0.31	10.955	0.15	0.5

Based on the capacities estimated in Table 3, the following conclusions could be made.

a) GD silica adsorbents display higher CO_2 adsorption capacities at the same PEI loadings as compared to SG silica adsorbents.

b) 1.5 monolayer PEI loadings on both SG silica and GD silica adsorbents have the highest CO_2 adsorption capacities as compared to lower PEI loadings on both adsorbents. It may be concluded that the adsorption capacities are directly proportional to the PEI loadings.

c) The 1.5 monolayer PEI loaded adsorbents would be tested further for their CO_2 adsorption capacities at higher temperatures, i.e. 75^0C.

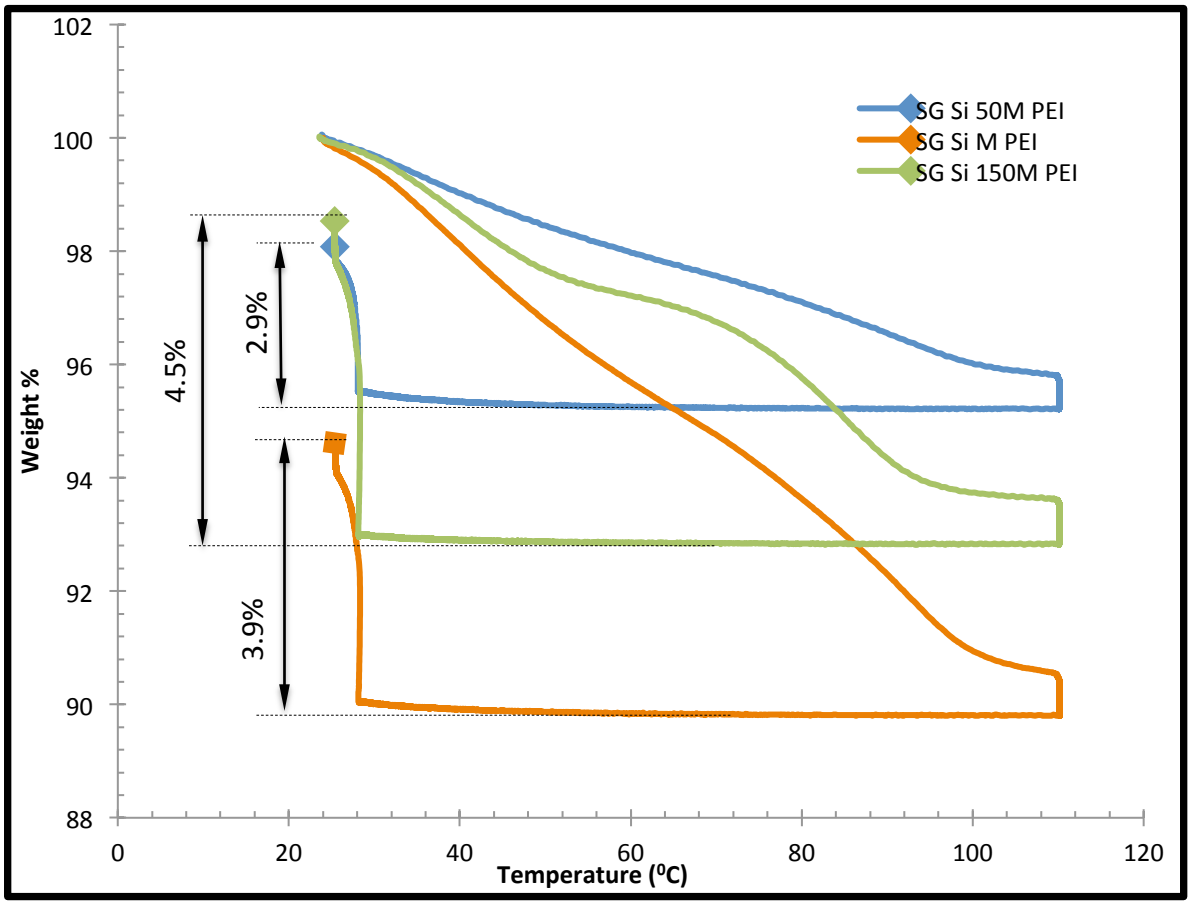

Fig 10: CO_2 adsorption capacities of Batch – I Saint Gobain silica adsorbents with PEI loadings of 0.5 monolayer, one monolayer and 1.5 monolayer, respectively, at 25^0C in 12 vol. % CO_2 in He.

Adsorption capacities at 75^0C

Approximately 10 mg of adsorbent sample was placed in a TGA alumina pan under the flow of helium at 100 ml/min. The sample was heated to 110^0C at 10^0C/min and kept at that temperature for one hour to remove moisture and adsorbed gases. The temperature of the sample was brought down to 75^0C at 10^0C/min under He flow and kept at 75^0C for one hour. The gas flow was then switched to 12 vol. % CO_2 in He at 100 ml/min while maintaining the temperature at 75^0C for a period of six hours. This experiment was conducted only on the promising adsorbents, which showed the highest CO_2 capture capacities in 25^0C. The following table (Table 4) shows information on capture capacities and amine efficiencies at 75^0C, calculated in the same manner as the experiments conducted at 25^0C. The TGA curves for other Batch I adsorbents in 12 vol. % CO_2 in He at 25 and 75^0C can be found in Appendix B.2 and B.2.1.

Table 4. CO_2 adsorption capacity and amine efficiency of Batch I adsorbents in 12 vol. % CO_2 at 75^0C.

		Based on TGA estimate of PEI loading		Based on PEI used in synthesis		Stoichiometry
SAMPLES	**mmol of CO_2 / g - ads**	**Amine Loading**	**Amine Efficiency**	**Theoretical Amine Loading**	**Theoretical Maximum Amine Efficiency**	**Maximum Efficiency**
SG Si 150M PEI	1.6	4.7	0.34	7.8	0.16	0.5
GD Si 150M PEI	1.73	5.1	0.34	10.9	0.15	0.5

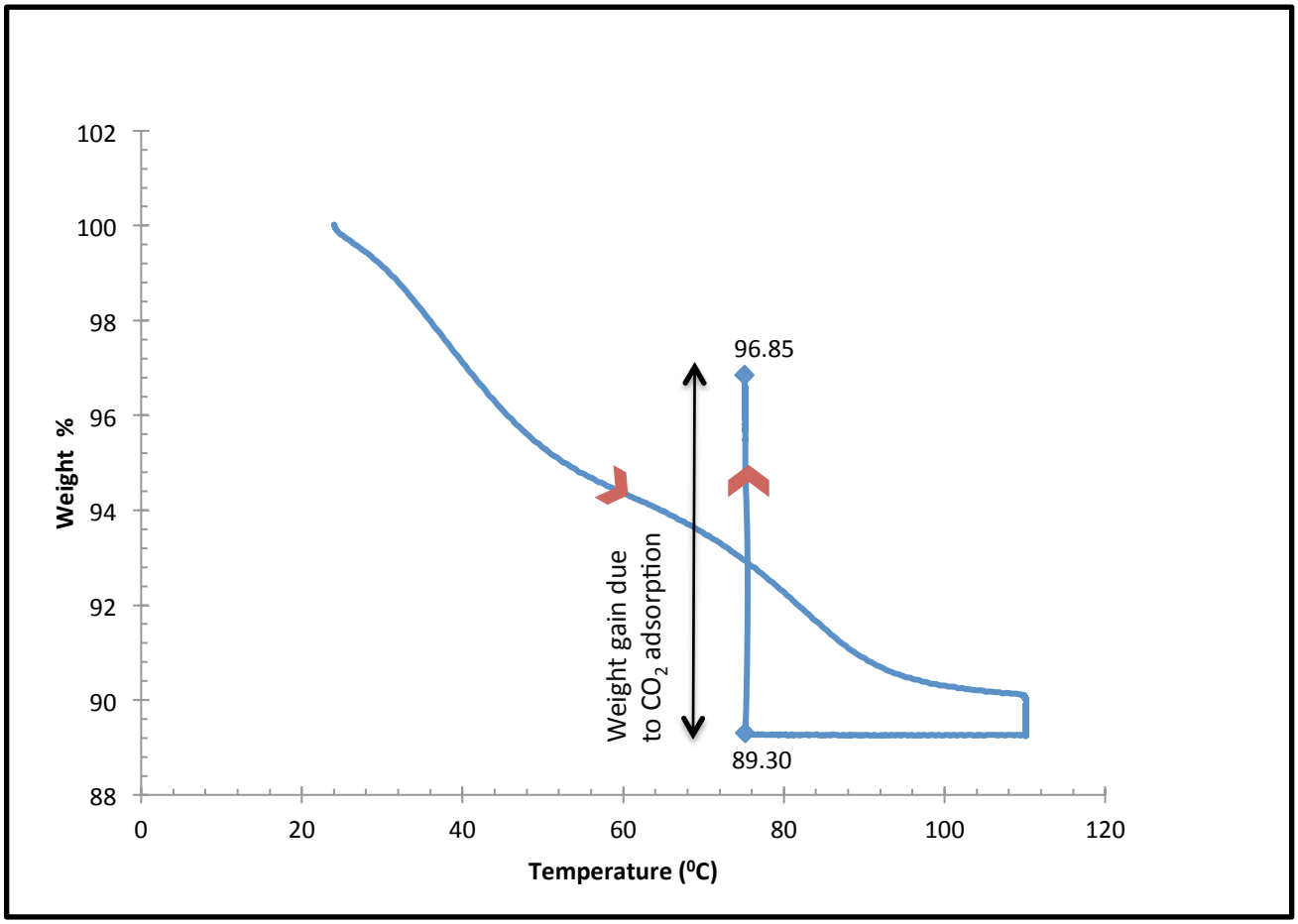

Fig 11: TGA curve for CO_2 adsorption on GD Si 150M PEI under 12 vol. % CO_2 in He flow at 75^0C.

The CO_2 adsorption capacities for Batch I adsorbents with 1.5 monolayer of PEI loading at 25 and 75^0C show that adsorption capacities are higher when adsorption takes place at 75^0C. Considering the fact that the capture capacities have proven to be proportional to the PEI content and since the actual PEI loadings were considerably lower than the theoretical values, it was concluded that the CO_2 adsorption capacities would be higher if the PEI loading process was optimized to enhance PEI content. Hence, the second batch of adsorbents was prepared with modified synthesis methods, improving upon the process of PEI impregnation.

2.3.2 Second Batch Adsorbents

To enhance PEI loadings, diffusion length calculations were performed shown in appendix A.2 to determine the amount of time needed to ensure all of PEI was loaded on to the adsorbent. Instead of calculating the time required for PEI molecules to diffuse through the pores of the silica and carbon supports, the size of support particles needed for synthesis time of 6 hrs and 24 hrs respectively, were calculated. These calculations demonstrated that a period of 6 hours was enough to allow PEI to completely diffuse the pore structure of the support. Refer to Appendix A.2 for estimation of the diffusion mechanism involved and diffusivity calculations.

To minimize mass transfer resistances, the support pellets were crushed to micron-sized dimensions prior to PEI loading, while PEI-loaded silica particles were separated from the synthesis slurry by filtration instead of solvent evaporation.

To compare the PEI loadings on these supports, four PEI loaded samples of each support were prepared using the same procedure and same amounts of PEI on two crushed and two granular supports. While one set of crushed and granular adsorbents was obtained by evaporation, the other set was filtered. Table 5 illustrates the classification of Batch-II adsorbents.

Table 5. Classification of Batch-II adsorbents

Saint Gobain	1.5 Monolayer	Granular	Filtered
			Evaporated
		Crushed	Filtered
			Evaporated
	1 Monolayer	Granular	Filtered
			Evaporated
		Crushed	Filtered
			Evaporated

Procedure: Batch II adsorbents

The granular supports of Saint Gobain Silica (SS 61138), Grace Davison Silica (SI 1101), Akzo Nobel Activated Carbon (EC 600JD) and Cabot Carbon Black (BP 2000) were oven dried in a vacuum oven at 105^0C for a period of 24 hrs. The desired amount of PEI for a particular loading (Table 1) was mixed with 20 ml of methanol and stirred using a magnetic stirrer for two hours to form a uniform solution.

Method A: Granular supports

1g of dried support was mixed with 15 ml of methanol in a plastic container to form a slurry, to which the PEI-methanol solution was added. The resultant slurry was allowed to sit overnight.

i) Evaporation: The sample slurry was allowed to dry in an oven at 40^0C for 72 hours to yield the adsorbent.
ii) Filtration: The sample slurry was filtered and washed with methanol and later dried in an oven at 40^0C for duration of 2 hours.

Method B: Crushed supports

The dried supports were crushed to fine powder using a mortar and pestle. 1g of crushed support was mixed with 15 ml of methanol in a plastic container to form a slurry, to which the PEI-methanol solution was added. The resultant slurry was allowed to sit overnight and the adsorbents were obtained by evaporation and filtration, following the procedures mentioned above.

For the convenience of comparison of the Batch II adsorbents, the discussion begins with comparing the dried and filtered adsorbents and later concentrates on performances of granular and crushed supports within those categories.

Dried adsorbents

The silica adsorbents made with granular supports, retained the color and shape of the original supports. They were non-sticky, with almost no PEI residue on the inner walls of the container in which the slurry was dried, unlike the case of Batch I adsorbents.

The silica adsorbents with crushed supports retained their powdery consistency with no trace of PEI on the surface of the adsorbents or the walls of the container and did not form aggregates. The Cabot carbon black adsorbents (crushed and granular), formed aggregates with excess PEI on the outer surface of the supports and the walls of the container. These adsorbents had a paste-like consistency and were deemed unsuitable for future experiments.

The adsorbents prepared with Akzo Nobel Activated Carbon supports (granular and crushed) retained the color and shape of the original supports, were non-sticky, with almost no PEI residue in the inner walls of the container. There was a slightly noticeable agglomeration in supports with higher PEI loading but the adsorbents were not sticky. The adsorbents made with granular supports were crushed to micron-sized particles using a mortar and pestle.

Estimation of PEI content in Batch II (Dried) adsorbents

The PEI content in the Batch II adsorbents was determined by the same procedure that was followed for Batch I adsorbents (see Section 2.3.1). While performing the experiment in the TGA, the carbon supports underwent combustion in the presence of air at higher temperatures, contributing to the weight loss data used to assess PEI content and making the procedure unsuitable for carbon supports. To maintain consistency in the data analysis of all adsorbents, it was required that the method of PEI estimation for carbonaceous adsorbents be performed on the TGA. Since the only issue with evaluating PEI-contributed weight loss in the carbonaceous adsorbents, was the presence of air in the experiments, it was speculated that using an inert gas environment instead, could produce the same results.

In order to evaluate the accuracy of the experiment conducted in the inert, helium atmosphere, a plain silica support and a silica adsorbent were tested in TGA under helium and the results were compared with the same experiment performed in the presence of air. The figures 12, 13, 14 and 15 show the comparison in weight loss patterns for a silica and a carbon adsorbent under helium and air. The TGA curves for silica adsorbents clearly demonstrate that even though the weight loss patterns are slightly different, the weight loss under both the atmospheres is similar. Since the most important data in this experiment is the weight loss, it can be concluded that the PEI content in carbonaceous adsorbents may be estimated by TGA in He. The TGA curves used to determine PEI content in the Batch II adsorbents may be found in Appendices B.3 and B.3.1. Detailed calculations for PEI estimation can be found in Appendix A.5. The PEI content in these adsorbents is shown in the Table 6.

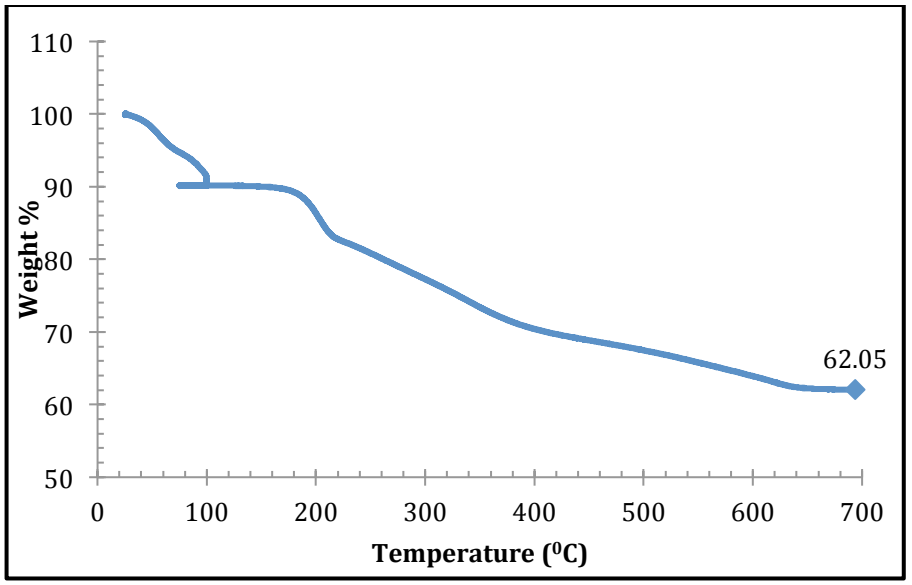

Fig 12: TGA curve of SG Si 150M PEI in air, when temperature is increased from 25°C to 700°C at 10°C/min.

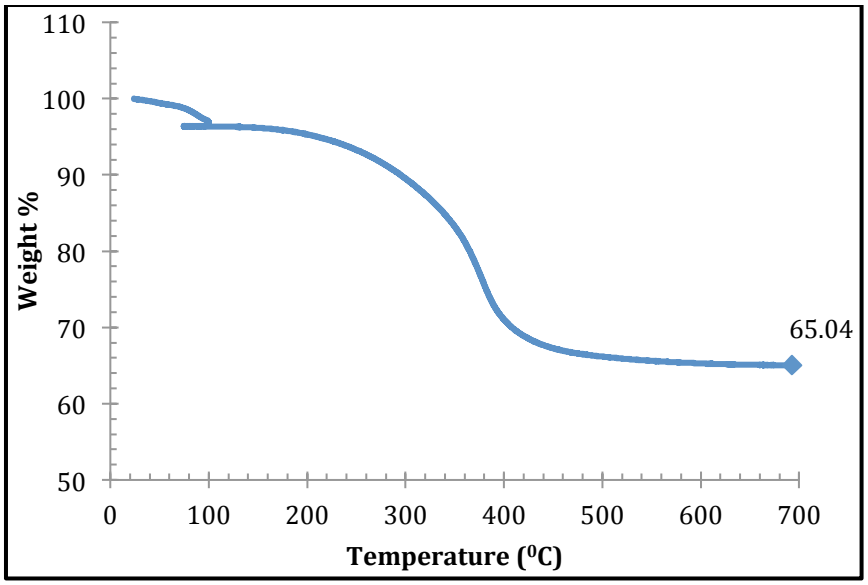

Fig 13: TGA curve of SG Si 150M PEI in helium, when temperature is increased from 25°C to 700°C at 10°C/min.

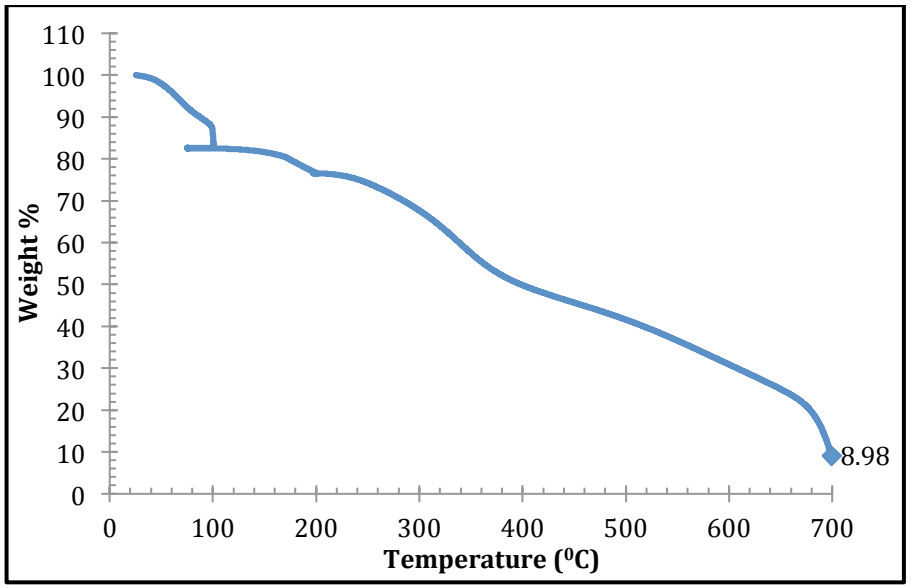

Fig 14: TGA curve of AN C 150M PEI in air, when temperature is increased from 25°C to 700°C at 10°C/min.

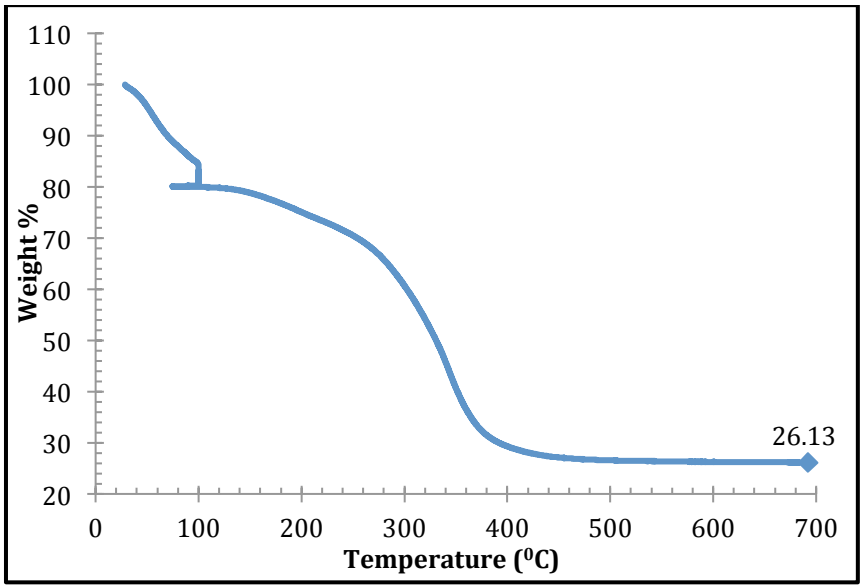

Fig 15: TGA curve of AN C 150M PEI in helium, when temperature is increased from 25°C to 700°C at 10°C/min.

Table 6. PEI content in Batch II (Dried) adsorbents.

SAMPLES		Amount of PEI estimated by TGA	Amount of PEI added during synthesis	Difference in the amounts calculated
		(%)	(%)	(%)
UNCRUSHED	GD Si M PEI	39.7	44.7	4.9
CRUSHED	GD Si M PEI	37.0	43.9	6.9
UNCRUSHED	GD Si 150 M PEI	59.7	65.1	5.4
CRUSHED	GD Si 150 M PEI	60.8	66.2	5.4
UNCRUSHED	SG Si M PEI	29.9	32.4	2.5
CRUSHED	SG Si M PEI	28.9	31.1	2.1
UNCRUSHED	SG Si 150M PEI	43.2	45.7	2.5
CRUSHED	SG Si 150M PEI	44.5	47	2.5

SAMPLES		Amount of PEI estimated by TGA	Amount of PEI added during synthesis	Difference in the amounts calculated
		(%)	(%)	(%)
UNCRUSHED	AN C M PEI	121.7	178	57.3
CRUSHED	AN C M PEI	148.1	179.1	31
UNCRUSHED	AN C 150M PEI	224.9	268.6	43.8
CRUSHED	AN C 150M PEI	205	268	62.1
UNCRUSHED	Cabot M PEI	123.1	184.8	61.8
CRUSHED	Cabot M PEI	124.6	183.8	59.3
UNCRUSHED	Cabot 150M PEI	Agglomerated sticky supports		
CRUSHED	Cabot 150M PEI			

From Table 6, it is evident that the PEI loadings on the SG Si samples were more effective when compared to the GD Si samples. Comparing the Batch II GD Si samples to the Batch I samples, it can be concluded that the synthesis procedure followed in this case provided much better PEI impregnation on the GD Si samples. As far as the carbon supports are concerned, the greater amount of PEI impregnated was due to their larger surface areas as compared to the silica supports. However, the PEI content shown in Table 6 indicated that only

67-76 % of PEI was actually loaded onto the adsorbent, which could be attributed to pore diffusion resistance, since the pore diameter of the carbon supports is ca. 7-9 nm. This also explains the deposition of PEI on the external surface of the carbon supports.

It can also be concluded from the data shown in Table 6 that reducing the particle size of the support prior to impregnation does not improve PEI loading. This in turn suggests the absence of significant diffusion limitations during PEI impregnation of both pelletized and crushed supports. However, the reduced particle size may improve the CO_2 adsorption capacities. The following section focuses on CO_2 adsorption capacities of Batch II adsorbents.

Carbon dioxide adsorption on Batch II (dried) adsorbents– 12% CO_2 balanced in helium

Since it has been established for Batch I adsorbents that the adsorption capacities in 12 vol. % CO_2 are higher at 75^0C than at 25^0C, the Batch II adsorbents were measured for their capacities at 75^0C only, following the same procedure followed for Batch I adsorbents. Figure 16 outlines the difference in CO_2 adsorption capacities of Batch I and Batch II Saint Gobain Silica adsorbents, measured in identical conditions. Using the data from the TGA experiments, the amount of CO_2 adsorbed (mmoles CO_2/g-ads) was calculated along with amine loading and amine efficiency. A detailed table with calculations can be found in Appendix A.6. Table 7 presents the CO_2 capture capacity and comparisons between theoretical and actual amine efficiencies of each adsorbent.

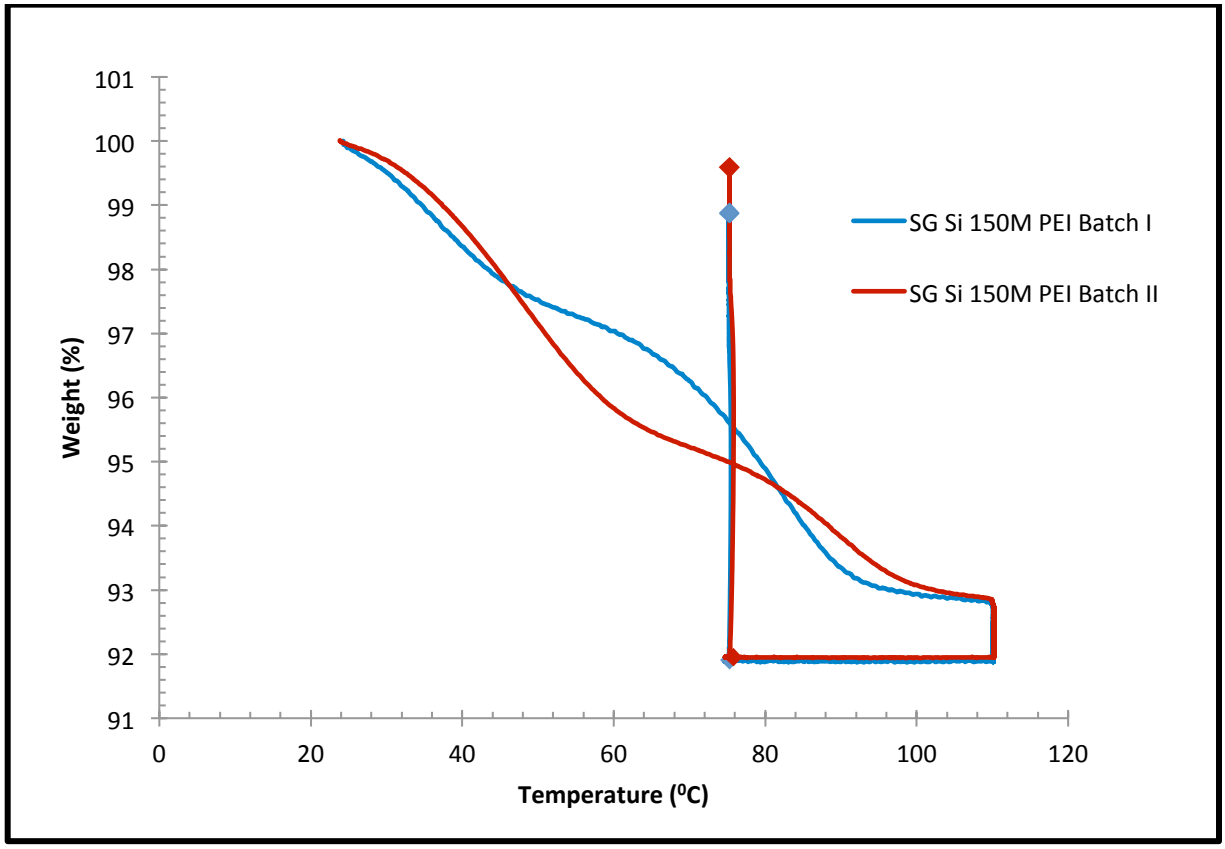

Fig 16. TGA curves for CO_2 adsorption on SG Si 150M PEI of Batch I and Batch II (dried) under 12 vol % CO_2 in He at 75^0C.

Table 7. Estimation of CO_2 capture capacity and amine efficiency of Batch II adsorbents in 12 vol% CO_2 at 75^0C.

			Based on TGA estimate of PEI loading		Based on PEI used in synthesis		Stoichiometry
	SAMPLES	mmol of CO_2 / g - ads	Amine Loading	Amine Efficiency	Theoretical Amine Loading	Theoretical Maximum Amine Efficiency	Maximum Efficiency
UNCRUSHED	SG Si M PEI	1.32	3.67	0.36	5.58	0.24	0.5
CRUSHED	SG Si M PEI	1.28	3.55	0.36	5.37	0.24	0.5
UNCRUSHED	SG Si 150M PEI	1.73	5.02	0.35	7.88	0.22	0.5
CRUSHED	SG Si 150M PEI	1.59	4.82	0.33	8.10	0.20	0.5
UNCRUSHED	GD Si M PEI	1.43	4.49	0.32	7.21	0.20	0.5
CRUSHED	GD Si M PEI	1.36	3.55	0.38	7.31	0.19	0.5
UNCRUSHED	GD Si 150M PEI	1.65	5.10	0.32	10.96	0.15	0.5
CRUSHED	GD Si 150M PEI	1.51	5.72	0.26	10.83	0.14	0.5
UNCRUSHED	AN C M PEI	2.10	8.30	0.25	31.08	0.07	0.5
CRUSHED	AN C M PEI	2.01	9.06	0.22	31.10	0.06	0.5
UNCRUSHED	AN C 150M PEI	2.60	10.33	0.25	46.66	0.06	0.5
CRUSHED	AN C 150M PEI	2.73	9.43	0.29	46.55	0.06	0.5
UNCRUSHED	CABOT M PEI	2.00	8.47	0.24	31.50	0.06	0.5
CRUSHED	CABOT M PEI	1.80	8.29	0.22	31.33	0.06	0.5
UNCRUSHED	CABOT 150 M PEI	Sticky Agglomerates					
CRUSHED	CABOT 150 M PEI						

Table 8. Comparison of estimated PEI loading amounts in Batch I vs. Batch II adsorbents.

		BATCH I			BATCH II		
		Amount of PEI estimated by TGA	Amount of PEI added during synthesis	Difference in the amounts calculated	Amount of PEI estimated by TGA	Amount of PEI added during synthesis	Difference in the amounts calculated
		(%)	(%)	(%)	(%)	(%)	(%)
UNCRUSHED	GD Si M PEI	39.7	44.6	4.9	19.3	45.9	26.6
CRUSHED	GD Si M PEI	37.02	43.9	6.9	-	-	-
UNCRUSHED	GD Si 150 M PEI	59.7	65.1	5.4	47.5	66.9	19.4
CRUSHED	GD Si 150 M PEI	60.8	66.2	5.4	-	-	-
UNCRUSHED	SG Si 150M PEI	43.2	45.7	2.5	39.9	45.4	5.4
CRUSHED	SG Si 150M PEI	44.5	47.01	2.5	-	-	-
UNCRUSHED	SG Si M PEI	29.9	32.4	2.5	28	31.4	3.4
CRUSHED	SG Si M PEI	28.9	31.1	2.1	-	-	-

From Table 8, it can be established that the Batch II adsorbents have higher PEI loadings owing to the improved PEI impregnation method and better CO_2 capture capacities at 75^0C. The Batch II SG Silica adsorbents with 1.5 monolayer PEI loadings have a higher CO_2 adsorption capacity as compared to Batch I adsorbents. It can also be concluded that crushing the supports prior to impregnation does not have an impact on improvement of CO_2 adsorption capacities. Figure 17 illustrates the comparison of adsorption capacities for crushed and granular supports for each adsorbent. The Akzo Nobel and Cabot adsorbents have shown particularly high adsorption capacities due to their higher surface areas. The CO_2 adsorption capacity per g-ads of AN C 150M PEI is 1.5 times more than its SG Si equivalent.

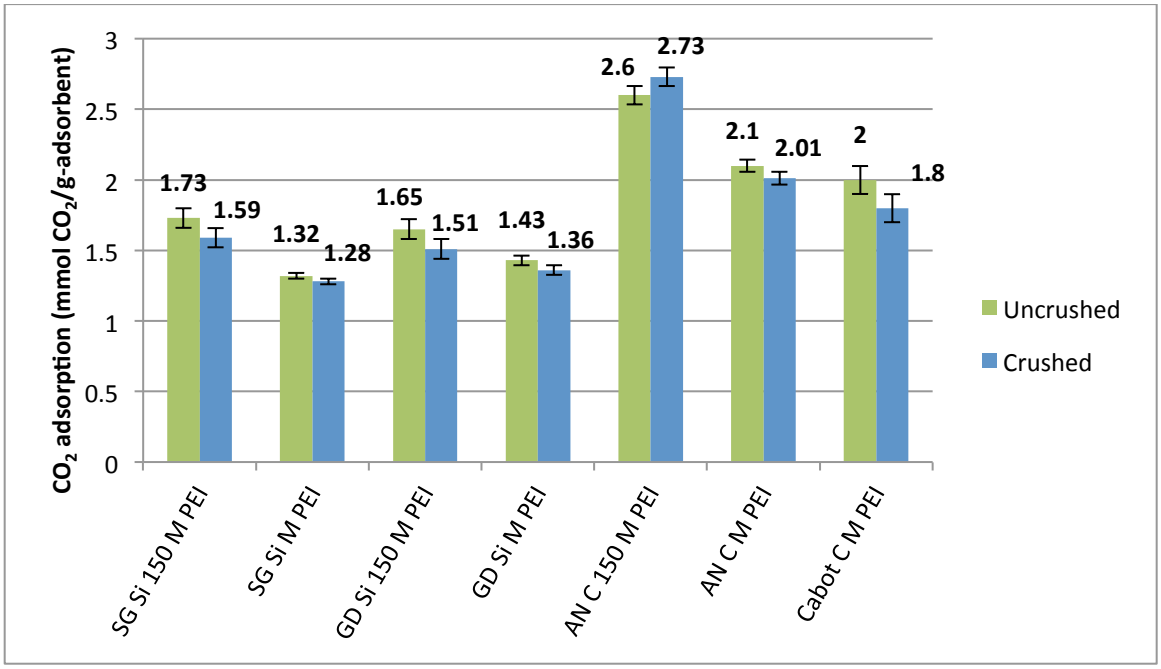

Fig 17. Graph depicting the carbon dioxide adsorption capacities of Batch II adsorbents under the flow of 12% CO_2 at 75^0C.

Filtered adsorbents

In order to find an alternative and faster synthesis method, filtration was used as an alternative method to obtain the adsorbents from the slurry mixture. The adsorbents made from granular and crushed supports retained the color and shape of the original supports and were non-sticky. The granular adsorbents were crushed to micron-sized particles using a mortar and pestle.

Carbon-dioxide adsorption on Filtered Adsorbents – 12 vol% CO_2 in He

Since the dried adsorbents were already tested in TGA and exhibited better PEI loadings and CO_2 adsorption capacities than their Batch I counterparts, the filtered adsorbents were directly evaluated for their CO_2 adsorption properties in 12 vol% CO_2 in He at 75^0C, following the same method described in Section 2.3.1. Figure 18 shows the difference in CO_2 adsorption capacities for dried and filtered adsorbents under the same conditions.

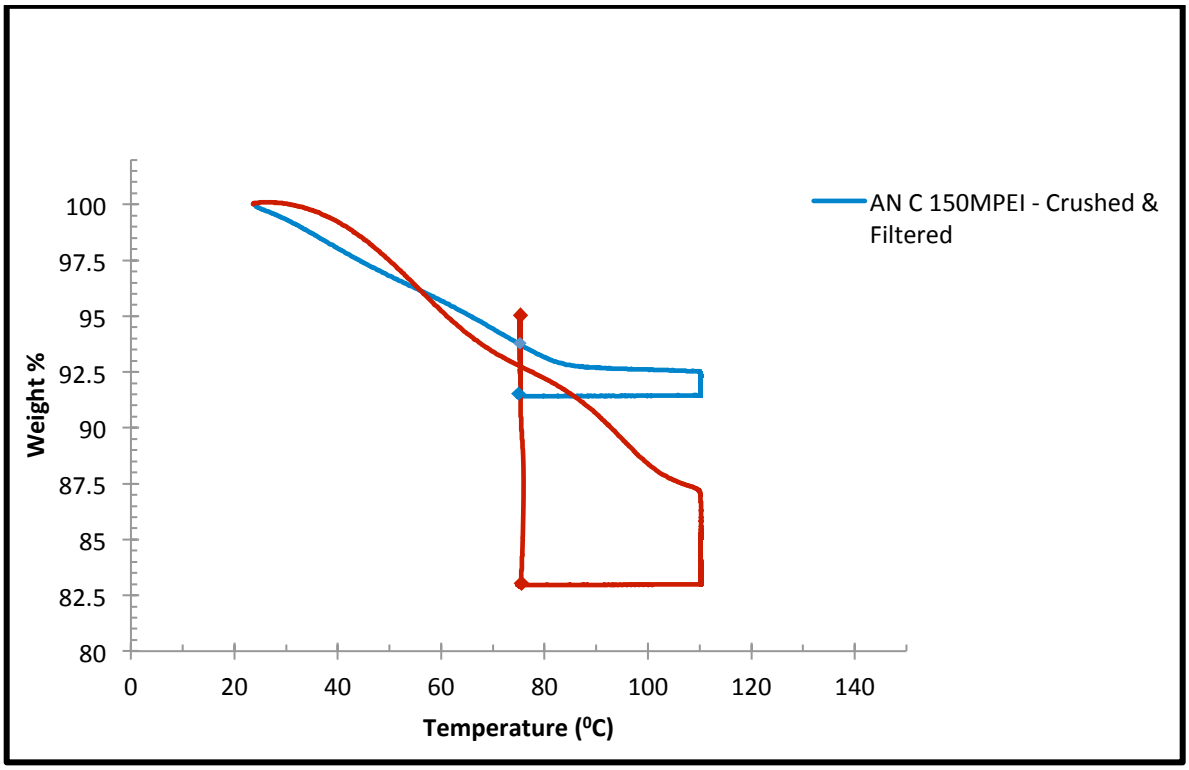

Fig 18. TGA curves of CO_2 adsorption on Batch II AN C 150M PEI under 12 vol% CO_2 in He at 75^0C synthesized by (i) drying and (ii) filtration.

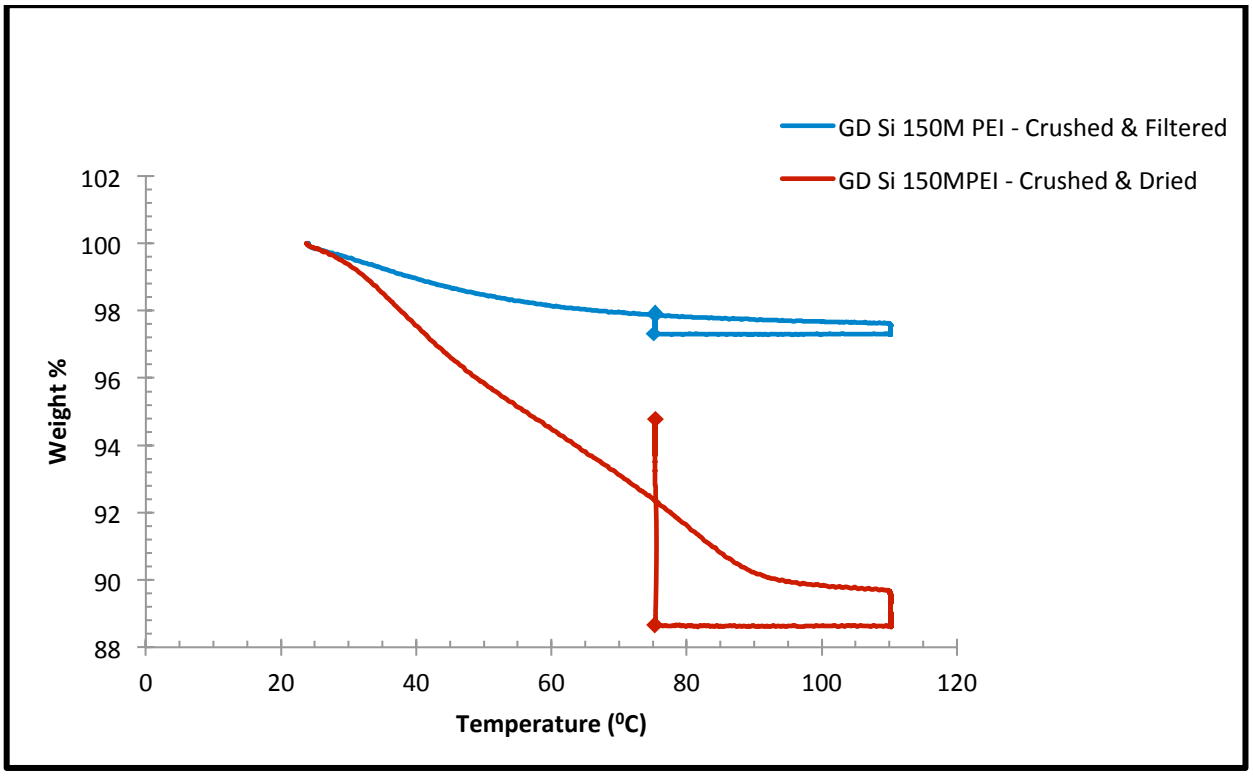

Fig 19. TGA curves of CO_2 adsorption on Batch II SG Si 150M PEI under 12 vol% CO_2 in He at 75^0C synthesized by (i) drying and (ii) filtration.

Figures 18 and 19 clearly show that the adsorption capacities of the filtered adsorbents are less than 20% of the capacities of the dried adsorbents. Similar experiments conducted on the rest of the Batch-II (filtered) adsorbents provided similar results and confirmed that the method of filtration of the adsorbent slurry to obtain the adsorbents was ineffective and thus was not pursued further. Comparing the adsorption capacities to studies conducted previously, the maximum capacities in this study in 12 vol% CO_2 on carbon and silica adsorbents are 120 and 76 mg CO_2/g-ads respectively. Comparing these values to the studies mentioned previously, the capacities measured are only half the values reported in other studies. However, the highest PEI loading in this study in only 30 wt%, which is also less than the half the loading values in these studies. However, the capacity of 35 wt% PEI loaded on an MCM-41 (Xu et al. 2002) was observed to be 68.7 mg/g-ads, which is closer to the capacities determined in this study.

2.3.3 Carbon dioxide adsorption – 400 ppm CO_2 balanced in helium

Since the dried Batch II adsorbents have been established to be the best candidate adsorbents for future experiments, they were subjected to further TGA runs under the flow of 400 ppm of CO_2 balanced in helium to investigate the CO_2 adsorption capacities of these adsorbents from ambient air.

Approximately 10 mg of SG Si 150M PEI adsorbent sample was placed in a TGA alumina pan under the flow of helium at 100 ml/min. The sample was heated to 110^0C at 10^0C/min and kept at that temperature for an hour to remove impurities, if any. While still maintaining helium flow, the temperature of the sample was brought down to 75^0C at 10^0C/min and kept isothermal for an hour. The gas flow was then switched to 400 ppm CO_2/He at 100 ml/min while maintaining the temperature at 75^0C for a period of six hours.

The CO_2 adsorption capacity seemed to be much lower than expected and the experiment was conducted again only to yield the same result. Since the ultimate purpose of these experiments is to capture CO_2 from ambient air, the same experiment was run in a TGA but the adsorption was allowed to take place at an ambient temperature of 25^0C instead of 75^0C.

The CO_2 adsorption capacity of the adsorbent now was much higher compared to its performance at 75^0C. Figure 20 shows the difference in magnitude of CO_2 adsorption from 400 ppm of CO_2 balanced in helium at 25 and 75^0C.

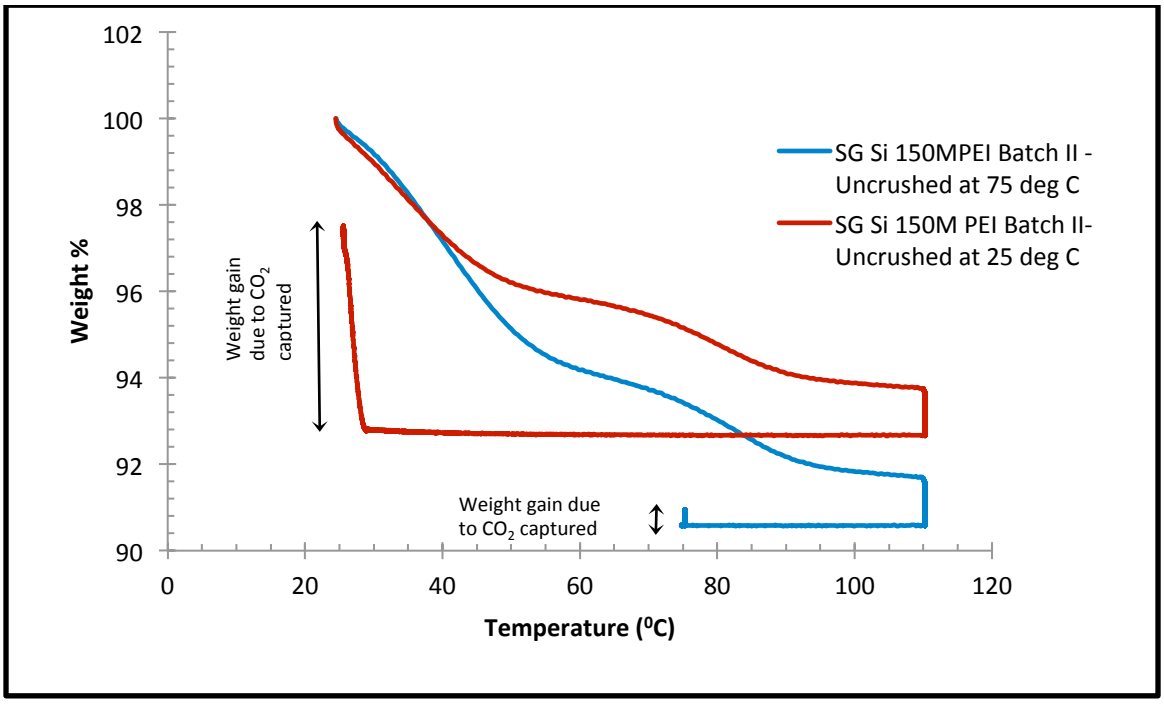

Fig 20. TGA curve of CO_2 adsorption on Batch II SG Si 150M PEI under 400 ppm CO_2 in He at 75^0C and 25^0C.

Figure 20 clearly shows the difference in CO_2 adsorption capacities of the adsorbent sample, SG Si 150M PEI (Batch II) IN 400 ppm CO_2 at different temperatures. Similar experiments were conducted for other Batch II adsorbents, which also exhibited lower CO_2 adsorption capacities at 75^0C. It was hence decided to perform all TGA experiments with 400 ppm of CO_2 balanced in helium at 25^0C. Table 9 shows the adsorption capacity, amine loading and amine efficiency of the adsorbents in 400 ppm CO_2. A detailed table with calculations can be found in Appendix A.7. Also, the TGA curves for all the experiments can be found in Appendix B.4.

Table 9. Estimation of CO_2 capture capacity and amine efficiency of Batch II adsorbents in 400 ppm CO_2/He at 25^0C.

			Based on TGA estimate of PEI loading		Based on PEI used in synthesis		Stoichiometry
	SAMPLES	**mmol CO_2 / g-ads**	**Amine Loading**	**Amine Efficiency**	**Theoretical Amine Loading**	**Theoretical Maximum Amine Efficiency**	**Maximum Efficiency**
UNCRUSHED	GD Si M PEI	1.05	4.49	0.23	7.21	0.15	0.5
CRUSHED	GD Si M PEI	0.97	4.15	0.23	7.31	0.13	0.5
UNCRUSHED	GD Si 150 M PEI	1.30	5.50	0.24	10.66	0.12	0.5
CRUSHED	GD Si 150 M PEI	1.09	5.72	0.19	10.83	0.10	0.5
UNCRUSHED	SG Si 150M PEI	1.11	5.02	0.22	7.88	0.14	0.5
CRUSHED	SG Si 150M PEI	1.02	4.82	0.21	8.10	0.13	0.5
UNCRUSHED	SG Si M PEI	0.83	3.67	0.22	5.58	0.15	0.5
CRUSHED	SG Si M PEI	0.78	3.55	0.22	5.37	0.15	0.5
UNCRUSHED	AN C M PEI	0.41	8.30	0.05	31.08	0.01	0.5
CRUSHED	AN C M PEI	0.34	9.06	0.04	31.10	0.01	0.5
UNCRUSHED	AN C 150M PEI	0.78	10.33	0.08	46.66	0.02	0.5
CRUSHED	AN C 150M PEI	0.37	9.43	0.04	46.55	0.01	0.5
UNCRUSHED	Cabot M PEI	0.34	8.47	0.04	8.47	0.04	0.5
CRUSHED	Cabot M PEI	0.32	8.29	0.04	8.29	0.04	0.5
UNCRUSHED	Cabot 150M PEI	Sticky Agglomerates					
CRUSHED	Cabot 150M PEI						

Table 9 and Figure 21 show that the adsorption capacities of carbon supports in 400 ppm of CO_2 are much lower than their silica support counterparts. Figure 21 clearly illustrates that the highest adsorption capacity achieved by a carbonaceous adsorbent in this experiment is equivalent to the lowest capture capacity of a silica adsorbent. This is in stark contrast to CO_2 adsorption capacities in 12 vol. % CO_2 where the CO_2 capacities of silica adsorbents were only half the capacities of the carbon adsorbents. These experiments have ruled out the possibility of using carbon adsorbents to capture CO_2 from ambient air at atmospheric conditions.

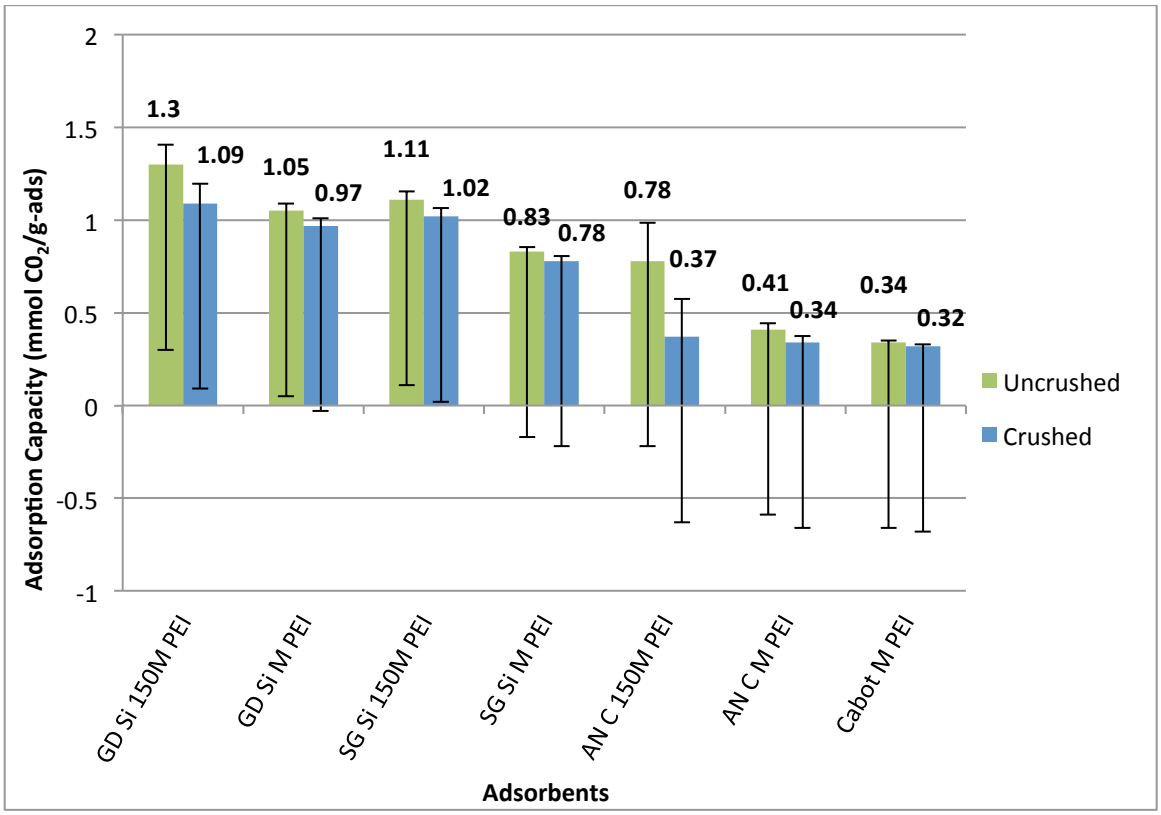

Fig 21. Adsorption capacities of Batch II adsorbents under 400 ppm CO_2 in He at 25^0C.

The highest adsorption capacities in 400 ppm CO_2 reported in this study were by GD Si 150M PEI (35 wt% PEI) and SG Silica 150M PEI (30 wt% PEI). They exhibited adsorption capacities of 57.2 and 48.4 mg CO_2/g-ads respectively, which when compared to a similar study by Dr. Jones' group (Choi et al. 2011) and Chen et al. (2013), shows only 50% of the capacity. Although, the PEI loading amount in their experiments were 45% and 50% respectively, the adsorption capacities are still considerably low.

2.3.4 Study of adsorbent regenerability

A candidate adsorbent must not only exhibit good CO_2 capture capacity but should also have the ability to be regenerated and reused multiple times without experiencing significant deterioration in its performance. The parameters that make an adsorbent attractive for regeneration are its chemical, mechanical and thermal stability over the cycles. A study was

conducted by Choi et al. (2011) to investigate the performance of three different kinds of adsorbents in a 4-cycle experiment in TGA under an environment containing 400 ppm CO_2 balanced in Argon.

The samples were initially subjected to temperatures starting at 25^{o}C (adsorption cycle) and then desorbed at 110^{o}C and this cycle was repeated a few times. It was observed that the PEI impregnated silica degraded significantly, losing about 30% of its capture capacity over the four cycles, suggesting that they might exhibit high adsorption capacities initially but will eventually have limited stability over cycles. In this project, the samples were tested in TGA under constant flow of 12% CO_2 in helium and 400 ppm CO_2 in helium for more than six cycles to observe losses in stability or performance.

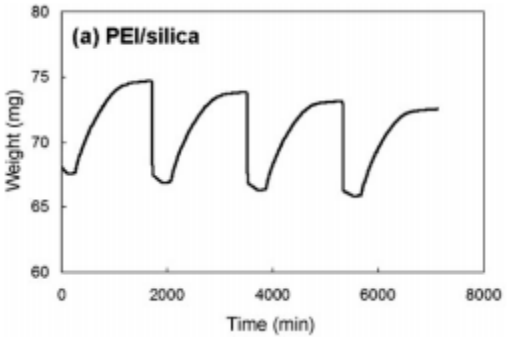

Table Changes of the adsorption capacities of the solid amine-based adsorbents from cyclic performance measurements in mol kg^{-1}. Each adsorbent was tested by using a TGA instrument using CO_2 dry gases (400 ppm in Ar) at ambient temperature.

	PEI/silica
Cycle 1	2.36
Cycle 2	2.08
Cycle 3	1.85
Cycle 4	1.65

Fig 22. Multicycle TGA adsorption curves of 45 wt% PEI/Silica. The adsorption experiments were performed by using a TGA instrument and repeated for four cycles, for which the adsorption step was traced usinga dry CO_2 mixture (400 ppm in Ar) at room temperature (Choi, et al. 2011).

The regenerability tests were performed on TGA at atmospheric pressures for adsorption from 400 ppm of CO_2 in helium at room temperature and at 75^{o}C to test adsorption performance in 12% CO_2 in helium. The adsorbents were initially purged with helium at 110^{0}C for an hour, after which the temperature was brought down to the adsorption conditions. The gas flow was switched to the desired concentration of CO_2 and maintained isothermal for 2 hours to allow for maximum adsorption, followed by desorption of the adsorbents by raising the temperature to

110°C. The adsorption cycle was performed again by cooling the environment to the respective temperature followed by desorption at 110^{0}C. This procedure was repeated over multiple cycles, while maintaining a constant CO_2 flow throughout the whole experiment. A trial experiment run on Saint Gobain Silica with 30 wt% PEI loading (150M PEI), under the flow of 12% CO_2 at 75^{0}C and under 400 ppm CO_2 at 25^{0}C, was performed following the above-mentioned procedure and the following figures (Fig 23, 24) and tables (Table 10, 11) illustrate the performance of the adsorbent over multiple cycles.

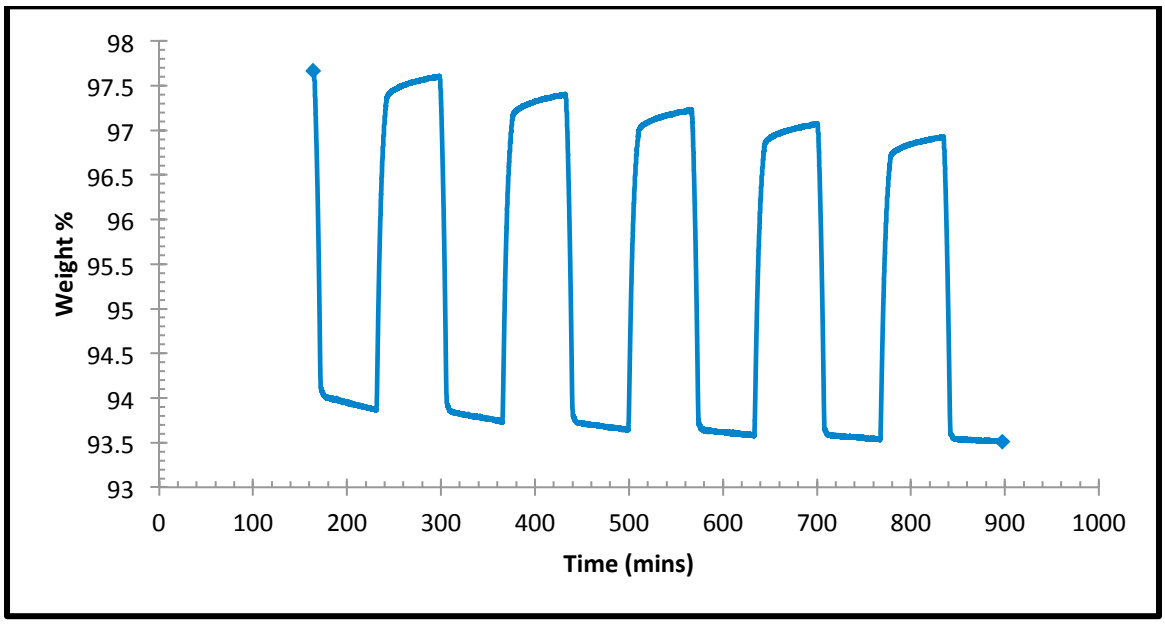

Fig 23. Multicycle TGA adsorption curves of SG Si 150M PEI, repeated for 6 cycles in 12 vol% CO_2 in He at 75°C.

Table 10. Adsorption capacities of CO_2 on Batch II SG Si 150M PEI over multi-cycle adsorption in 12 vol% CO_2 in He at 75^{0}C.

	mmol/g-adsorbent
Cycle 1	0.84
Cycle 2	0.83
Cycle 3	0.81
Cycle 4	0.79
Cycle 5	0.77

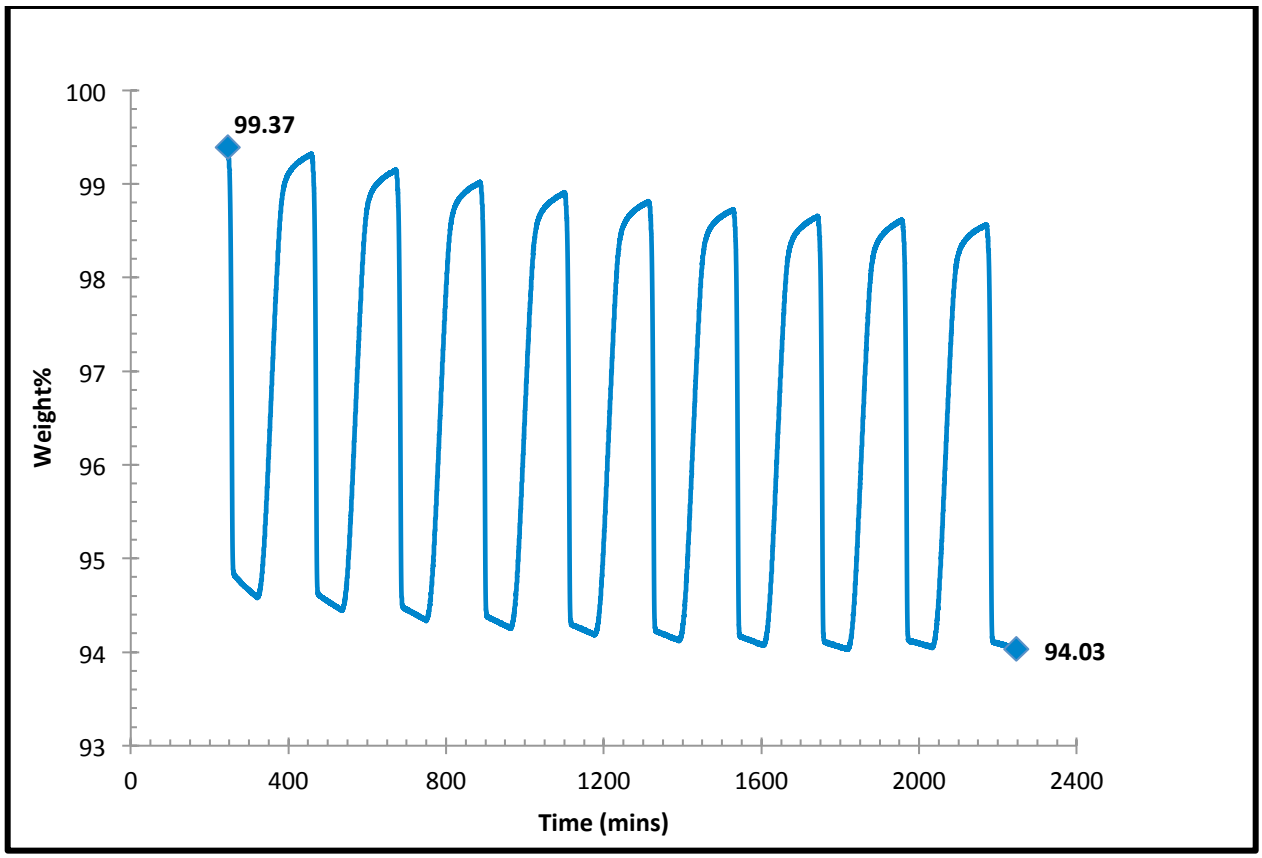

Fig 24. Multicycle TGA adsorption curves of SG Si 150M PEI, repeated for 10 cycles in 400 ppm CO_2 in He at 25^{o}C.

Table 11. CO_2 adsorption capacities of Batch II-SG Si 150M PEI over multicycle adsorption in 400 ppm CO_2 in He at 25^{0}C.

	milli mol CO_2/g-adsorbent
Cycle 1	1.061
Cycle 2	1.061
Cycle 3	1.059
Cycle 4	1.046
Cycle 5	1.049
Cycle 6	1.042
Cycle 7	1.033
Cycle 8	1.040
Cycle 9	1.016

Figure 24 and Table 11 clearly demonstrate that the adsorption capacities do not deteriorate considerably over multiple cycles of adsorptions and regenerations. It must be noted however, that the capacities of SG Si 150M PEI in 12 vol% CO_2 in He over successive cycles are much lower than the capacity achievable by a fresh pellet or a pellet regenerated in an inert atmosphere. The initial adsorption capacity after purging in helium at 110^0C is 1.67 mmol CO_2/g-ads and drops to almost half its capacity in subsequent cycles. This could be attributed to desorption/regeneration in a CO_2 environment and thus the inability of the adsorbent to completely be desorbed.

These experiments prove that the silica adsorbents prepared with the highest loading of PEI, i.e., 1.5 monolayer, could be candidate adsorbents for capturing CO_2 from ambient air at atmospheric conditions. They have high CO_2 adsorption capacities and are relatively stable mechanically, chemically and thermally.

To test these adsorbents for their application for the removal of dilute CO_2 from ambient air, the experiments were conducted on a larger scale employing a small-scale adsorber as described in Chapter 3. Although both GD-Si-150M-PEI and SG-Si-150M-PEI adsorbents were highly promising, the small-scale adsorber tests described in chapter 3 were conducted using SG Si adsorbents due to limited availability of the Grace Davison support.

CHAPTER 3
Small-scale Adsorber system

3.1 Introduction

For the purpose of studying adsorbent performance under realistic conditions, the findings from the TGA experiments were used to design and assemble a small-scale adsorber system, packed with the candidate adsorbent, SG Si 150M PEI. The adsorption capacities of the candidate adsorbent were measured using a temperature swing adsorption (TSA) process. The TSA process allows for a bed of adsorbent to selectively adsorb one or more species from the feed stream. The preferential adsorption of a single species and its adsorption capacity can be enhanced by performing the adsorption step under specific temperatures and pressures, since both the parameters influence the extent of adsorption of the particular species. The adsorbent bed is later regenerated by raising the temperature of the bed, to liberate the adsorbed species, since adsorption isotherms are strongly influenced by temperature.

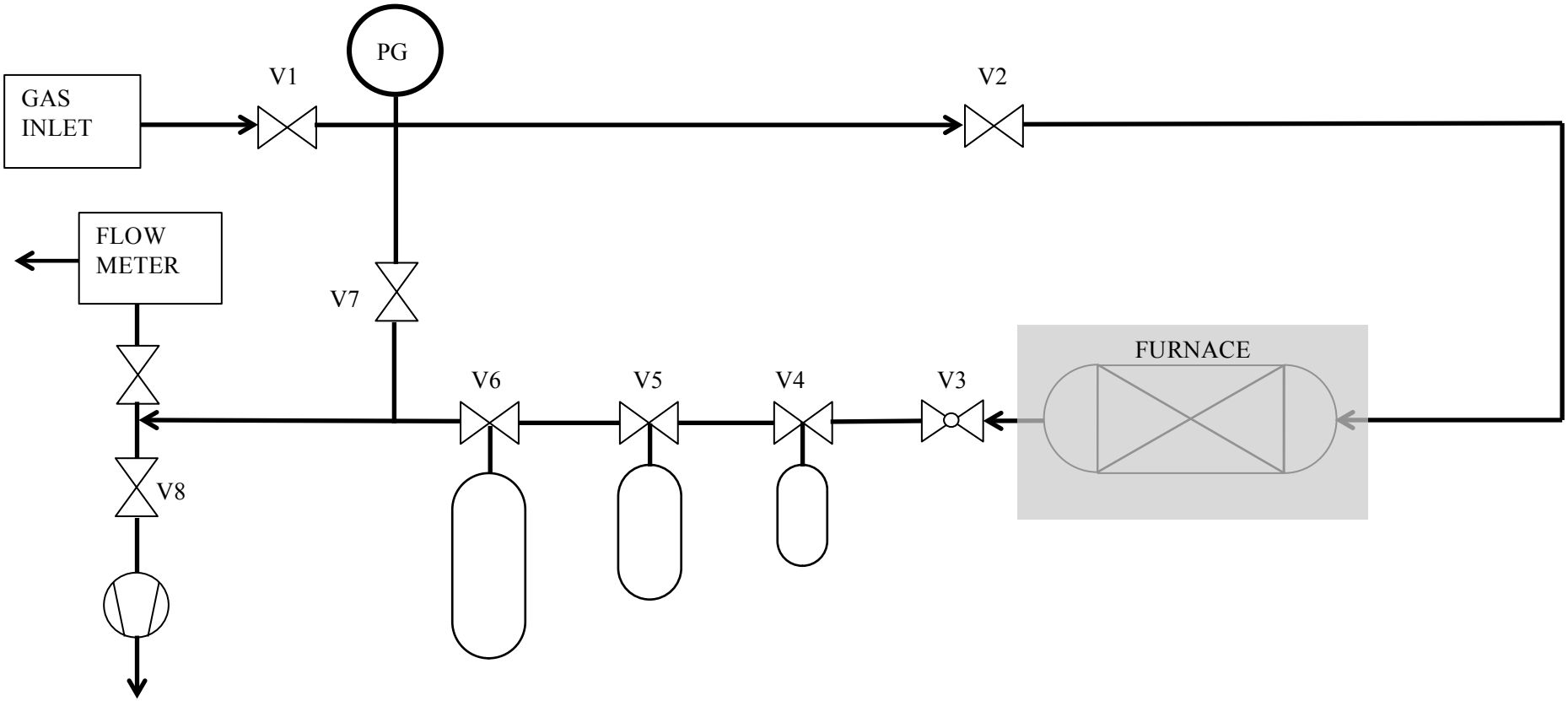

Fig 25. PID for the adsorber experiment.

3.2 TSA Cycles

3.2.1 Experimental Setup

The 97 cc. adsorber was packed with pellets of Saint Gobain Silica 150M PEI, weighing approximately 32 grams, while Zirconia (Alfa Aesar) served as a filler. Both inlet and outlet were packed with glass wool and sieve discs to prevent displacement of the pellets in the packed bed during the experiments. The adsorber was placed in a Lindberg Blue tube furnace, which served to change and maintain the temperature of the bed.

The inlet to the adsorber was connected to a gas source, such as a cylinder or an air compressor. The temperature of the bed was raised to high temperature and helium was allowed to flow through the adsorber to purge and remove impurities, if any. The temperature was then reduced to the adsorption step temperature and pressure, and the feed gas (containing CO_2) was allowed to flow through the adsorber at the desired flowrate, exiting from the flow controller. After sufficient time was allowed to achieve maximum adsorption, the feed gas was stopped, the inlet (V2) and exit (V3) valves of the adsorber were closed and temperature of the bed was raised to liberate the CO_2. Since, amount of CO_2 could not be directly measured, the exit valve (V3) was opened to the fill one of the previously evacuated cylinders of volume, 75 cc, 200 cc and 300cc respectively. A pressure gauge operated by valve (V7), was placed on the line exiting the cadsorber and the cylinders to monitor the pressure of liberated CO_2.

3.2.2 Extrapolation of TGA data

Upon analysis of the TGA data of CO_2 adsorption on SG Si 150M PEI under 400 ppm CO_2 in He (Fig. 26), it was noted that most of the adsorption (up to 92%) takes place in less than

2 hours and though the adsorption curve after that point has a very low slope, it is ever increasing and never reaches equilibrium.

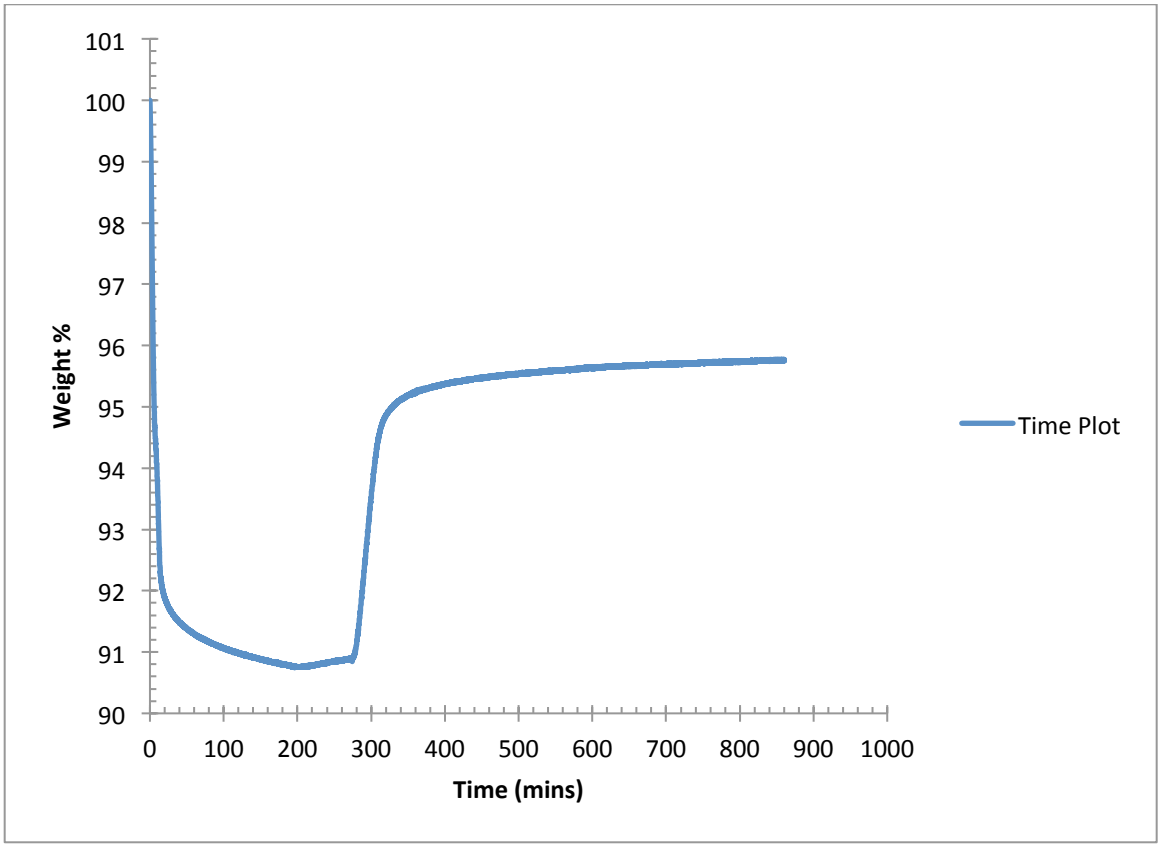

Fig 26. TGA curve for CO_2 adsorption on Batch II - SG Si 150M PEI under 400 ppm CO_2 in He for 10 hrs at 25^{o}C.

Therefore, in order to calculate the amount of air that would be required to attain the same level of adsorption in the adsorber experiment, the comparison was made to estimate the time required for 90% adsorption in TGA. The amount of PEI present in 32 grams of adsorbent was calculated using the data in Table 6 and the adsorption capacity of these adsorbents is shown in Table 9. From the information available, the maximum amount (moles) of CO_2 that could be adsorbed by these adsorbents was estimated. Assuming that the CO_2 content in the air is 400 ppm by volume, the amount (liters) of air containing the estimated amount of CO_2 was

determined. The air flowrate to be fed to the adsorber was chosen to be in the range of 2.5-5 LPM (liters per minute) in order to allow for 90% adsorption as shown in Figure 26. The calculations can be found in Appendix A.8.

3.2.3 Calibration of the adsorber system

Since the estimation of CO_2 adsorption in these experiments was based on pressure monitoring a cylinder of known volume, it was necessary that the volumes in the system were accounted for, in order for the calculation to be precise. The internal volumes including those of the lines, the adsorber and the dead volumes were estimated by an experiment using Boyle's Law.

Helium was allowed to flow through the entire setup exiting through the flow meter. Valve, V4 was opened to allow the gas to enter the 75cc cylinder and V7 was opened to monitor the pressure in the system and once the pressure was stable at 35 psi, valve (V4) to the 75cc cylinder was closed. The exit valve from the flow meter was now sealed and the whole system except the 75 cc cylinder was evacuated using the vacuum pump.

After complete evacuation, all valves but V7 were closed and the reading on the pressure gauge was noted. Valve V4 was then opened to release the helium into the lines around the cylinder and Valve V3 was later opened to allow the gas to travel through the adsorber. Finally, the valve (V6) to the 300 cc cylinder was released and the pressure changes after each step was recorded.

Using the pressure changes associated with change in volumes, the Boyle's law was applied to the computation and the collective volumes of the lines in the system and the adsorber was determined. The calculations can be found in Appendix A.10.

3.2.4 Estimation of CO_2 adsorption capacity in the adsorber

Procedure

The furnace was initially set to a temperature of 110^{o}C and helium was allowed flow through the system at 80 ml/min and exit through the flowmeter for a period of one hour, in order to purge the system. The helium flow was then stopped and the furnace temperature brought down to 25^{o}C. Once the temperature was stable at 25^{o}C, the feed source was changed to an air compressor and the air flow-rate was set at 5 LPM. According to preliminary calculations, the least amount of time that would be required for the air to flow in order to achieve an equivalent adsorption capacity in the adsorber was determined to be approximately 11 hours (Refer Section 3.3). In Run 1, the period of air flow was set for 17 hours, after which, the valves V1, V2 and V3 were closed, the air flow was stopped and the system was evacuated with the help of the vacuum pump. Once the system was under vacuum, all valves were closed except that of the pressure gauge (V7). The furnace was now heated to 110^{o}C and the exit valve (V3) from the adsorber was opened along with valve V4, allowing the now liberated CO_2 to enter the previously evacuated, 75cc cylinder. The pressure in the cylinder and adjacent lines was noted at intervals of every 5 minutes until it was stable and all the CO_2 desorbed.

Interpretation of pressure data

The data acquired from the above mentioned experiment indicates pressure changes in known volumes as the bed of adsorbents is desorbed at higher temperatures. As the CO_2 is liberated, the pressure in these volumes slowly increases until it becomes stable at one point since the adsorbents are now completely desorbed, and neither increases nor decreases. This stable pressure indicates the pressure exerted by the amount of CO_2 that was adsorbed and has now been desorbed into the cylinder.

In order to continue with these initial calculations, two assumptions had been made. The first being that N_2 and O_2 do not compete with CO_2 during adsorption and second assumption being that the amount of CO_2 adsorbed in the adsorber is completely liberated during desorption. These assumptions and their validity will be addressed in the following sections. Using the ideal gas equation, the number of moles of CO_2 exerting the said pressure was found and hence, the milli-moles of CO_2 captured per gram of adsorbent were determined. The calculations involved in estimating capture capacity can be found in Appendix A.11. Further experiments were conducted with varying flow rates and adsorption periods. The results of these experiments and the comparison of adsorption performance to that in the TGA will be discussed in the next section.

3.3 Results and Discussions

In this section, we will discuss the data gathered from six of several experiments conducted following the procedure mentioned in Section 3.2.4. Although initial set of experiments were performed with flow rate of air set at 5 LPM during the adsorption cycle, later experiments were conducted with a flow rate of 2.5 LPM with varying lengths of adsorption cycle. The following table shows adsorption capacity achieved in each of these experiments.

Table 12. CO_2 adsorption capacities by SG Si 150M PEI in the small-scale adsorber experiment.

RUN #		I	II	III	IV	V	VI	TGA
Flow of air	LPM	5	5	2.5	2.5	2.5	2.5	-
Period of adsorption	Hrs.	17	36	42	100	163	192	-
Adsorption capacity per gram of adsorbent	mmol/g	0.15	0.14	0.13	0.15	0.15	0.15	1.11

It can be observed from the table above that though the adsorption capacity is comparatively higher at higher flowrates and lower adsorption time (for example Run I), increasing the duration of adsorption does not provide higher capacities and in fact, affects the performance of the adsorbents. Also, the adsorption system in question was incapable of handling flow rates of that velocity or higher.

Switching to a lower flow-rate with a longer adsorption time did not result in better capacities either but with increase in lengths of adsorption periods, an increase in performance could be noticed, which however was insignificant. Comparing these capacities to that obtained from TGA, the highest capacity attained is only 13.6% of that achieved in a TGA experiment and it is apparent that the adsorber experiment has failed to deliver the results expected. Since the experiments conducted in the TGA were performed in a highly controlled environment, on a very small sample with a known concentration of CO_2 and no known competition during

adsorption, these factors must be considered in order to determine the factors affecting adsorption in the adsorber system.

Investigation into low CO_2 adsorption capacities

The purpose of this section is to identify and validate the factors that could possibly be affecting adsorption capacities in the adsorber experiment. As discussed above (Refer Section 3.2.4.2), one of the reasons could be competition from nitrogen and/or oxygen. Others being mass transfer limitations, loss of PEI from the adsorbent, formation of urea during thermal regeneration and adsorption of CO_2 by the filler material Zirconia. These issues will be addressed in the following sections.

Competition with nitrogen

A single pellet of SG Silica 150M PEI was tested in a TGA under nitrogen flow and subjected to the same procedure (Refer Section 2.3.1) as that used to determine CO_2 adsorption capacities. The purpose of this experiment was to examine the affinity of the adsorbent towards N_2 alone. The following figure (Fig. 27) shows the adsorption curve obtained from the experiment and it can be noted that hardly any N_2 is adsorbed. Upon estimation, the amount of nitrogen captured by 1 gram of adsorbent was found to be only 0.05 mmoles as that compared to 1.11 mmoles of CO_2. It can thus be concluded that nitrogen is not competing with CO_2 during adsorption. To confirm this statement, another similar experiment was performed on the TGA with air, sourced from a cylinder. Air was allowed to pass over the sample for a short period of two hours, the same as that for the 400 ppm CO_2/He mix, in order to compare the CO_2 adsorption capacities in presence of other elements with that estimated in controlled environments.

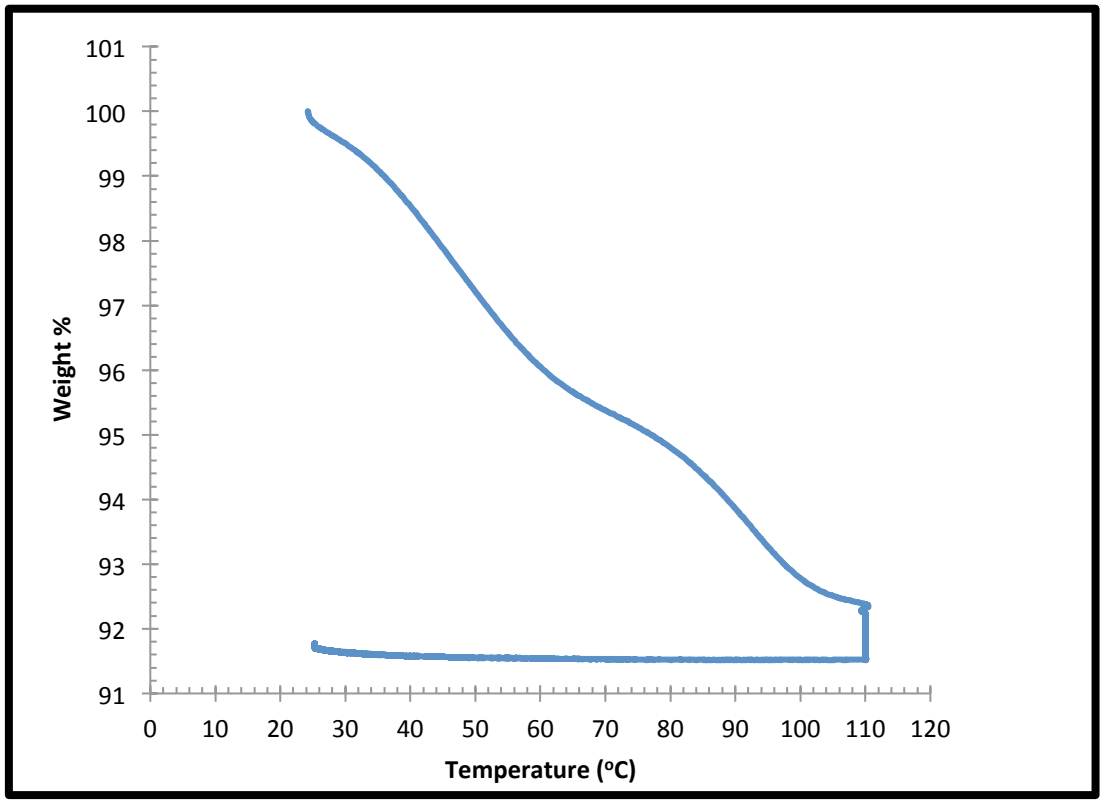

Fig 27. Estimation of N_2 capture capacity by Saint Gobain Silica 150M PEI at 25°C in TGA.

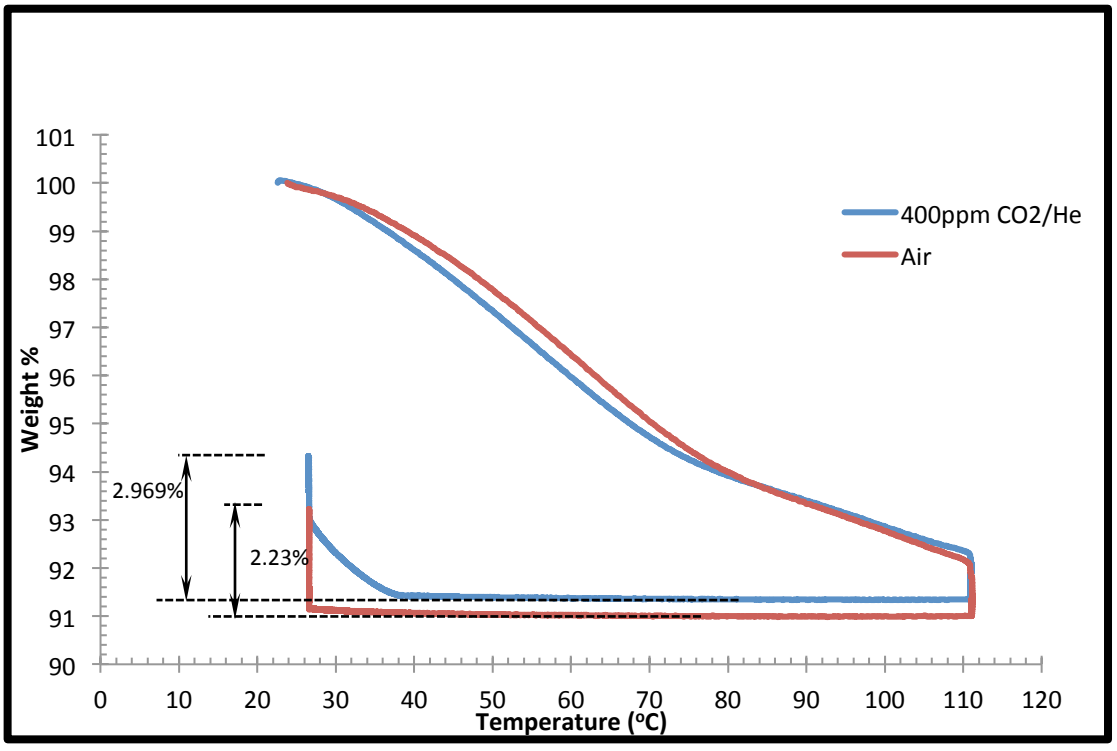

Fig 28. Estimation of CO_2 capture capacity by Saint Gobain Silica 150M PEI in TGA, at 25°C in air vs. 400 ppm CO_2 in He.

From Figure 28, it can be deduced that though the capture capacity of the adsorbent from ambient air is not on par with that achieved in a controlled environment, its capacity is comparatively much better in a TGA environment (75% of max. capacity attainable) than in the small-scale adsorber (13.6%). Since, the competition with N_2 has been ruled out and according to Aroua et al. (2008) and Xu et al. (2005), O_2 does not compete with CO_2 as well, other factors must now be probed into.

Competition with Zirconia

Zirconia (ZrO_2) was used as a filler material in the adsorber experiment and was chosen among other candidates for its low surface area (90 m^2/g) compared to silica (324 m^2/g) and its low affinity for CO_2 under ambient conditions. To estimate its affinity for CO_2, a single pellet of ZrO_2 was tested in a thermogravimetric analyzer (TGA) at 25^oC following the procedure mentioned in Section 2.3.3. It can be observed from the TGA curve in Figure 28, that the weight gained by the ZrO_2 sample is only 0.5% and upon calculation, the CO_2 capture capacity of ZrO_2 in 400 ppm CO_2/He was estimated to be only 0.127 mmol CO_2/ g ads, which is approximately 10% of the adsorption capacity of SG Si 150M PEI. It can be thus concluded that zirconia is not a strong competitor for CO_2 and hence the only possible explanation for low CO_2 adsorption capacity would be mass transfer limitations and loss of active amine sites.

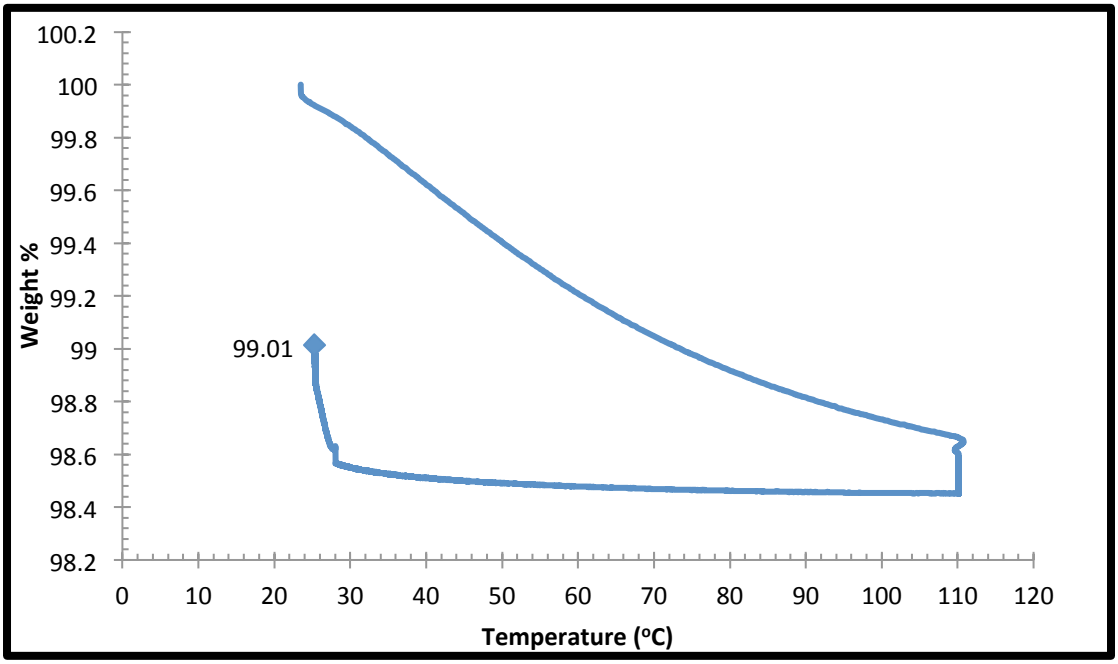

Fig 29. Estimation of CO_2 capture capacity of ZrO_2 pellet in TGA at 25°C in 400ppm CO_2 in He.

Loss of PEI and irreversible formation of urea

Deterioration in adsorption capacities can also occur due to physical loss of PEI and degradation of amine sites due to formation of urea. Goeppert et al. (2010) and Hicks et al. (2008) have reported PEI leaching in small amounts in temperatures in excess of 80°C. The causes for leaching have been attributed to low molecular weight impurities present in PEI, evaporation of PEI and slow decomposition of the amine over several cycles.

Studies conducted by Drage et al. (2008) and Sayari et al. (2010), state that a reduction in CO_2 capacity is noticeable over successive adsorption/desorption cycles and anhydrous conditions due to irreversible formation of urea. This formation can be a result of a direct reaction of CO_2 with PEI and/or a secondary reaction between carbamate ions and amine groups. At temperatures in the range of 130-140°C, desorption of adsorbents in a CO_2-rich atmosphere, results in reaction between CO_2 and amine groups, yielding urea.

$$R_2NH_2^+ + R_2NCOO^- \leftrightarrow R_2NCONR_2 + H_2O$$
$$2R_2NH + CO_2 \leftrightarrow R_2NCONR_2 + H_2O$$

Fig 30. Reactions involved in formation of urea at 130^{o}C (Drage et al. 2008).

Thermal regeneration of adsorbents at higher temperatures is a compromise between degradation of the adsorbent and successful regeneration. Solutions proposed to counter formation of urea have been (i) lowering temperatures of desorption, while compromising on adsorption capacity (ii) use of an inert stripping gas and (iii) use of humid streams during desorption or as a treatment for deactivated adsorbents (Sayari et al. 2010).

The desorption-cycles in this adsorber experiment were performed consistently at 110^{o}C and in CO_2 rich atmospheres as well, followed by purging of the adsorber with an inert gas. Also, experiments conducted in TGA to test thermal stability over multiple cycles (Refer Section 2.3.4), did not demonstrate significant decline in adsorption capacity over cycles. However, the regenerability of the adsorbent was examined over a maximum of ten cycles and the assumption that their performance over further adsorption/desorption cycles would be similar, cannot be made. Several researchers (Xu et al. 2002, Li et al. 2015) have tested adsorption capacities at temperatures in ranges as high as 90-105^{o}C with promising results. It is thus hard to say, whether formation of urea is an issue in this case, although loss of PEI over higher temperatures and cycles is a high possibility.

Mass Transfer Limitations

The classic steps for a gas-solid reaction involve:

i) Diffusion of reactants from the bulk-phase to the external surface of the adsorbent surface

ii) Diffusion of reactants into the pores of the adsorbent

iii) Adsorption of reactants onto the inner adsorbent surface

iv) Reaction at active sites on the surface

In the case of the adsorber experiment, CO_2 has to diffuse through the bulk phase of ambient air to the surface of the Si-PEI adsorbent pellets. CO_2 must then diffuse through the pores of the pellet, while diffusing into the bulk of PEI present in the pores and react with PEI forming carbamates under anhydrous conditions and bicarbonates in the presence of moisture.

Diffusion Limitations

To determine the diffusion controlling step in the adsorption process, the Biot number was calculated for the adsorber system as well as the TGA experiments. The Biot number, Bi, denotes ratio of the internal resistance to mass transfer by diffusion to the external resistance to mass transfer by convection. For $0.1<Bi<10$, both internal and external mass transfer resistances are significant (Basmadjian, 2007). Initially, the average particle size of the powdered SG Si 150M PEI (Uncrushed) sample used in TGA was estimated to be 13.78 microns, using SEM images of the sample. The equivalent diameter of 100 discrete particles were measured and their average was found. The particle size distribution curve can be found in the Appendix B.5. The particle Reynold's numbers (Re_p) calculated for both cases were 27.24 and 1.7 for the adsorber and TGA respectively. The Bi number for the adsorber was estimated to be 4.03 and 5.21 for the TGA tests(Appendix A.12). The values of the Biot number determined for both experiments are close and lie in range to 0.1-10, where both internal and external mass transfer are diffusion

limited. It can thus be deduced that the reduced particle size does not contribute to the higher CO_2 adsorption capacities observed in the TGA experiment.

Pore Diffusion Limitations

Adsorption studies conducted by Xu et al. (2002) and Li et al. (2015) at higher temperatures in the range of 90-110^oC have been promising, which implies that adsorption is still occurring at higher temperatures. Raising the temperature allows the PEI molecules to be more flexible, thus allowing more accessible sites for CO_2. However, the PEI- amine interactions are weaker at higher temperatures like 75^oC and further raising the temperature only weakens the amine-CO_2 interaction even though accessibility of CO_2 to amines increases. Ultimately, the overall adsorption capacity decreases. In this case, the CO_2 is liberated inside the adsorber at 110^oC and at higher partial pressures of CO_2, it is possible that adsorption continues to take place and not all CO_2 is fully desorbed. Therefore, the low adsorption capacities may not be because of loss in the adsorbent's stability over multiple cycles or degradation of PEI.

To prove this theory, a single SG Si 150M PEI pellet (regenerated multiple times) was removed from the adsorber before the desorption cycle and tested in the TGA. The pellet was first desorbed at 110^oC under 400 ppm CO_2 in He and then, its adsorption capacity was measured similar to previous experiments. The adsorption capacity of the pellet was determined to be 1.09 mmol CO_2/g-ads, which is comparable to the capacity of a fresh adsorbent (1.11 mmol CO_2/g-ads) under identical conditions. The calculations and TGA curves for adsorption capacity of a single pellet can be found in Appendix A.13 and B.6 respectively. This experiment confirms that the adsorption capacity of the pellets after multiple regenerations has not diminished and that the reason for lower capacities reported in the adsorber experiment is the continual adsorption of CO_2 under high partial pressures at 110^oC, which is absent in TGA. Comparing the adsorption capacities in the adsorber experiment and the TGA, the recovery ratio would be 0.13, implying

that the efficiency of the these TSA cycles are very low. To avoid adsorption at higher temperatures, the adsorber may be purged with an inert gas while running the desorption cycle, to remove the liberated CO_2 and the capture the gas mixture in an evacuated cylinder. However, given the present set-up of the system and in the absence of a CO_2-analyzer, the estimation of the amount of CO_2 adsorbed and later liberated, would be difficult.

In recent studies regarding pore diffusion resistance, Kumar et al. (2008) reported diffusion limitations in their MCM-48 membranes caused by strong interactions of CO_2 and PEI, enhanced by presence of moisture, which hinders further CO_2 diffusion into the pores of the adsorbent. Sayari et al. (2011) also reported that CO_2 adsorption into amine-impregnated supports was mainly diffusion limited and discussed the different factors contributing to diffusion limitations to be the pore size of the support, amount of PEI loaded, size of the particle and the temperature of adsorption.

Ahn's group (Son et al. 2008) studied and demonstrated the effects of pore size on CO_2 diffusion and kinetics. Their studies stated that the pore size of the support material was directly proportional to the rate of CO_2 adsorption. Xu et al. (2002) and Chen et al. (2010) reported that the PEI loading was a crucial factor in reaching maximum adsorption capacities. Although, the adsorption capacities increased with increasing PEI content, for PEI loadings above 60 wt. %, a slight drop in the amine efficiency was observed. With further increase in the PEI loading in the support, the capture capacities dropped as well, mostly due to pore blockage and additional resistance to diffusion because of excess PEI coated on the outer surface.

It has been reported that lower loadings of PEI allow for better dispersion of PEI within the pores of the support, providing easier access to CO_2 to active amino sites. Supports with higher surface area, pore size and pore volume further enhance capture capacities at lower loadings (Goeppert et al. 2014, Son et al. 2008).

Goeppert et al. (2014) also studied the effects of particle size on CO_2 capture capacities in air at ambient temperatures. They tested particles sizes in the ranges <0.2 mm, 0.2-0.5 mm, 0.5-1.7 mm and >1.7 mm and reported that the adsorption kinetics were fastest with smaller particle sizes and decreased considerably when the particle size increased. Similar behavior was observed during desorption cycles of the adsorbent as well. Their studies conclude that the diffusion of CO_2 into the adsorbent is more difficult with increasing particle size and that particles in the range of 0.2-0.5 mm were suited best for CO_2 captures. However, in this study it has been proved that the reduced particle size of the adsorbent does not improve the mass transfer limitations.

Xu et al. (2002) investigated the effects of temperature on adsorption capacities and stated that, with decrease in adsorption temperatures from 75^{o}C to 25^{o}C, the adsorption capacities reduced. The formation of bulk-like PEI aggregates inside the pores of the support at lower temperatures, hinders CO_2 adsorption and leads to a diffusion limited process (Sayari et al. 2011). Increase in adsorption temperatures, facilitates flexibility in the PEI molecules, exposing more CO_2-affinity sites and allowing for higher diffusion rates of CO_2 into the bulk-like PEI. Increased reaction rate of CO_2 with PEI can thus be observed and as a result, higher capture capacities were reported. However, as mentioned before, the CO_2-amine interactions get weaker when temperature is increased. An optimal temperature in between has to determined, where the accessibility to bulk PEI and strong CO_2-amine interactions can both co-exist. However, these experiments were performed in pure CO_2 atmospheres or simulated flue gas conditions and it is uncertain if the findings would be applicable to dilute CO_2 streams.

Considering the above-mentioned factors, the parameters that could affect the adsorption capacity in the adsorber experiment could be the desorption of the adsorbents in CO_2-rich environment at higher temperatures, and the temperature of adsorption, since the pore size of the support (10.9 nm) and the PEI amount (45 wt. %) in this case are ideal for CO_2 adsorption.

Conclusions

Four mesoporous supports, namely, Saint Gobain Silica (SG Si), Grace Davison (GD Si), Cabot BP Carbon Black (Cabot C) and Akzo Nobel Carbon Black (AN C) were investigated as candidate supports for CO_2 capture from ambient air. These supports were impregnated with varying amounts of polyethylenimine (PEI) and their capture capacities were initially tested under flue-gas simulated (12 vol. % CO_2) conditions in a thermogravimetric analyzer. At 75^oC, the maximum adsorption capacities were exhibited by the AN-C-150M-PEI adsorbents, with capture capacities of 2.73 mmol of CO_2/g of adsorbent. The capture capacity of its silica counterpart (SG Si), with the same PEI loading was 1.73 mmol of CO_2/g of adsorbent. Further adsorption tests conducted in TGA under ambient conditions and simulated ambient air atmospheres, determined weak capture capacities by carbon black adsorbents at lower temperatures, eliminating them from further experiments for CO_2 capture from ambient air. Meanwhile, the silica adsorbents displayed capacities of 1.11 and 1.30 mmol of CO_2/g of adsorbent by SG Si and GD Si adsorbents respectively. The regenerability and stability of these adsorbents were investigated over multiple cycles using TGA to test adsorption performances at 25^oC in 400-ppm CO_2 atmospheres and at 75^oC in 12% CO_2 atmospheres and, desorption performances at 110^oC. The capacities were found to not deteriorate considerably over multiple cycles, while providing relatively high capacities compared to a single cycle and the adsorbents were determined to be chemically, thermally and mechanically stable.

Although both silica adsorbents were promising candidates for CO_2 capture in air, further experiments for practical applications were conducted on the SG Si adsorbent due to limited availability of GD Si support for larger scale testing. SG–Si-150M-PEI pellets were packed in a small adsorber and tested for CO_2 capture from ambient air at ambient conditions over extended

periods of time. The recovery ratio of CO_2 in the adsorber when compared to the TGA experiment was found to be only 0.13. Investigation into lower adsorption capacities eliminated certain possibilities of competition with nitrogen and oxygen, competition with filler material (zirconia) and led to more probable causes, namely, the leaching and degradation of PEI impregnated onto supports, and, most importantly, mass transfer limitations during CO_2 adsorption.

Future Work

Considering the obstacles faced in achieving high CO_2 capture capacities from ambient air in the adsorber experiment, one of the first steps would be to test for urea formation by the chemical reaction between CO_2 and surface amino groups. If urea formation is observed, the adsorbent can be treated under humid conditions to reverse the urea formation and regenerate the adsorbent. The experiments can also be performed with use of a stripping gas during regeneration to prevent urea formation. A comparison of adsorption capacities achieved under these new conditions with capacities reported for dry atmospheres can be made to eliminate or validate the presence of PEI degradation and its effect on capture capacities. Another approach should be to use lower regeneration temperatures to avoid degradation and loss of PEI altogether and examine the resulting capacities.

The regeneration cycle of the adsorber system can be optimized to allow a purge gas to remove the liberated CO_2 and use an analyzer to measure the concentration of CO_2 from the CO_2-purge gas mixture. The temperature of the regeneration may be increased to facilitate CO_2 desorption, but it in turn may lead to increased degradation and loss of PEI.

References

Aroua, M.K., Daud, W.M.A.W., Yin, C-Y and Adinata, D. "Adsorption capacities of carbon dioxide, oxygen, nitrogen and methane on carbon molecular basket derived from polyethyleneimine impregnation on microporous palm shell activated carbon." *Separation and Purification Technology*, 2008, 62 (3), 609-613.

Atabani, A.E., Silitonga, A.S., Badruddin, I.A., Mahlia, T.M.I., Masjuki, H.H., Mekhilef, S., "A comprehensive review on biodiesel as an alternative energy resource and its characteristics." *Renewable and Sustainable Energy Reviews*, 2012, 16(4), 2070-2093.

Azar, C., Rodhe, H., "Targets for Stabilization of Atmospheric CO_2." *Science*, 1997, 276, 1818.

Basmadjian,D., "Mass Transfer and Separation Processes: Principles and Applications." 2007.

Behr, A., Henze, G., "Use of carbon dioxide in chemical syntheses via a lactone intermediate." *Green Chemistry Volume*, 2011, 13(1), 25-39.

Belmabkhout, Y.; Serna-Guerrero, R.; Sayari, A., "Amine-bearing mesoporous silica for CO_2 removal from dry and humid air." *Chemical Engineering Science*, 2010, 65 (11), 3695 – 3698.

Berggren, C., Magnusson, T., "Reducing automotive emissions — The potentials of combustion engine technologies and the power of policy." *Energy Policy*, 41, 2012, 636–643.

Chaffee, A.L., Knowles, J.P., Liang, Z., Zhang, J., Xiao, P., Webley. P.A., "CO_2 capture by adsorption: Materials and process development." *International Journal of Greenhouse Gas Control*, 2007, 1(1), 11–18.

Chapman, L., "Transport and climate change: a review." *Journal of Transport Geography*, 2007, 15(5), 354–367.

Chen, C., Son, W.J., You, K.S., Ahn, J.W., Ahn, W.S., " Carbon dioxide capture using amine-impregnated HMS having textural mesoporosity." *Chemical Engineering Journal*, 2010, 161, 46–52.

Chen, Z., Deng, S.,Wei, H., Wang, B., Huang, J., Yu, G., "Polyethylenimine-Impregnated Resin for High CO_2 Adsorption: An Efficient Adsorbent for CO_2 Capture from Simulated Flue Gas and Ambient Air." *ACS Applied Materials and Interfaces*, 2013, 5, 6937–6945.

Chew, T.L., Ahmad, A.L. and Bhatia, S., "Ordered Mesoporous Silica (OMS) as an Adsorbent and Membrane for Separation of Carbon Dioxide (CO_2)." *Advances in Colloid and Interface Science*, 2010, 153, 43–57.

Choi, S., Gray, M.L., Jones, C.W., "Amine-Tethered Solid Adsorbents Coupling High Adsorption Capacity and Regenerability for CO_2 Capture From Ambient Air." *ChemSusChem*, 2011, 4, 628 – 635.

Choi, S., Drese, J. H., Jones, C. W., "Adsorbent materials for carbon dioxide capture from large anthropogenic point sources." *ChemSusChem*, 2009, 2, 796– 854.

Conway, T. and Tans, P., NOAA/ESRL (www.esrl.noaa.gov/gmd/ccgg/trends/))

Darensbourg, D.J., "Making plastics from carbon dioxide: Salen metal complexes as catalysts for the production of polycarbonates from epoxides and CO_2." *Chemical Reviews*, 2007, 107(6), 2388-2410.

Drage, T. C., Arenillas, A., Smith, K. M., Snape, C. E., "Thermal stability of polyethylenimine based carbon dioxide adsorbents and its influence on selection of regeneration strategies." *Microporous and Mesoporous Materials*, 2008, 116, 504 – 512.

Drese, J.H., Choi, S., Lively, R., Gray, M., Fauth, D. J., Jones, C. W., "Synthesis-Structure-Property Relationships for Hyperbranched Aminosilica CO_2 Adsorbents."Adv. Funct.Mater. 2009, 19, 3821 – 3832.

Elliott, S., Lackner, K.S., Ziock, H.J., Dubey, M.K., Hanson, H.P., Barr, S., Ciszkowski, N.A., Blake, D.R., "Compensation of atmospheric CO_2 buildup through engineered chemical shrinkage." *Geophysical Research Letters*, 2001, 28(7), 1235-1238.

Erdinc, O., Uzunoglu, M., "Optimum design of hybrid renewable energy systems: Overview of different approaches." *Renewable and Sustainable Energy Reviews*, 2012, 16(3), 1412-1425.

Falk Pederson, O., Dannstrom, H., Gronvold, M., Stuksrud, D., Ronning, O., "Gas treating using membrane gas/liquid contactors." Fifth International Conference of Greenhouse Gas Control Technologies, Cairns, Australia. 2000.

Figueroa, J.D., Fout, T., Plasynski, S., McIlvried, H., Srivastava, R.D., "Advances in CO_2 capture technology—The U.S. Department of Energy's Carbon Sequestration Program" *International Journal of Greenhouse Gas Control*, 2008, 9-20.

Filburn, T., Helble, J.J. and Weiss, R.A., "Development of Supported Ethanolamines and Modified Ethanolamines for CO_2 Capture." *Industrial & Engineering Chemistry Research*, 2005, 44, 1542–1546.

Geerlings, H., Zevenhoven, R., "CO_2 Mineralization—Bridge Between Storage and Utilization of CO_2." *Annual Review of Chemical and Biomolecular Engineering*, 2013, 4, 103-117.

Goeppert, A., Meth, S., Surya Prakash, G. K., Olah, G. A., "Nanostructured silica as a support for regenerable high-capacity organoamine-based CO_2 sorbents." *Energy & Environmental Science*, 2010, 3, 1949–1960.

Goeppert, A., Zhang, H., Czaun, M., May, R. B., Surya Prakash, G. K., Olah, G. A., Narayanan, S. R., "Easily Regenerable Solid Adsorbents Based on Polyamines for Carbon Dioxide Capture from the Air." *ChemSusChem*, 2014, 7, 1386 – 1397.

Hansen, J., Sato, M., Kharecha, P., Beerling, D., Berner, R., Masson-Delmotte, V., Pagani, M., Raymo, M., Royer, D.L., and Zachos, J.C., "Target Atmospheric CO_2: Where Should Humanity Aim?" *Open Atmospheric Science Journal*, 2008, 2, 217-231.

Harrison, D.P., "The role of solids in CO_2 capture: A mini review." 7th International Conference on Greenhouse Gas Control Technologies Vancouver, CA, 2004, 1101-1106.

Herzog, H.J., *Environmental Science and Technology*, 2001, 35, 148A-153A.

Hicks, J. C., Drese, J. H., Fauth, D. J., Gray, M. L., Qi, G. G., Jones, C. W., "Designing Adsorbents for CO_2 Capture from Flue Gas-Hyperbranched Aminosilicas Capable of Capturing CO_2 Reversibly."*Journal of the American Chemical Society*, 2008, 130, 2902 – 2903.

Hiyoshi, N.; Yogo, K.; Yashima, T., "Adsorption characteristics of carbon dioxide on organically functionalized SBA-15." *Microporous and Mesoporous Materials*, 2005, 84, 357.

Hsu, S.C., Lu, C., Su, F., Zeng, W. and Chen, W., "Thermodynamics and Regeneration Studies of CO_2 Adsorption on Multiwalled Carbon Nanotubes." *Chemical Engineering Science*, 2010, 65, 1354–1361.

IEA. International energy agency statistics, 2002.

IPCC: Summary for policymakers. In: Climate Change 2014: Impacts, Adaptation, and Vulnerability. Part A: Global and Sectoral Aspects. Contribution of Working Group II to the Fifth Assessment Report of the Intergovernmental Panel on Climate Change [Field, C.B., V.R. Barros, D.J. Dokken, K.J. Mach, M.D. Mastrandrea, T.E. Bilir, M. Chatterjee, K.L. Ebi, Y.O. Estrada, R.C. Genova, B. Girma, E.S. Kissel, A.N. Levy, S. MacCracken, P.R. Mastrandrea, and L.L.White (eds.)]. Cambridge University Press, Cambridge, United Kingdom and New York, NY, USA, 2014, 1-32.

Karkezi, S., Majoro, L., Johnson, T. M., "Climate change mitigation in the urban transport sector: priorities for the World Bank." The World Bank, Washington D.C. 2003.

Khatri, R.A., Chuang, S.S.C., Soong, Y., Gray, M., "Thermal and chemical stability of regenerable solid amine sorbent for CO_2 capture." *Energy and Fuels*, 2006, 20 (4), 1514–1520.

Keeling, R., Scripps Institution of Oceanography (scrippsco2.ucsd.edu/)

Knowles, G.P., Graham, J.V., Delaney, S.W., Chaffee, A.L., "Aminopropyl-functionalized mesoporous silica as CO_2 adsorbents." *Fuel Processing Technology*, 2005, 86, 1435.

Kumar, P., Kim, S., Ida, J., Guliants, V.V., "Polyethylenimine-Modified MCM-48 Membranes: Effect of Water Vapour and Feed Concentration on N_2/CO_2 Selectivity." *Industrial and Engineering Chemistry Research*, 2008, 47, 201-208.

Kuppler, R.J., Timmons, D.J., Fang, Q.R., Li, J.R., Makal, T.A., Young, M.D., Yuan, D., Zhao, D., Zhuang, W. and Zhou, H.C., "Potential Applications of Metal Organic Frameworks." *Coordination Chemistry Reviews*, 2009, 253, 3042– 3066.

Lackner K.S.; Ziock, H.J., "From low to no emissions" *Modified Power Systems*, 2000, 20, 31.

Lal, R., "Soil carbon sequestration to mitigate climate change." *Geoderma*, 2004, 123(1–2), 1-22.

Lee, S., Filburn, T.P., Gray, M., Park, J.W. and Song, H.J., "Screeening Test of Solid Amine Sorbents for CO_2 Capture." *Industrial and Engineering Chemistry Research*, 2008, 47, 7419–7423.

Li, J.R., Kuppler, R.J. and Zhou, H.C., "Selective Gas Adsorption and Separation in Metal-Organic Frameworks." *Chemical Society Reviews*, 2009, 38, 1477–1504.

Li, J.R., Ma, Y., McCarthy, M.C., Sculley, J., Yu, J., Jeong, H.K., Balbuena, P.B. and Zhou, H.C., "Carbon Dioxide Capture-related Gas Adsorption and Separation in Metal-organic Frameworks." *Coordination Chemistry Reviews*, 2011, 255, 1791–1823.

Li, K., Jiang, J., Tian, S., Yan, F., Chen, X., "Polyethyleneimine–nano silica composites: a low-cost and promising adsorbent for CO_2 capture." *Journal of Materials Chemistry A*, 2015, 3, 2166–2175.

Liu, X., Li, J., Zhou, L., Huang, D. and Zhou, Y. "Adsorption of CO_2, CH_4, and N_2 on Ordered Mesoporous Silica Molecular Sieve." *Chemical Physical Letters*, 2005, 415, 198–201.

Lund, H., Mathiesen, B.V. "The role of Carbon Capture and Storage in a future sustainable energy system." *Energy*, 2012, 44(1), 469-476.

Ma, X., Wang, X. and Song, C.,"Molecular Basket" Sorbents for Separation of CO_2 and H_2S from Various Gas Streams." *Journal of the American Chemical Society*, 2005, 131, 5777–5783.

Mazloomi, K., Gomes, C., "Hydrogen as an energy carrier: Prospects and challenges." *Renewable and Sustainable Energy Reviews*, 2012, 16(5), 3024-3033.

McNutt B.D., Johnson L.R., "Competing against entrenched technology: implications for U.S. government policies and fuel cell development." Pre-Symposium Workshop of the Sixth Grove Fuel Cell Symposium, London, UK, 1999.

Meehl, G. A. et al in Climate Change 2007: The Physical Science Basis

Melzer, L.S., "Carbon Dioxide Enhanced Oil Recovery (CO_2 EOR): Factors Involved in Adding Carbon Capture, Utilization and Storage (CCUS) to Enhanced Oil Recovery" 2012.

Millward, A.R. and Yaghi, O.M., "Metal-Organic Frameworks with Exceptionally High Capacity for Storage of Carbon Dioxide at Room Temperature." *Journal of the American Chemical Society*, 2005, 127, 17998–17999

Pachauri, R.K., Reisinger, A. (ed.). IPCC Report on Climate Change, IPCC, Geneve, Switzerland. 2007.

Pandey, V.C., Singh, K., Singh, J.S., Kumar, A., Singh, B., Singh, R.P., "Jatropha curcas: A potential biofuel plant for sustainable environmental development." *Renewable and Sustainable Energy Reviews*, 2012, 16(5), 2870-2883.

Plaza, M.G., García, S., Rubiera, F., Pis, J.J. and Pevida, C., "Post-Combustion CO_2 Capture with a Commercial Activated Carbon: Comparison of Different Regeneration Strategies." *Chemical Engineering Journal*, 2010, 163, 41–47.

Plaza, M.G., Pevida, C., Arenillas, A., Rubiera, F. and Pis, J.J., "CO_2 Capture by Adsorption with Nitrogen Enriched Carbons." *Fuel*, 2007, 86, 2204–2212.

Plaza, M.G., Pevida, C., Arias, B., Fermoso, J., Arenillas, A., Rubiera, F. and Pis, J.J., "Application of Thermogravimetric Analysis to the Evaluation of Aminated Solid Sorbents for CO_2 Capture." *Journal of Thermal Analysis and Calorimetry*, 2008, 92, 601–606.

Puppan, D., "Environmental evaluation of biofuels." *Period Polytech Ser Soc. Man. Sci.*, 2002, 10, 95–116.

Qi, G., Wang, Y., Estevez, L., Duan, X., Anako, N., Park, A.H.A., Li, W., Jones, C.W. and Giannelis, E.P., "High Efficiency Nanocomposite Sorbents for CO_2 Capture Based on Amine-functionalized Mesoporous Capsules." *Energy and Environmental Science*, 2011, 4, 444–452.

Rochelle, G., Chen, E., Dugas, R., Oyenakan, B., Seibert, F., "Solvent and process enhancements for CO_2 absorption/ stripping." In: 2005 Annual Conference on Capture and Sequestration, Alexandria, VA.

Roddy, D.J. "Development of a CO_2 network for industrial emissions." *Applied Energy Volume*, 2012, 91(1), 459–465.

Saha, D. and Deng, S., "Adsorption Equilibrium and Kinetics of CO_2, CH_4, N_2O, and NH_3 on Ordered Mesoporous Carbon." *Journal of Colloid and Interface Sciences*, 2010, 345, 402–409.

Sakakura, T., Choi, J.C., Yasuda, H., "Transformation of carbon dioxide." *Chemical Reviews*, 2007, 107(6), 2365-2387.

Sayari, A. and Belmabkhout, Y., "Stabilization of Amine-Containing CO_2 Adsorbents: Dramatic effect of Water Vapor." *Journal of American Chemical Society*, 2010, 132, 6312–6314.

Sayari, A., Belmabkhout, Y. and Serna-Guerrero, R., "Flue Gas Treatment via CO_2 Adsorption." *Chemical Engineering Journal*, 2011, 171, 760–774.

Siriwardane, R.V., Shen, M.S., Fisher, E.P., Poston, J.A. "Adsorption of CO_2 on molecular sieves and activated carbon." *Energy Fuels*, 2001, 15, 279.

Son, W.J., Choi, J.S., Ahn, W.S., "Adsorptive removal of carbon dioxide using polyethyleneimine-loaded mesoporous silica materials." *Microporous and Mesoporous*

Materials, 2008, 113, 31–40.

Song, C., "Global challenges and strategies for control, conversion and utilization of CO_2 for sustainable development involving energy, catalysis, adsorption and chemical processing." *Catalysis Today*, 115(1–4), 2006, 2–32.

Su, F., Lu, C., Cnen, W., Bai, H. and Hwang, J.F., "Capture of CO_2 from Flue Gas via Multiwalled Carbon Nanotubes." *Science of the Total Environment*, 2009, 407, 3017–3023.

Sun, Y., Liu, X.W., Su, W., Zhou, Y. and Zhou, L., "Studies on Ordered Mesoporous Materials for Potential Environmental and Clean Energy Appilcations." *Applied Surface Science*, 2007, 253, 5650–5655.

Tans, P., NOAA/ESRL (www.esrl.noaa.gov/gmd/ccgg/trends/)

Wang, D., Ma, X., Shalaby, C., Song, C., "Development of Carbon-Based "Molecular Basket" Sorbent for CO_2 Capture." *Industrial and Engineering Chemistry Research*, 2012, 51, 3048−3057.

Wang, J., Chen, H., Zhou, H., Liu, X., Qiao, W., Long, D., Ling, L., "Carbon dioxide capture using polyethylenimine-loaded mesoporous carbons." Journal of Environmental Sciences, 2013, 25(1) 124–132.

Wang, Q., Luo, J., Zhong, Z. and Borgna, A., "CO_2 Capture by Solid Adsorbents and Their Applications: Current Status and New Trends." *Energy and Environmental Science*, 2011, 4, 42–55.

Wang, X., Ma, X., Song, C., Locke, D.R., Siefert, S.,Winans, R.E., Mollmer, J., Lange, M., Moller, A., Glaser, R., "Molecular basket sorbents polyethylenimine–SBA-15 for CO_2 Capture from flue gas: Characterization and sorption properties." *Microporous and Mesoporous Materials*, 2013, 169, 103-111.

Wang, X., Schwartz, V., Clark, J.C., Ma, X., Overbury, S.H., Xu, X. and Song, C., "Infrared Study of CO_2 Sorption over "Molecular Basket" Sorbent Consisting of Polyethylenimine-Modified Mesoporous Molecular Sieve." *The Journal of Physical Chemistry C*, 2009, 113, 7260–7268.

Xu, X. Song, C., Miller, B.G., Scaroni, A.W., "Adsorption separation of carbon dioxide from flue gas of natural gas-fired boiler by a novel nanoporous "molecular basket" adsorbent." *Fuel Processing Technology*, 2005, 86, 1457 – 1472.

Xu, X., Song, C., Andresen, J.M., Miller, B.G. and Scaroni, A.W., "Novel Polyethylenimine-Modified Mesoporous Molecular Sieve of MCM-41 Type as High Capacity Adsorbent for CO_2 Capture." *Energy Fuels*, 2002, 16, 1463–1469.

Xu, X., Song, C., Miller, B.G. and Scaroni, A.W., "Influence of Moisture on CO_2 Separation from Gas Mixture by a Nanoporous Adsorbent Based on Polyethylenimine-Modified Molecular Sieve MCM-41." *Industrial and Engineering Chemistry Research*, 2005, 44, 8113–8119.

Yu, C., Huang, C., Tan, C., "A Review of CO_2 Capture by Absorption and Adsorption." *Aerosol and Air Quality Research*, 2012, 12, 745–769.

Yue, M.B., Chun, Y., Cao, Y., Dong, X. and Zhu, J.H., "CO_2 Capture by As-Prepared SBA-15 with an Occluded Organic Template." *Advanced Functional Materials*, 2006, 16, 1717–1722.

Yue, M.B., Sun, L.B., Cao, Y., Wang, Y., Wang, Z.J. and Zhu, J.H., "Efficient CO_2 Capturer Derived from As-Synthesized MCM-41 Modified with Amine." *Chemistry- A European Journal*, 2008, 14, 3442–3451.

APPENDIX A

TABLES

A.1. Calculation of the amount of PEI to be impregnated.

Diameter of PEI molecule (m)		1.00E-09			
Cross sectional area of PEI molecule(m^2)		7.85398E-19			
		Grace Davison	**Saint Gobain**	**Akzo Nobel**	**Cabot**
		Silica	Silica	Carbon	Carbon
		SI 1101	SS 61138	EC 600JD	BP 2000
Surface Area (m^2/g) BET		324.3591	236.2667	1400	1400
Number of PEI molecules per 1 g of support		4.12987E+20	3.00824E+20	1.7825E+21	1.7825E+21
Avagadro's number, NA		6.023E+23			
Number of moles per 1 g of support		0.000685683	0.000499459	0.00295955	0.00295955
Molecular weight of PEI		600			
Weight of PEI per 1 g of support (g)	Monolayer	0.411	0.300	1.776	1.7757284
	Half Monolayer	0.206	0.150	0.888	0.888
	1.5 times Monolayer	0.617	0.450	2.664	2.664

A.2. Diffusion Length Calculation

In order to confirm the presence of Knudsen Diffusion, the mean free path of PEI molecule was calculated using the following equation (Perry 2008).

$$\lambda = \frac{3.2}{P}\mu\left(\frac{RT}{2\pi M}\right)^{1/2}$$

When mean free diameter >> pore diameter, Knudsen diffusion prevails.

Instead of calculating the time required for PEI to diffuse into the pores of the supports, the calculation was back tracked to the size of particle required for synthesis in 6 hrs and 24 hrs. From Apprendix A.2.1, it is evident that the size of particles to allow for PEI diffusion in 6 hrs is much larger than the size of particles used in this study.

1) $$D_K = \frac{\epsilon_b}{\tau}\frac{d_p}{3}\sqrt{\frac{8RT}{\pi M}}$$

Where,

K = Boltzmann Constant 1.38E-23 $m^2\ kg\ s^{-2}\ K^{-1}$

N = Avagadro's Number 6.02E+23

ε_b = Porosity of the particle

τ = Tortuosity

2) Diffusion Length = $2\sqrt{Dt}$

3) Particle size (dia) = Diffusion length /2

A.2.1. Diffusion Length Calculation Spreadsheet

			At 25 C				
			Diffusivity	**DIFFUSION LENGTH (cm)**		**Particle size (dia) (cm)**	
	Pore dia. (nm)	Pore dia. (cm)	D_{KA} (cm^2/s)	6 hour synthesis	24 hour synthesis	6 hour synthesis	24 hour synthesis
SG Silica	10.9	0.0000011	0.00062	7.3	14.6	3.6	7.3
GD Silica	12.6	0.00000126	0.00072	7.8	15.7	3.9	7.8
SG Alumina	9	0.0000009	0.00051	6.6	13.3	3.3	6.6
Calgon Carbon	2.8	0.00000028	0.00016	3.7	7.4	1.8	3.7
Cabot Carbon	7.26	0.00000072	0.00041	5.9	11.9	2.9	5.9
Akzo Nobel Carbon	7	0.0000007	0.00040	5.8	11.7	2.9	5.8

			At 80 C				
			Diffusivity	**DIFFUSION LENGTH (cm)**		**Particle size (dia) (cm)**	
	Pore dia. (nm)	Pore dia. (cm)	D_{KA} (cm^2/s)	6 hour synthesis	24 hour synthesis	6 hour synthesis	24 hour synthesis
SG Silica	10.9	0.00000109	0.00068	7.6	15.2	3.8	7.6
GD Silica	12.6	0.00000126	0.00078	8.2	16.4	4.1	8.2
SG Alumina	9	0.0000009	0.00056	6.9	13.8	3.4	6.9
Calgon Carbon	2.8	0.00000028	0.00017	3.8	7.7	1.9	3.8
Cabot Carbon	7.26	0.00000073	0.00045	6.2	12.4	3.1	6.2
Akzo Nobel Carbon	7	0.0000007	0.00043	6.1	12.2	3.06	6.1

A.3. PEI estimation for Batch-I adsorbents

									Based on TGA estimate of PEI loading	
SAMPLES	**Initial weight (mg)**	**Weight at 100^0C**	**Weight at 700^0C**	**Weight loss observed**	**Weight loss due to surface hydroxyls**	**Amount of PEI estimated by TGA**	**Amount of PEI added during synthesis**	**Difference in the amounts calculated**	**Amine Loading**	**Theoretical Amine Loading**
				(%)	**(%)**	**(%)**	**(%)**			
SG Pure silica	6.1	6.054	6.009	0.761	0.761	NA				
SG Si 50M PEI	7.7	7.479	6.507	14.941	0.761	14.179	15.553	1.374	0.972	0.201
SG Si M PEI	6.9	6.486	5.037	28.767	0.761	28.006	31.442	3.436	1.449	0.339
SG Si 150M PEI	11	10.373	7.370	40.746	0.761	39.985	45.381	5.396	3.003	0.448
GD Pure Silica	6.5	6.214	6.081	2.191	2.191	NA				
GD Si 50M PEI	11.6	11.020	7.627	44.487	2.191	42.295	23.602	-18.693	3.393	0.468
GD Si M PEI	7.5	7.238	5.955	21.537	2.191	19.345	45.965	26.620	1.283	0.255
GD Si 150M PEI	11	10.065	6.724	49.693	2.191	47.502	66.916	19.414	3.341	0.486

A.4.12% CO_2 adsorption capacities of Batch I adsorbents at 25 deg C

								Based on TGA estimate of PEI loading		Based on PEI used in synthesis		Stoichiometry
SAMPLES	Initial weight (mg)	Weight after 110^0C	Weight at 25^0C before adsorption Of CO_2	Weight after adsorption of CO_2	Amount of CO_2 adsorbed (mg)	Gram Mole of CO_2	mmol CO_2 / g-ads	Amine Loading	Amine Efficiency	Theoretical Amine Loading	Theoretical Maximum Amine Efficiency	Maximum Efficiency
SG Si 50M PEI	9.3	8.86	8.89	9.02	0.1302	2.96E-06	0.32	2.105	0.15	2.124	0.150	0.5
SG Si M PEI	8.4	7.53	7.56	7.95	0.3885	8.83E-06	1.05	3.559	0.30	5.420	0.194	0.5
SG Si 150M PEI	7.2	6.68	6.69	7.10	0.4032	9.16E-06	1.27	4.705	0.27	7.823	0.163	0.5
GD Si 50 M PEI	11.5	10.93	10.97	11.42	0.45425	1.03E-05	0.90	4.918	0.18	3.864	0.23	0.5
GD Si M PEI	7.6	6.96	6.992	7.4746	0.4826	1.1E-05	1.44	2.682	0.54	7.525	0.19	0.5
GD Si 150 M PEI	9	8.181	8.208	8.8425	0.6345	1.44E-05	1.60	5.104	0.31	10.955	0.15	0.5

12% CO_2 adsorption capacities of Batch I adsorbents at 75 deg C

							Based on TGA estimate of PEI loading		Based on PEI used in synthesis		Stoichiometry
SAMPLES	Initial weight (mg)	Weight at 25^0C (before desorption)	Weight after adsorption of CO_2	Amount of CO_2 adsorbed (mg)	Gram Mole of CO_2	mmol CO_2 / g-ads	Amine Loading	Amine Efficiency	Theoretical Amine Loading	Theoretical Maximum Amine Efficiency	Maximum Efficiency
SG Si 150M PEI	6.56	6.029	6.491	0.462	1.05E-05	1.602	4.705	0.340567371	7.823	0.163	0.5
GD Si 150M PEI	7.93	7.078	7.682	0.604	1.37E-05	1.732	5.104	0.34	10.955	0.15	0.5

A.5. PEI estimation for Batch II adsorbents

			Initial weight (mg)	Weight after 100°C	Weight at 700°C	Weight loss observed	Weight loss due to surface hydroxyls	Amount of PEI estimated by TGA	Amount of PEI added during synthesis	Difference in the amounts calculated	Amine loading	Theoretical amine loading
						(%)	(%)	(%)	(%)			
	GD Pure Silica		6.5	6.21	6.08	2.19	2.19					
UNCRUSHED	GD Si M PEI		10.5	9.58	6.75	41.91	2.19	39.72	44.65	4.93	4.49	7.21
CRUSHED	GD Si M PEI		10.2	9.05	6.50	39.22	2.19	37.02	43.93	6.91	3.55	7.31
UNCRUSHED	GD Si 150 M PEI		12.2	10.37	6.41	61.90	2.19	59.71	65.14	5.43	5.10	10.96
CRUSHED	GD Si 150 M PEI		8.8	7.79	4.78	62.98	2.19	60.79	66.17	5.38	5.72	10.83
	SG Pure silica		6.1	6.05	6.01	0.76	0.76	NA				
UNCRUSHED	SG Si M PEI		7.2	6.64	5.09	30.63	0.76	29.87	32.39	2.52	3.67	5.58
CRUSHED	SG Si M PEI		9.4	8.51	6.56	29.75	0.76	28.99	31.13	2.14	3.55	5.37
UNCRUSHED	SG Si 150M PEI		14.9	14.16	9.83	43.94	0.76	43.18	45.70	2.52	5.02	7.88
CRUSHED	SG Si 150M PEI		8.5	7.67	5.28	45.28	0.76	44.52	47.02	2.50	4.82	8.10
	Pure AN C		4.97	4.94	4.93	0.14	0.14	NA				
UNCRUSHED	AN C M PEI		13.7	11.85	5.34	121.79	0.14	121.66	178.96	57.31	8.30	31.08
CRUSHED	AN C M PEI		7.7	6.69	2.70	148.21	0.14	148.08	179.06	30.99	9.06	31.10
UNCRUSHED	AN C 150M PEI		12	10.24	3.15	225.00	0.14	224.86	268.65	43.79	10.33	46.66
CRUSHED	AN C 150M PEI		6.4	5.13	1.68	206.11	0.14	205.97	268.04	62.07	9.43	46.55
	Pure Cabot		6.5	6.39	6.33	0.92	0.92	NA				
UNCRUSHED	Cabot M PEI		9.8	8.67	3.87	124.05	0.92	123.13	184.90	61.77	8.47	31.50
CRUSHED	Cabot M PEI		13.9	11.94	5.30	125.50	0.92	124.57	183.87	59.30	8.29	31.33
UNCRUSHED	Cabot 150M PEI		Agglomerated sticky supports									
CRUSHED	Cabot 150M PEI											

A.6. 12% CO_2 adsorption capacities of Batch II adsorbents at 75^0C

								Based on TGA estimate of PEI loading		Based on PEI used in synthesis		Stoichiometry
	SAMPLES	Initial weight (mg)	Weight at 110^0C	Weight after adsorption of CO_2	Amount of CO_2 adsorbed (mg)	Gram Mole of CO_2	mmol CO_2 / g-ads	Amine Loading	Amine Efficiency	Theoretical Amine Loading	Theoretical Maximum Amine Efficiency	Maximum Efficiency
UNCRUSHED	SG Si M PEI	9	8.22	8.74	0.52	1.19E-05	1.32	3.67	0.36	5.58	0.24	0.5
CRUSHED	SG Si M PEI	9.8	8.96	9.52	0.55	1.26E-05	1.28	3.55	0.36	5.37	0.24	0.5
UNCRUSHED	SG Si 150M PEI	15.6	14.35	15.54	1.19	2.71E-05	1.73	5.02	0.35	7.88	0.22	0.5
CRUSHED	SG Si 150M PEI	7.6	6.88	7.41	0.53	1.21E-05	1.59	4.82	0.33	8.10	0.20	0.5
UNCRUSHED	GD Si M PEI	8	7.08	7.59	0.50	1.15E-05	1.43	4.49	0.32	7.21	0.20	0.5
CRUSHED	GD Si M PEI	6.2	5.49	5.87	0.37	8.45E-06	1.36	3.55	0.38	7.31	0.19	0.5
UNCRUSHED	GD Si 150M PEI	7.9	7.07	7.65	0.57	1.3E-05	1.65	5.10	0.32	10.96	0.15	0.5
CRUSHED	GD Si 150M PEI	6.7	6.01	6.46	0.45	1.01E-05	1.51	5.72	0.26	10.83	0.14	0.5
UNCRUSHED	AN C M PEI	12.7	10.45	11.63	1.17	2.67E-05	2.10	8.30	0.25	31.08	0.07	0.5
CRUSHED	AN C M PEI	13.1	10.81	11.97	1.16	2.63E-05	2.01	9.06	0.22	31.10	0.06	0.5
UNCRUSHED	AN C 150M PEI	11.2	9.28	10.56	1.28	2.91E-05	2.60	10.33	0.25	46.66	0.06	0.5
CRUSHED	AN C 150M PEI	14	11.62	13.30	1.68	3.82E-05	2.73	9.43	0.29	46.55	0.06	0.5
UNCRUSHED	CABOT M PEI	10.5	8.51	9.43	0.92	0.000021	2.00	8.47	0.24	31.50	0.06	0.5
CRUSHED	CABOT M PEI	11.6	9.43	10.35	0.92	2.08E-05	1.80	8.29	0.22	31.33	0.06	0.5
UNCRUSHED	CABOT 150 M PEI	Sticky Agglomerates										
CRUSHED	CABOT 150 M PEI											

A.7. 400ppm CO_2 adsorption capacities of Batch II adsorbents at 25^0C.

									Based on TGA estimate of PEI loading		Based on PEI used in synthesis		Stoichiometry
	SAMPLES		Initial weight (mg)	Weight after 25°C	Weight after adsorption of CO_2	Amount of CO_2 adsorbed (mg)	Gram Mole of CO_2	mmol CO_2 / g-ads	Amine Loading	Amine Efficiency	Theoretical Amine Loading	Theoretical Maximum Amine Efficiency	Maximum Efficiency
UNCRUSHED	GD Si M PEI		16.12	14.19	14.93	0.74	1.69E-05	1.05	4.49	0.23	7.20	0.14	0.5
CRUSHED	GD Si M PEI		9.7	8.48	8.90	0.41	9.36E-06	0.96	4.14	0.23	7.31	0.13	0.5
UNCRUSHED	GD Si 150 M PEI		9.67	8.06	8.61	0.55	1.25E-05	1.3	5.49	0.23	10.66	0.12	0.5
CRUSHED	GD Si 150 M PEI		10.61	9.03	9.54	0.51	1.16E-05	1.09	5.72	0.19	10.83	0.10	0.5
UNCRUSHED	SG Si 150M PEI		7.1	6.45	6.8	0.34	7.87E-06	1.11	5.02	0.22	7.87	0.14	0.5
CRUSHED	SG Si 150M PEI		14.4	12.56	13.21	0.64	1.47E-05	1.02	4.82	0.21	8.10	0.12	0.5
UNCRUSHED	SG Si M PEI		6.77	5.98	6.23	0.24	5.59E-06	0.82	3.67	0.22	5.58	0.14	0.5
CRUSHED	SG Si M PEI		12.76	11.39	11.83	0.43	9.96E-06	0.78	3.54	0.22	5.36	0.14	0.5
UNCRUSHED	AN C M PEI		12.6	10.03	10.26	0.22	5.15E-06	0.41	8.30	0.05	31.08	0.01	0.5
CRUSHED	AN C M PEI		15.6	11.62	11.85	0.23	5.31E-06	0.34	9.06	0.03	31.09	0.01	0.5
UNCRUSHED	AN C 150M PEI		12.43	10.02	10.49	0.42	9.71E-06	0.78	10.32	0.07	46.65	0.01	0.5
CRUSHED	AN C 150M PEI		27.22	20.95	21.39	0.44	1.02E-05	0.36	9.43	0.03	46.55	0.01	0.5
UNCRUSHED	Cabot M PEI		13.2	9.97	10.17	0.19	4.5E-06	0.34	8.47	0.04	8.47	0.04	0.5
CRUSHED	Cabot M PEI		14.7	10.99	11.20	0.21	4.67E-06	0.31	8.29	0.03	8.29	0.03	0.5
UNCRUSHED	Cabot 150M PEI		Sticky agglomerates										
CRUSHED	Cabot 150M PEI												

A.8. Calculation for flow rate of air through small adsorber.

According to previous TGA experiments

1)	Flow rate of gas mixture		100	cc/min
2)	Concentration of CO_2		0.04	wt%
3)	Weight of adsorbent		7.65	mg
4)	Approx. Time taken for 90% adsorbance at a flow rate of 100cc/min		90	mins
5)	Amount of CO_2 adsorbed per mg of adsorbent in 0.04wt% CO_2 in He		1.11	mg CO_2/mg adsorbent

ADSORPTION

Present experiment

*	Amount of adsorbent available		32	g
*	Expected CO_2 adsorbance w.r.t TGA data	(or)	35520 35.52	mg g CO_2
	Amount of CO_2 in air		0.04	wt%
	Amount of air needed to provide 35.52 g CO_2		88800	g of air
	Moles of air		3062.068966	moles
	Volume of air needed		136.6141236	L
	Flow rate for 90% adsorption		1.517934706	LPM
	Flow rate to allow for maximum adsorption		**3**	**LPM**

A.9. Calculation for duration of air-flow for adsorber experiment.

Weight of SG Si adsorbent	32	g
Percentage of PEI by weight	44	%
Amount of PEI in 32g of adsorbent	14.08	g
Acc. to TGA data in 400 ppm CO_2, 5% of CO_2 by weight will be captured by the adsorbent		
Therefore, amount of CO_2 captured	32*0.05	
	1.6	g
Moles of CO_2 captured	1.6/44	
	0.036	moles
Moles of air carrying 0.036 moles of CO_2	0.036/0.0004	
at 400 ppm concentration	90.91	moles of air
Volume of air	90.91*22.4	
	2037.636	L
Average flow rate of air	3	LPM
Minimum duration for adsorbent to reach	679.21	mins
maximum capacity	11	hrs

A.10. Calibration of adsorber experiment.

	Procedure			
		Pressure		**Absolute Pressure (psi)**
1)	Helium allowed to flow through the entire setup.			
2)	Opened valve to 250 cc cylinder			
3)	**Pressure stabilizes at**	**28.14**	psi	**42.252**
4)	Cylinder valve closed			
5)	Whole system evacuated except 250 cc cylinder			
6)	All valves closed			
7)	**Pressure reading**	**-28.8**	in hg	**0**
8)	Opened valve to 250 cc cylinder			
9)	**Pressure reading**	**14.88**	psi	**28.992**
10)	Opened exit valve from adsorber			
11)	**Pressure reading**	**2.54**	in hg	**15.3566**
12)	Opened valve to 500 cc cylinder			
13)	**Pressure reading**	**-15.7**	in hg	**6.419**

A.10.1 Calculation of dead volumes in adsorber experiment using Boyle's law.

VT1	Tank I volume, cc	75	$\mathbf{P_t}$	Pressure in tank 1
V1	volume in lines (cc)		**P1**	Pressure in tank 1 + lines
V2	volume in adsorber (cc)		**P2**	Pressure in tank 1 + lines + adsorber
VT2	Tank II volume, cc	300	**P3**	Pressure in tank 1+ lines + adsorber + tank 2

$P_t*Vt1 = P1*(V1+Vt1)$

V1+ Vt1	109.30	
V1	34.30	cc

$P1*(V1+Vt1) = P2*(Vt1+V1+V2)$

(Vt1+V1+V2)	206.35	cc
V2	97.05	cc

Rounding up

V1	34	cc
V2	97	cc
V1 + V2	131	cc

Cross verification

$P2*(Vt1+V1+V2) = P3*(Vt1+V1+V2+VT$

LHS	3168.90	
RHS	3250.29	
From above formula, V1 + V2	140.46	cc

A.11. Calculation of adsorption capacity in adsorber experiments.

RUN I	at 5 LPM
T (min)	P (psi)
0	-7.84
5	-6.86
10	-5.978
15	-4.998
20	-4.165
25	-3.136
30	-2.45
40	-1.225
45	-0.784
50	-0.441
55	-0.196
60	-0.049
65	0.09
70	0.18
75	0.23
80	0.26
85	0.27
90	0.27

	Symbol/ Formula	**Units**	**Value**
Grams of adsorbent	w	g	32
Volume of cylinder + lines + adsorber	V	cc m3	206 0.000206
Universal gas constant	R	Pa-m3/mol-K	8.314
Temperature	T	K	298

Difference in pressure noted in 250 cc tank	P	(psi) Pa	8.11 56283.956
Moles of CO_2 milli-moles of CO_2	n = PV/RT moles * 1000	g-mol mmol	0.0047 4.68
mMoles/ g adsorbent	mmol/w	mmol/g	0.146

A.12 Estimating mass transfer correlations

A.12.1 Packed Bed:

Reynolds Number (Re)

$$Re = \frac{D_p V_s \rho}{(1-\varepsilon)\mu} = 27.24 \quad \text{(laminar)} \qquad (1)$$

Where, Dp = particle diameter = 1.5 mm

Vs = superficial velocity in bed = Q/A = 0.127 m/s

where

Q = volumetric flow rate = 2.5 LPM

A = cross-sectional area of adsorber = 3.14×10^{-4} m^2

P = density of air = 1.184 kg/m^3

μ = viscosity = 1.84×10^{-5} kg/m-s

ε = void fraction = 0.55

Mean Free Path (λ)

$$\lambda = \frac{K\,T}{\sqrt{2}\pi P \sigma^2} = 57.14 \text{ nm} \qquad (2)$$

where,

K = Boltzmann Constant = 1.38×10^{-23} m^2 kg s^{-2} K^{-1}

T = Temperature = 298 K

P = Pressure = 1 atm

σ = collision diameter of CO_2 = 0.4 nm

Pore diameter (D_{pore}) of Saint Gobain Silica = 10.9 nm.

Since, $\lambda >> D_{pore}$, the diffusion occurs under Knudsen regime.

Knudsen Coefficient (D_K)

$D_K = \frac{D_{pore}}{3} \frac{\varepsilon}{\tau} \sqrt{\frac{8KNT}{\pi M}} = 2.29 \times 10^{-5}\ m^2/s$ (3)

Where,

K = Boltzmann Constant = $1.38 \times 10^{-23}\ m^2\ kg\ s^{-2}\ K^{-1}$

T = Temperature = 298 K

N = Avagadro's Constant = 6.023×10^{-23}

M = Molecular Weight of CO_2 = 44 / mol

ε = Porosity of pellet = 0.5

τ = Tortuosity = 3

Schmidt Number (Sc)

$Sc = \frac{\mu}{\rho D_K} = 0.31$ (4)

Using eq. (3)

Where,

μ = viscosity of CO_2 = 1.4×10^{-5} kg/m-s

ρ = density of CO_2 = $1.977\ kg/m^3$

Sherwood Number (Sh)

$Sh = \frac{0.357}{\varepsilon} Re^{0.641} Sc^{0.33}$ for 3<Re<900 (Perry's handbook)

Also, $Sh = \frac{k_c L_p}{D_K}$, where k_c is the mass transfer coefficient.

Using eq (1) and (4),

Sh = 4.03

Biot Number (Bi)

$Bi = \frac{k_c L_p}{D} = Sh = 4.03$

A.12.2 Thermogravimetric Analysis (TGA):

Reynolds Number (Re)

$$Re = \frac{D_p V_s \rho}{(1-\varepsilon)\mu} = 1.7 \quad \text{(laminar)} \qquad (5)$$

Where, Dp = particle diameter = 13.78 microns (Appendix B.5)

Vs = superficial velocity in furnace = Q/A = 0.127 m/s

where

Q = volumetric flow rate = 100 ml/min

A = cross-sectional area of furnace = 5.06×10^{-4} m^2

P = density of air = 1.184 kg/m^3

μ = viscosity = 1.84×10^{-5} kg/m-s

ε = porosity = 0.5

It has been established in Appendix A.12.1, that the diffusion of CO_2 occurs in the Knudsen regime.

Knudsen Coefficient (D_K)

$$D_K = \frac{D_{pore}}{3}\sqrt{\frac{8KNT}{\pi M}} = 1.375 \times 10^{-6} \ m^2/s \qquad (6)$$

Where,

K = Boltzmann Constant = 1.38×10^{-23} m^2 kg s^{-2} K^{-1}

T = Temperature = 298 K

N = Avagadro's Constant = 6.023×10^{-23}

M = Molecular Weight of CO_2 = 44 / mol

Schmidt Number (Sc)

Sc = $\frac{\mu}{\rho D_K}$ = 5.16 (7)

Using eq. (3)

Where,

μ = viscosity of CO_2 = 1.4 x 10^{-5} kg/m-s

ρ = density of CO_2 = 1.977 kg/m^3

Sherwood Number (Sh)

Sh = $1.66\ Re^{0.33} Sc^{0.33}$ for laminar flow

Using Eq. 5 and Eq. 7,

Sh	= 5.21

As discussed in Appendix A.12.1,

Bi	= Sh	= 5.21

Appendix A.13 Estimation of CO_2 adsorption capacity for a single pellet removed from adsorber

SAMPLE		Initial weight (mg)	Weight at 25^0C (before desorption)	Weight after adsorption of CO_2	Amount of CO_2 adsorbed (mg)	Gram Mole of CO_2	milli moles of CO_2 / g of adsorbent
SG Si 150M PEI		5.48	4.36	4.63	0.26	5.97818E-06	1.09

APPENDIX B

FIGURES

B.1. TGA curves for estimation of PEI loading in Batch I adsorbents

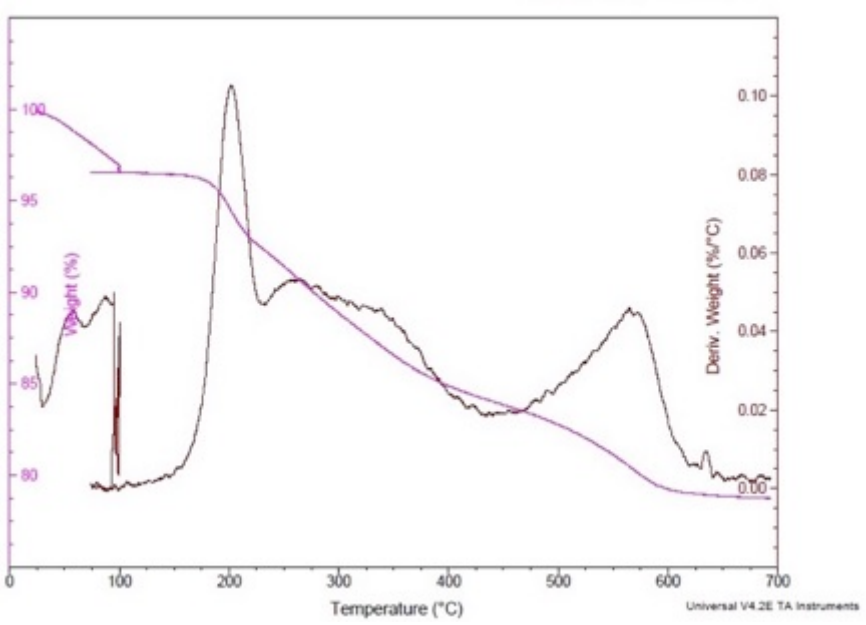

GD-Si -50M-PEI

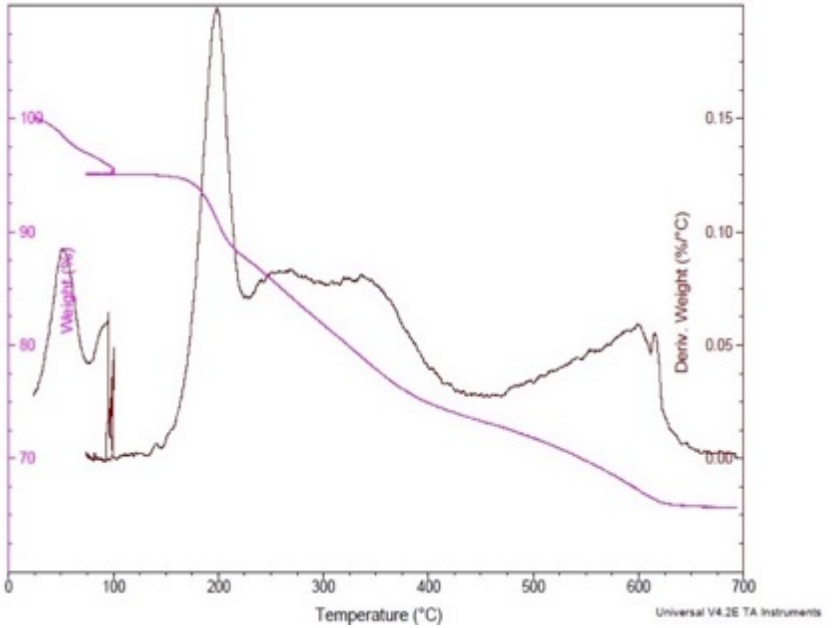

GD-Si -M-PEI

B.1. TGA curves for estimation of PEI loading in Batch I adsorbents (*continued*)

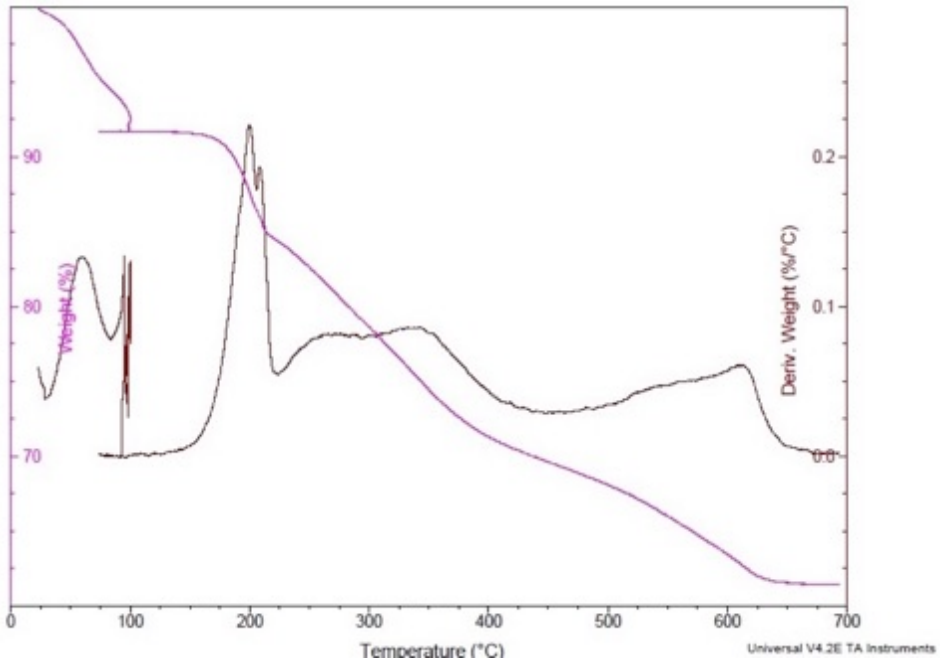

GD-Si -150M-PEI

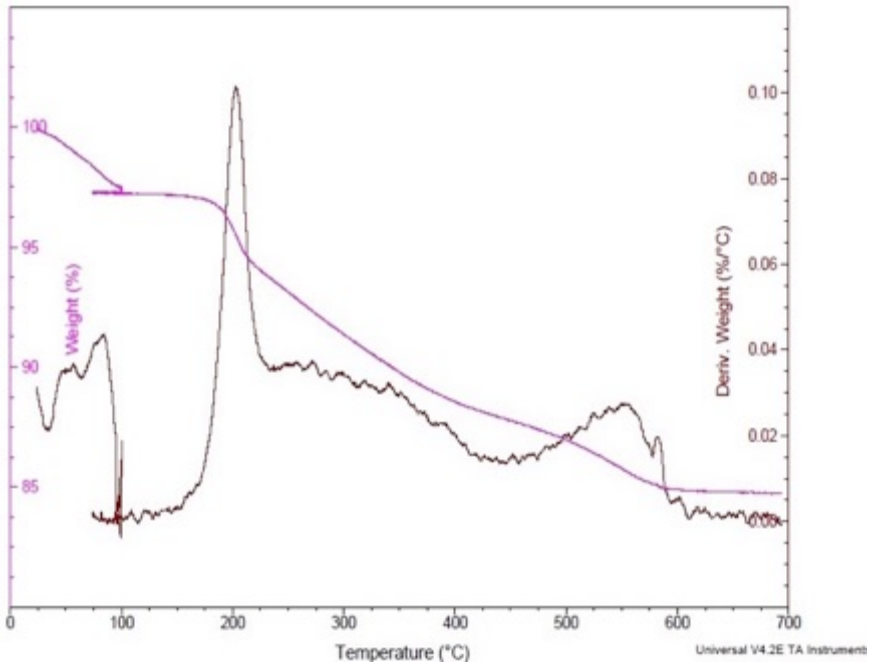

SG-Si -50M-PEI

B.1. TGA curves for estimation of PEI loading in Batch I adsorbents (*continued*)

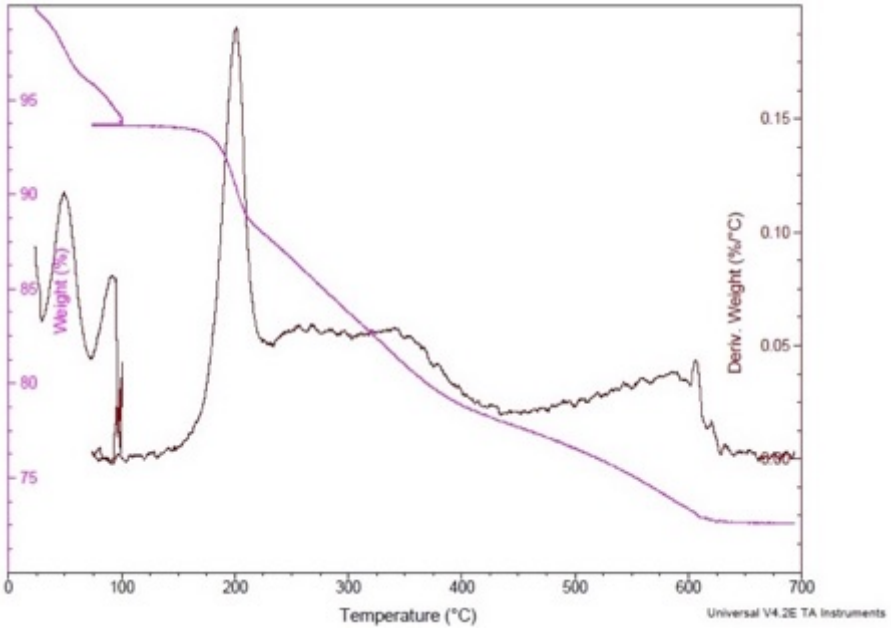

SG-Si -M-PEI

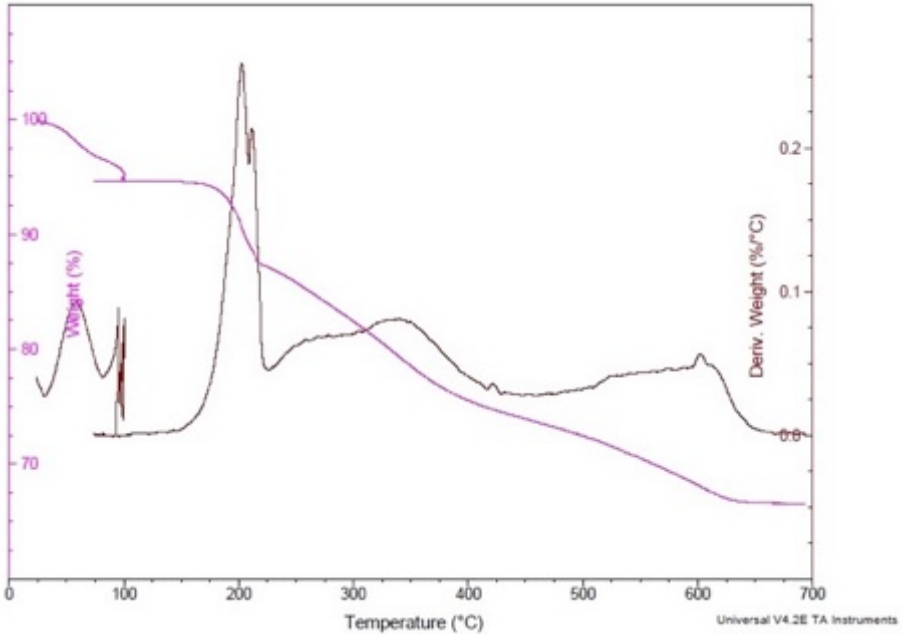

SG-Si -150M-PEI

B.2. TGA curves for CO_2 adsorption in atmospheres of 12% CO_2 in He at 25^{o}C.

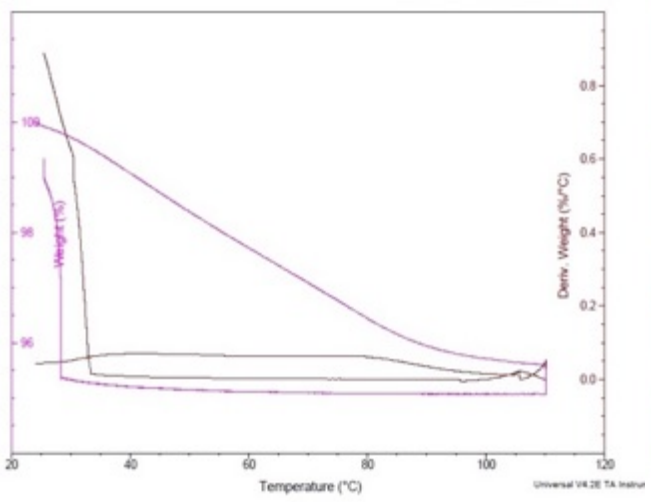

]
GD-Si-50M-PEI

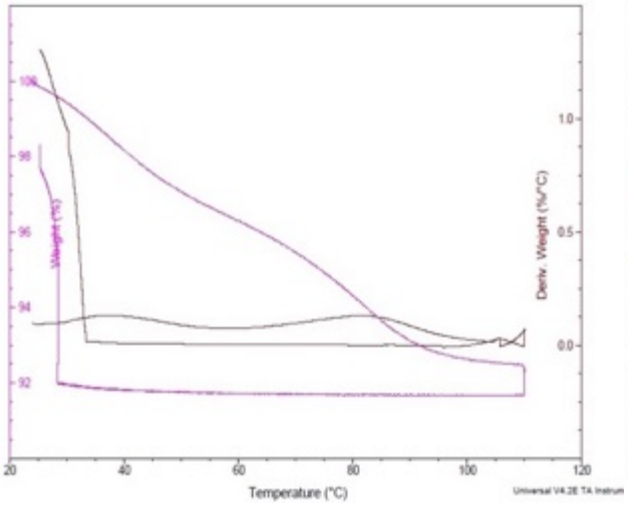

GD-Si-M-PEI

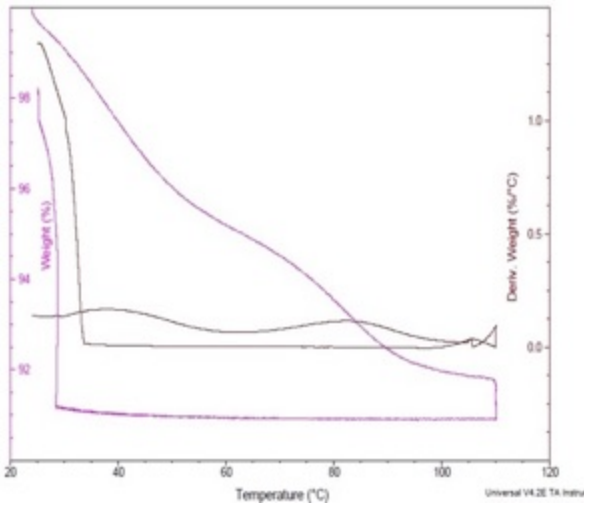

GD-Si-150M-PEI

B.2. TGA curves for CO_2 adsorption in atmospheres of 12% CO_2 in He at 25^{o}C (*continued*).

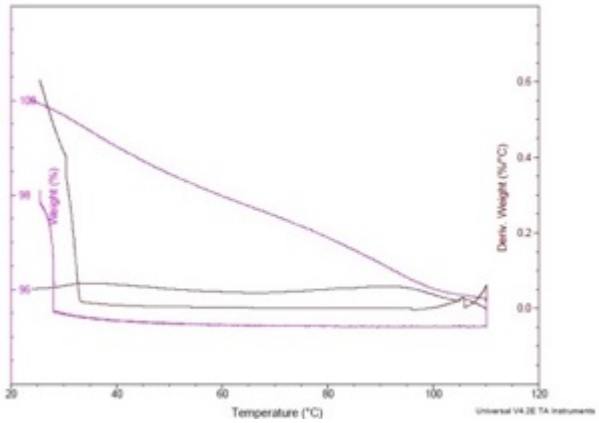

SG-Si-50M-PEI

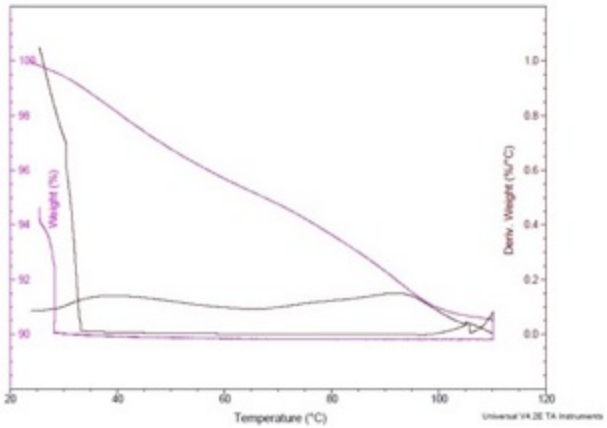

SG-Si-M-PEI

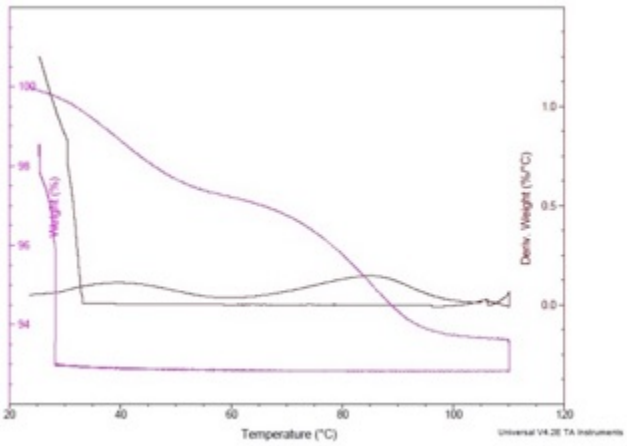

SG-Si-150M-PEI

B.2.1 TGA curves for CO_2 adsorption in atmospheres of 12% CO_2 in He at 75^{o}C.

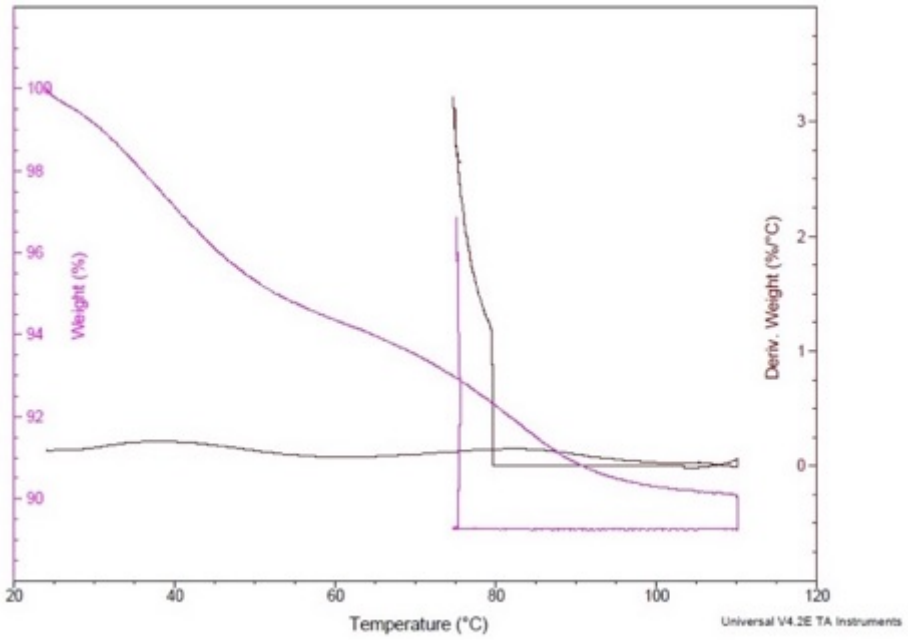

GD-Si-150M-PEI

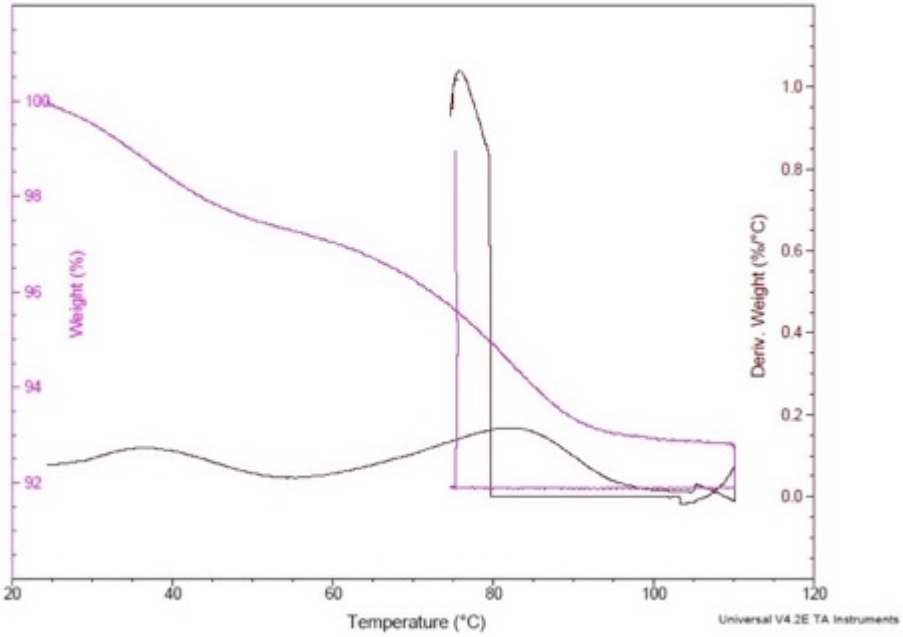

SG-Si-150M-PEI

B.3. TGA curves for PEI estimation of Batch II adsorbents (Uncrushed & Dried).

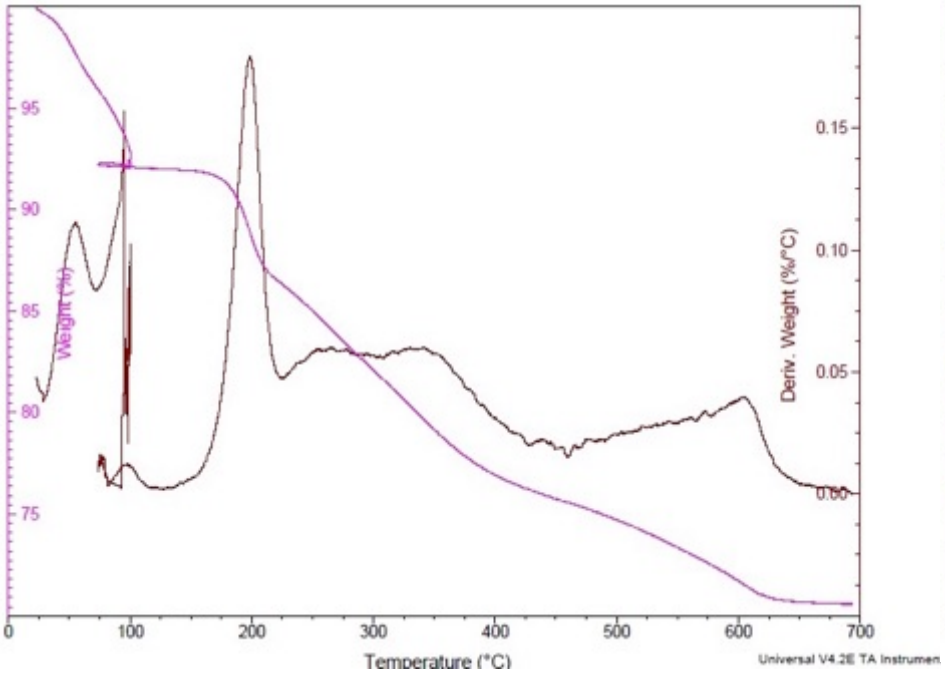

SG-Si-M-PEI

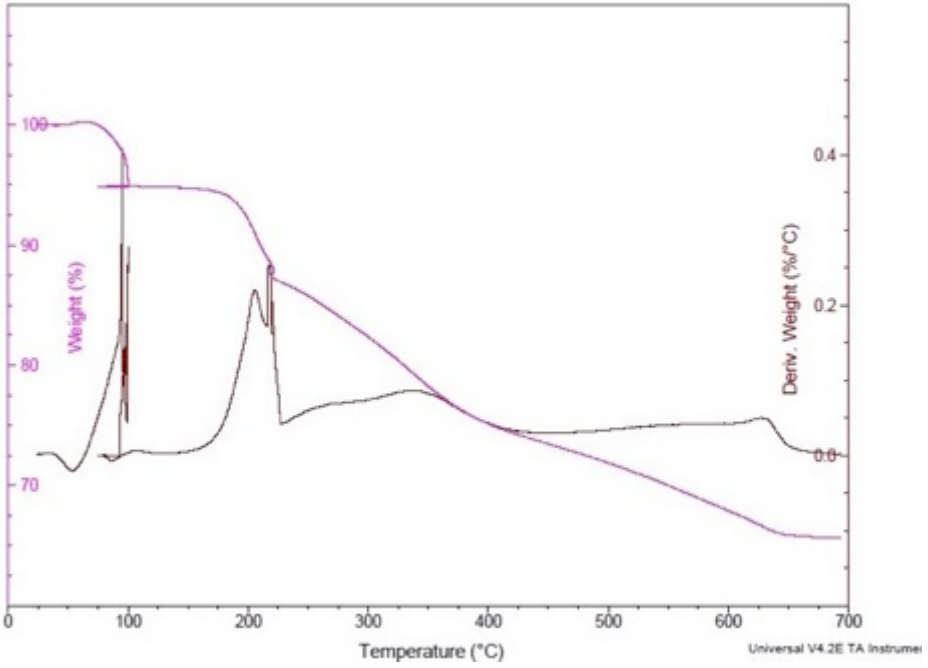

SG-Si-150M-PEI

B.3. TGA curves for PEI estimation of Batch II adsorbents (Uncrushed & Dried) (*continued*).

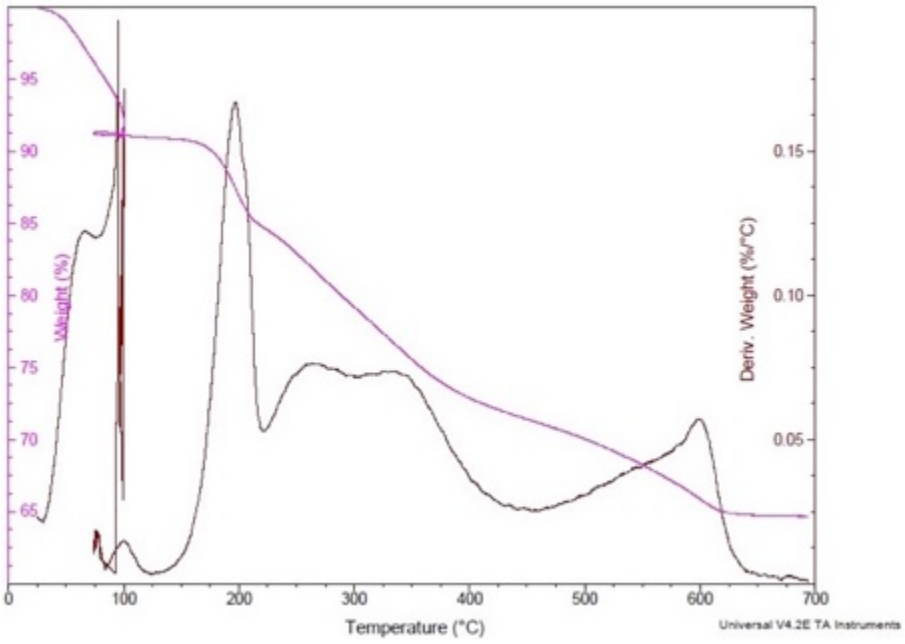

GD-Si-M-PEI

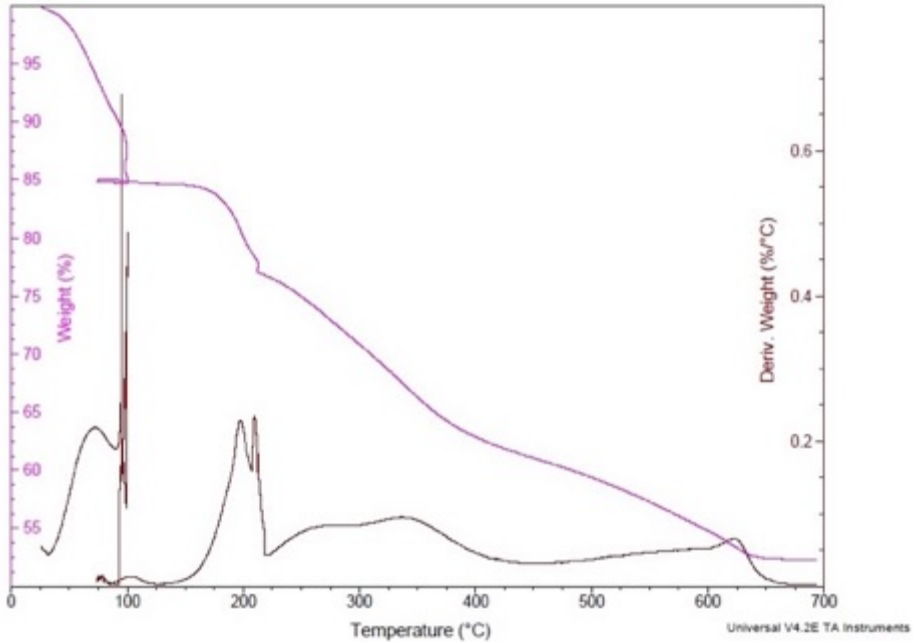

GD-Si-150M-PEI

B.3. TGA curves for PEI estimation of Batch II adsorbents (Uncrushed & Dried) (*continued*).

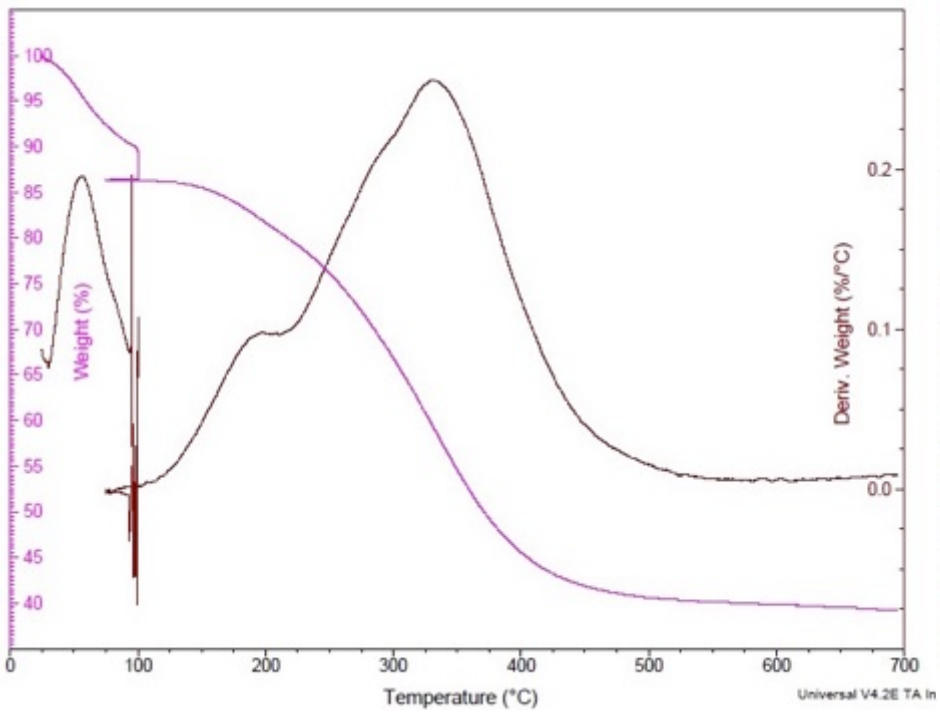

AN-C-M-PEI

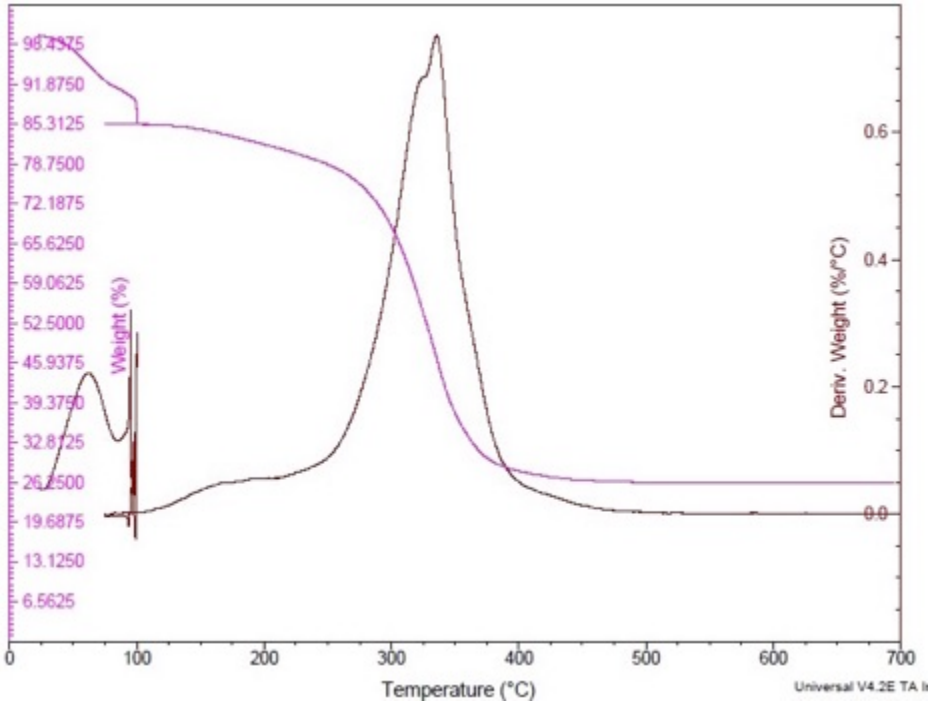

AN-C-150M-PEI

B.3. TGA curves for PEI estimation of Batch II adsorbents (Uncrushed & Dried) (*continued*).

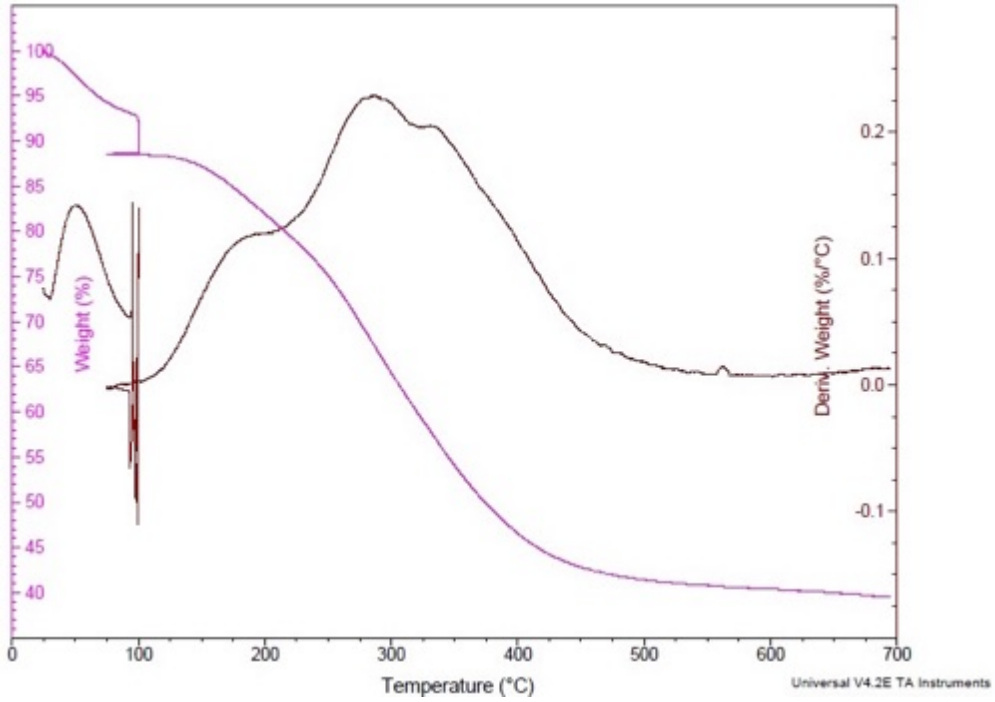

Cabot-C-M-PEI

B.3.1. TGA curves for PEI estimation of Batch II adsorbents (Crushed& Dried).

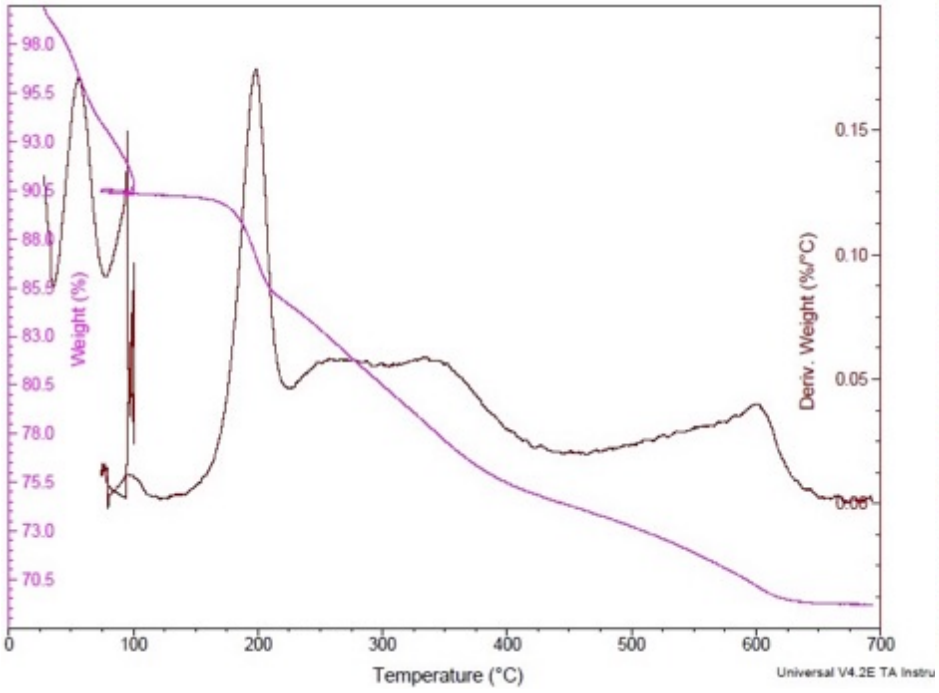

SG-Si-M-PEI

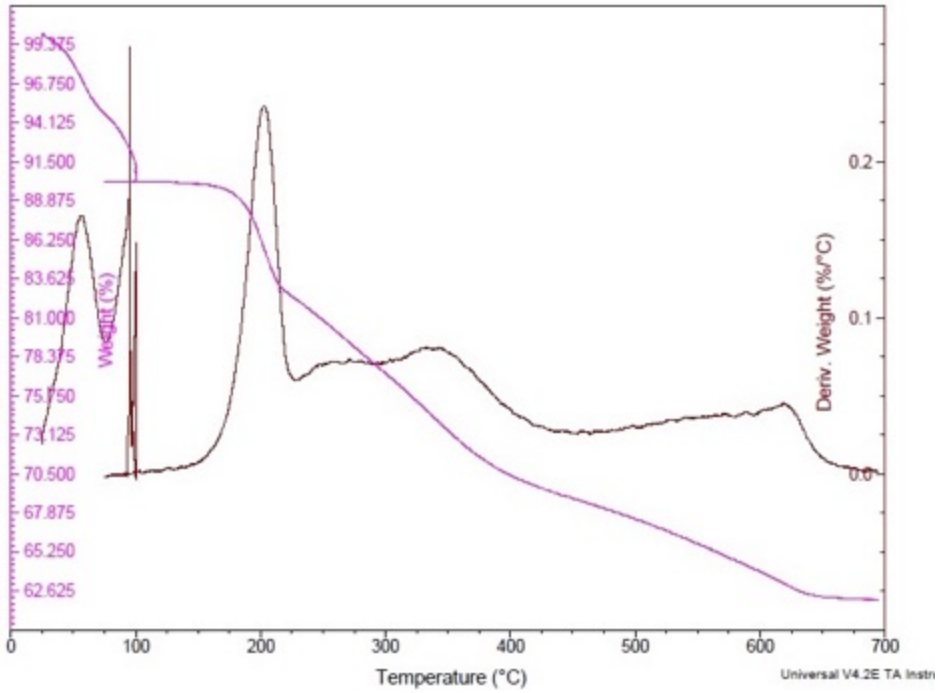

SG-Si-150M-PEI

B.3.1. TGA curves for PEI estimation of Batch II adsorbents (Crushed& Dried) *(continued)*.

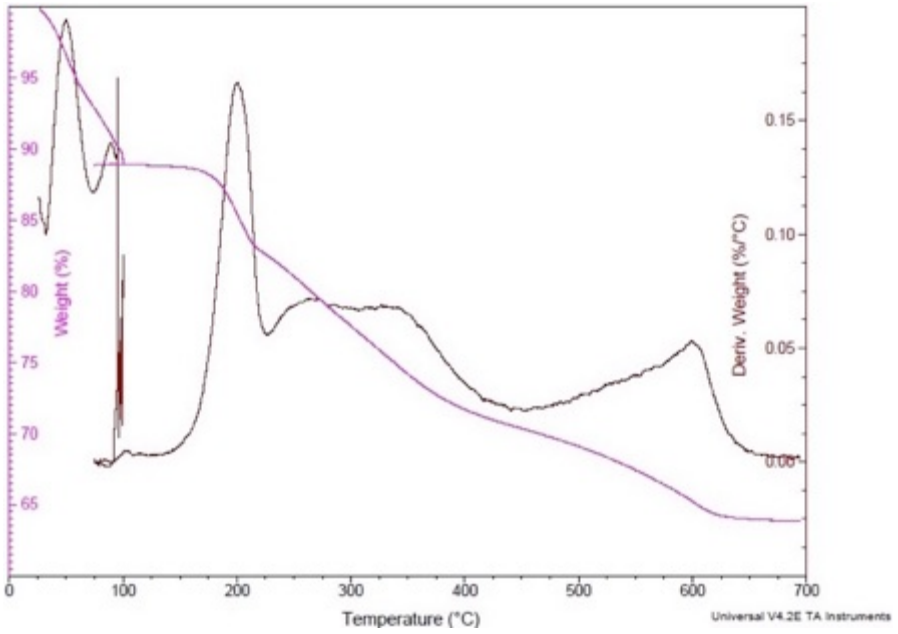

GD-Si-M-PEI

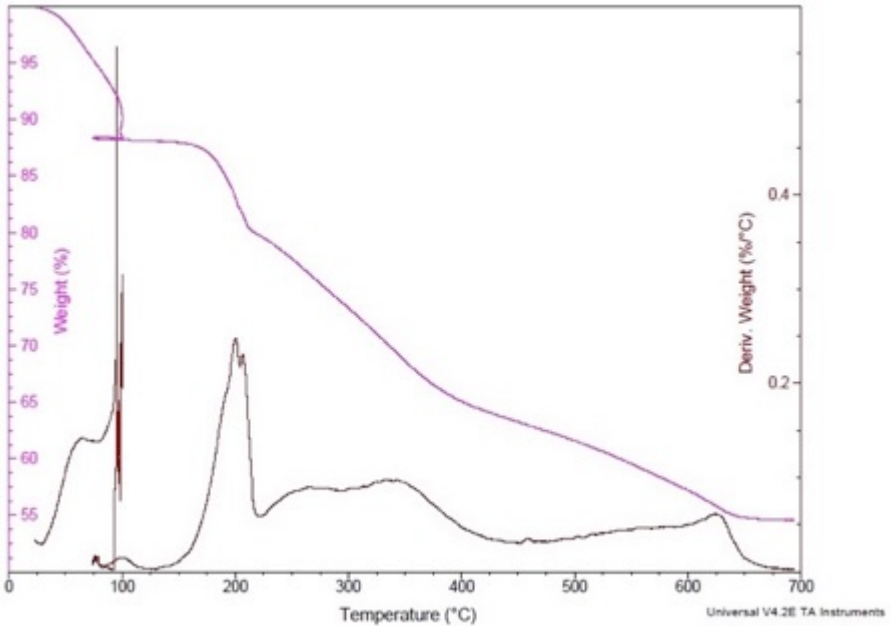

GD-Si-150M-PEI

B.3.1. TGA curves for PEI estimation of Batch II adsorbents (Crushed& Dried) *(continued)*.

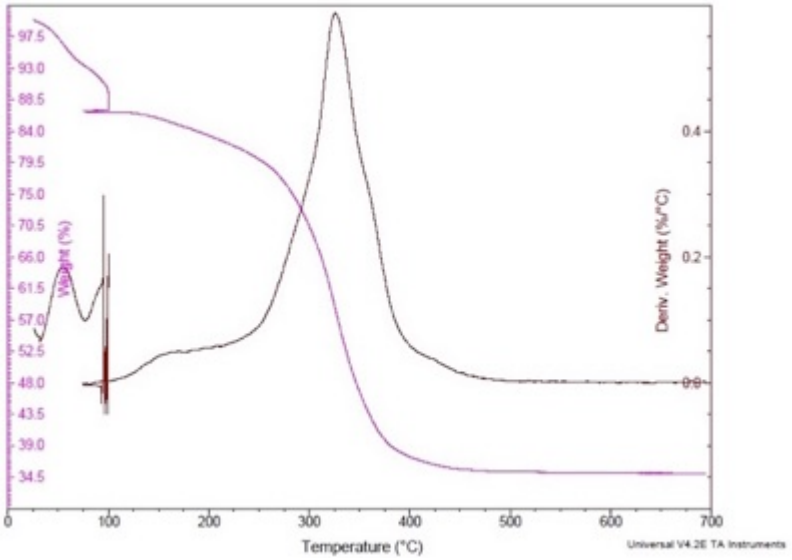

AN-C-M-PEI

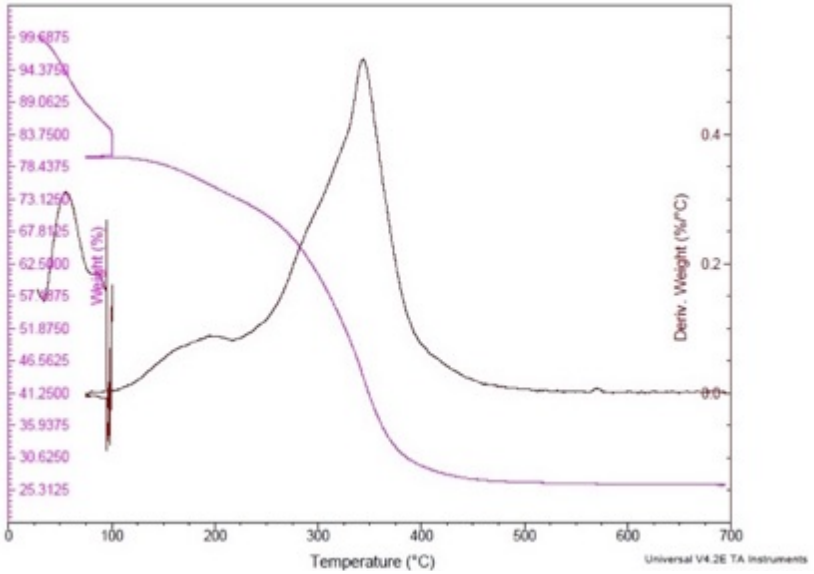

AN-C-150M-PEI

B.3.1. TGA curves for PEI estimation of Batch II adsorbents (Crushed& Dried) (*continued*).

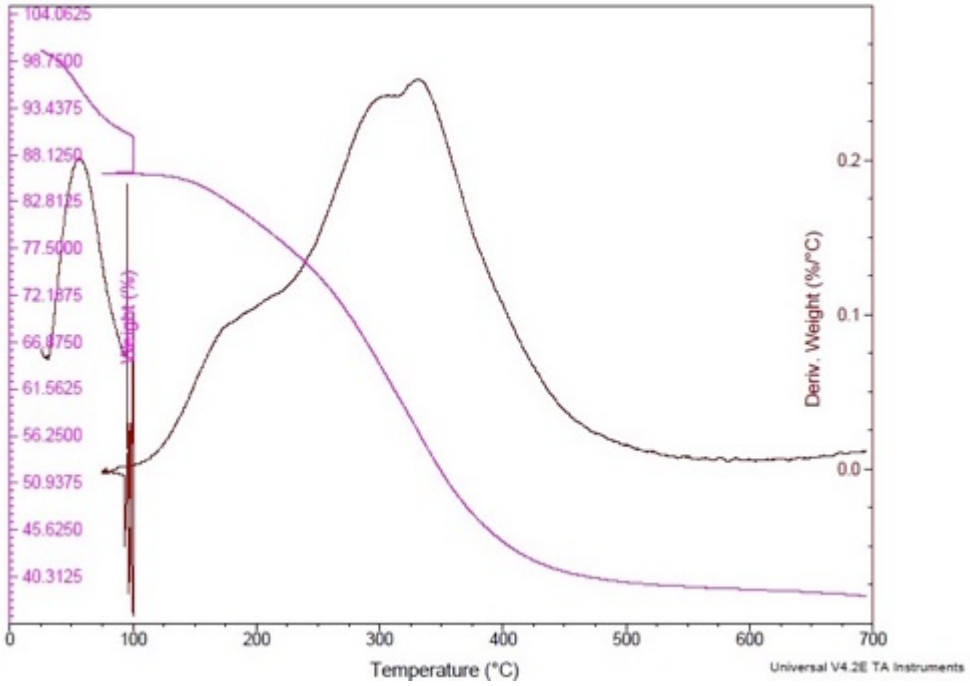

Cabot-C-M-PEI

B.4. TGA curves for CO_2 adsorption by Batch-II adsorbents in atmospheres of 400 ppm CO_2 in He at 25^{o}C (Uncrushed & Dried).

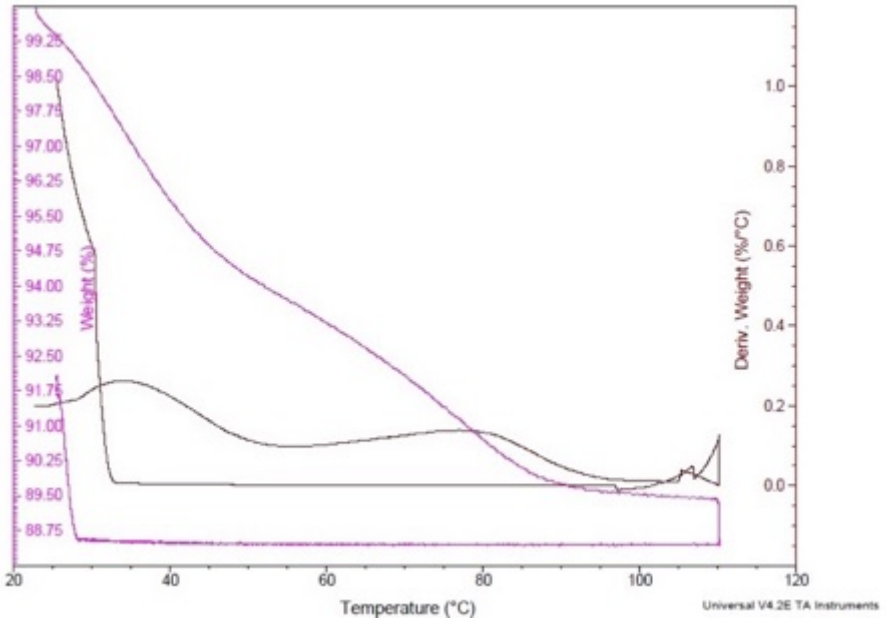

SG-Si-M-PEI

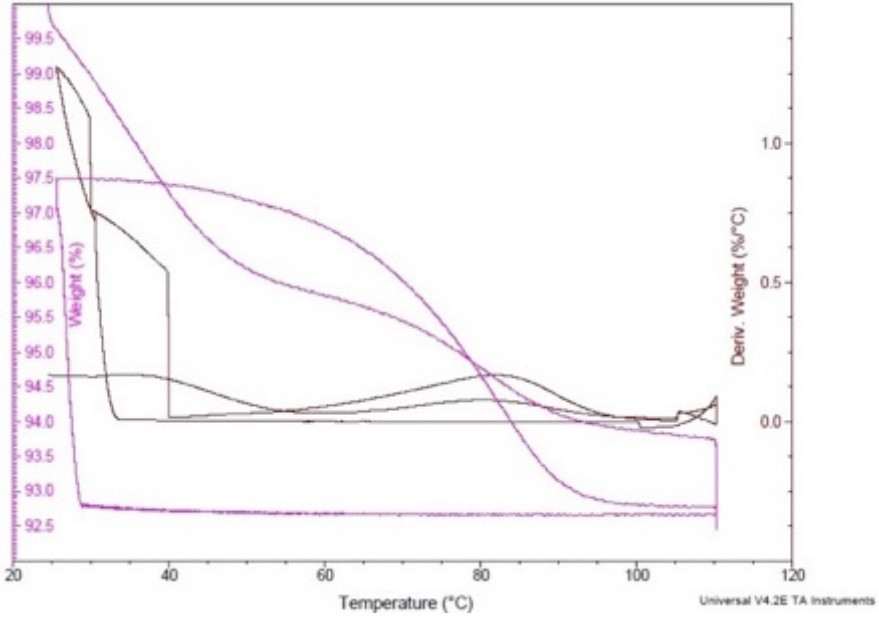

Adsorption and desorption curve for SG-Si-150M-PEI

B.4. TGA curves for CO_2 adsorption by Batch-II adsorbents in atmospheres of 400 ppm CO_2 in He at 25^{o}C (Uncrushed & Dried) (*continued*).

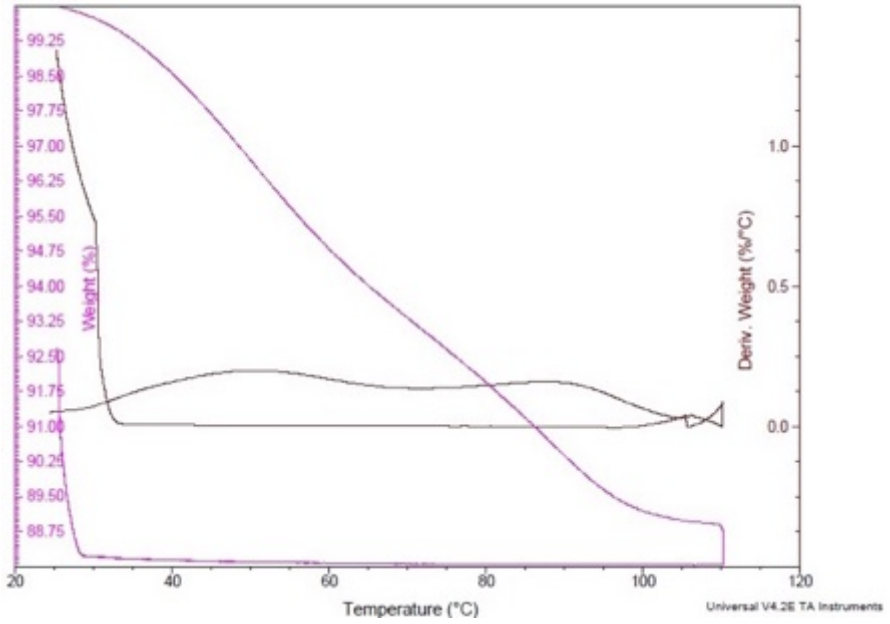

GD-Si-M-PEI

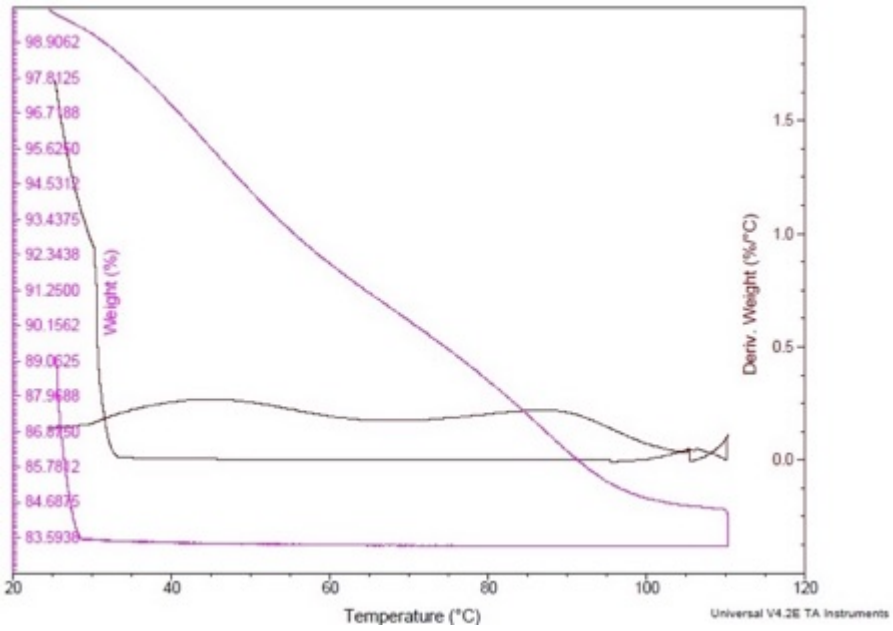

GD-Si-150M-PEI

B.4. TGA curves for CO_2 adsorption by Batch-II adsorbents in atmospheres of 400 ppm CO_2 in He at 25^{o}C (Uncrushed & Dried) (*continued*).

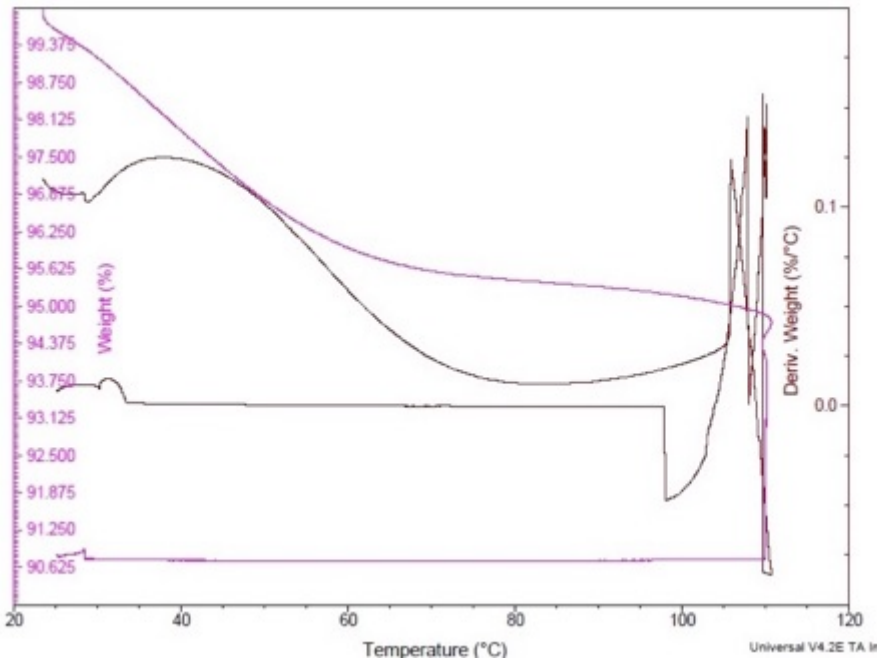

AN-C-M-PEI

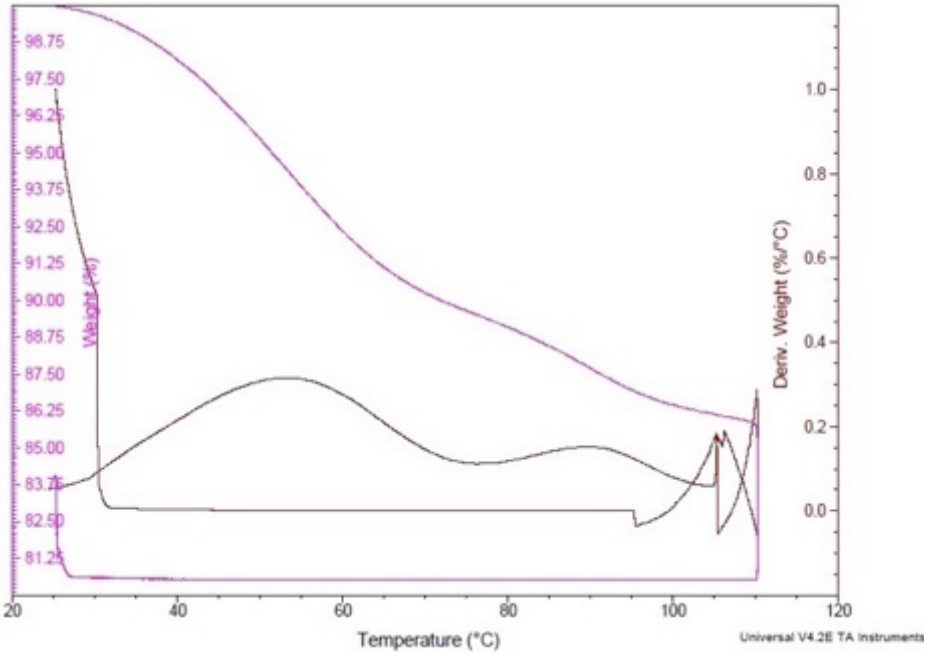

AN-C-150M-PEI

B.4. TGA curves for CO_2 adsorption by Batch-II adsorbents in atmospheres of 400 ppm CO_2 in He at 25°C (Uncrushed & Dried) (*continued*).

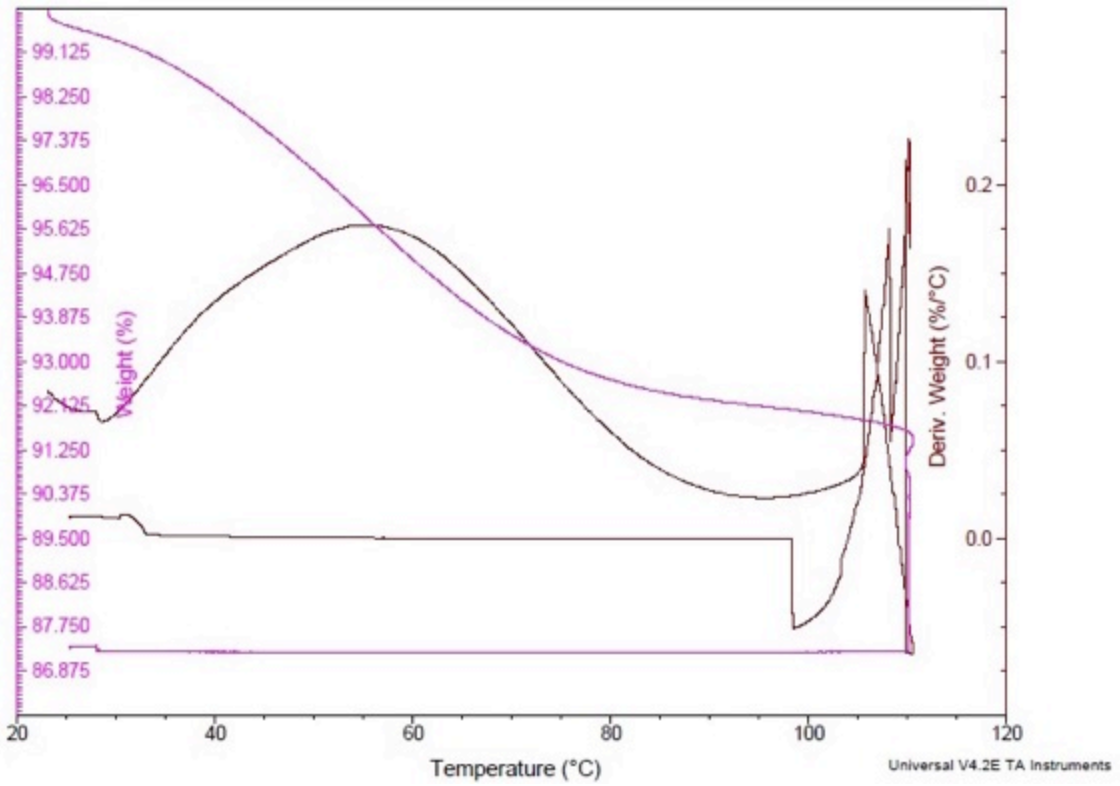

Cabot-C-M-PEI

B.4.1 TGA curves for CO_2 adsorption by Batch-II adsorbents in atmospheres of 400 ppm CO_2 in He at 25^{o}C (Crushed & Dried).

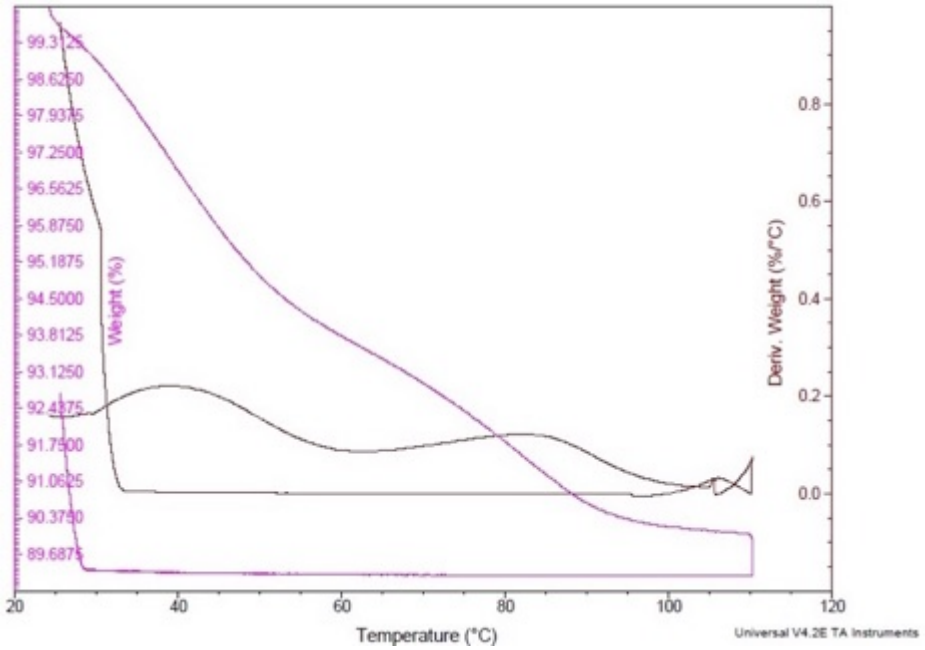

SG-Si-M-PEI

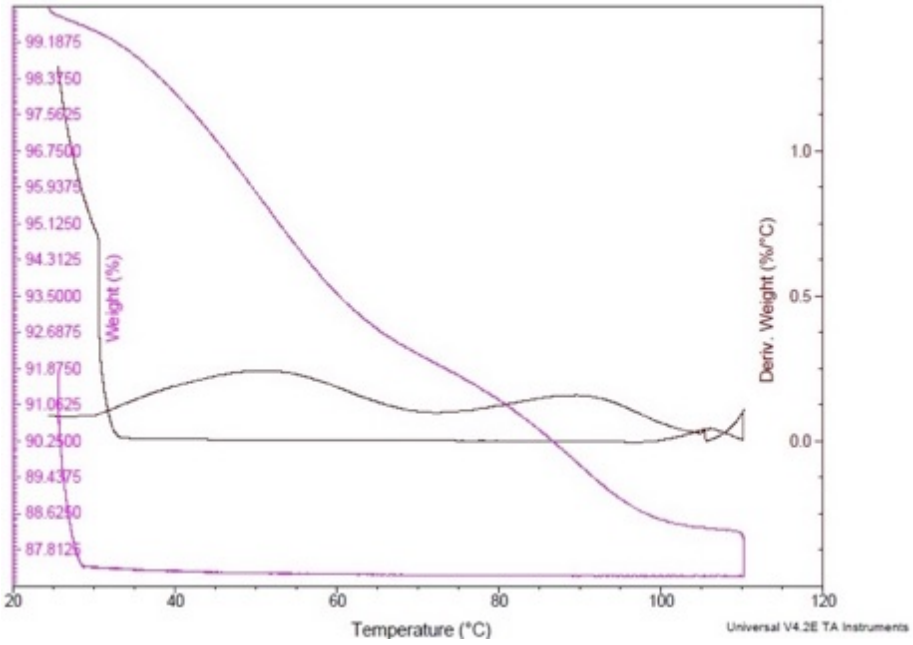

SG-Si-150M-PEI

B.4.1 TGA curves for CO_2 adsorption by Batch-II adsorbents in atmospheres of 400 ppm CO_2 in He at 25°C (Crushed & Dried) (*continued*).

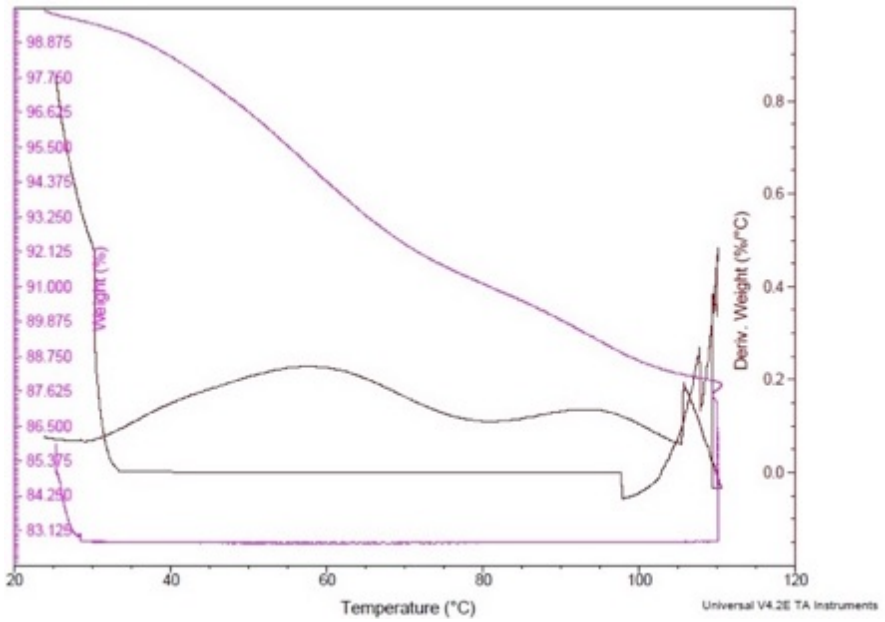

AN-C-M-PEI

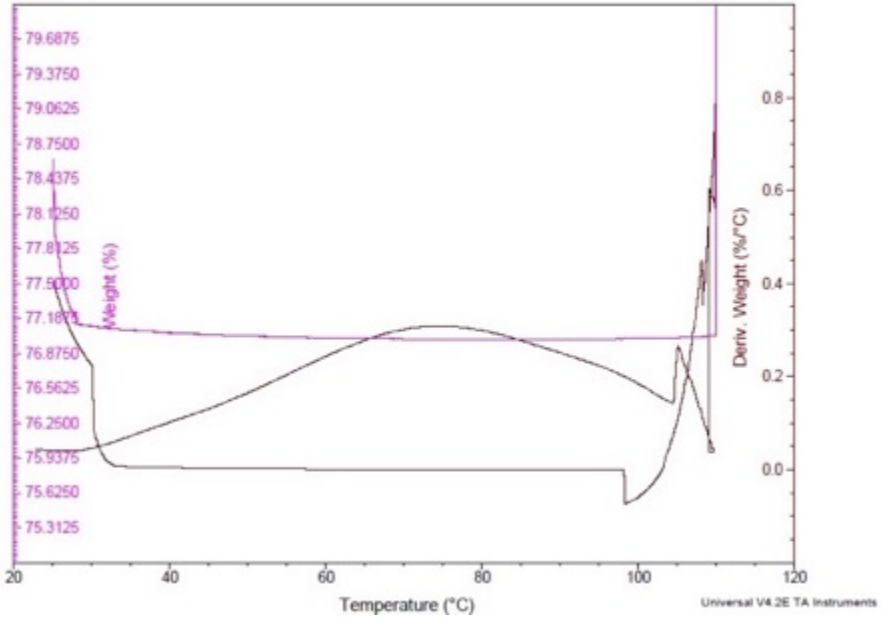

AN-C-150M-PEI

B.4.1 TGA curves for CO_2 adsorption by Batch-II adsorbents in atmospheres of 400 ppm CO_2 in He at 25°C (Crushed & Dried) (*continued*).

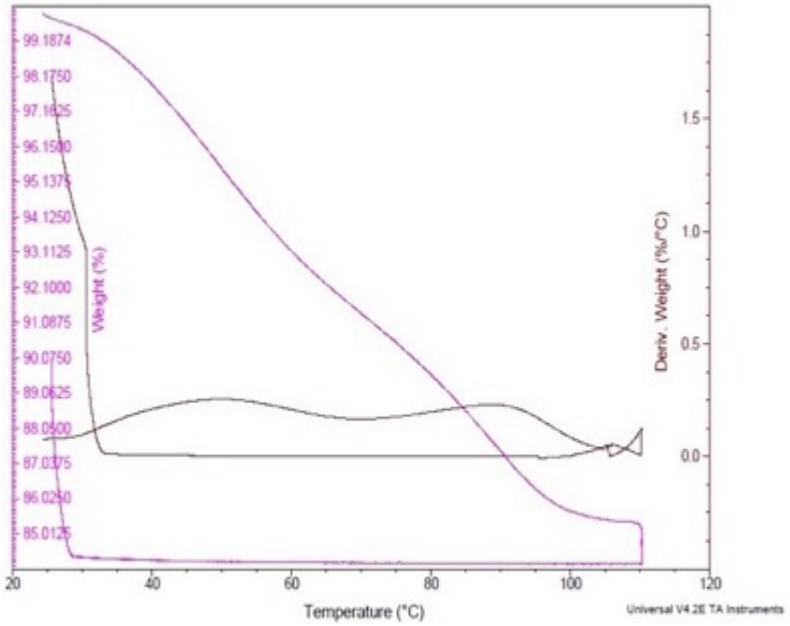

GD-Si-150M-PEI

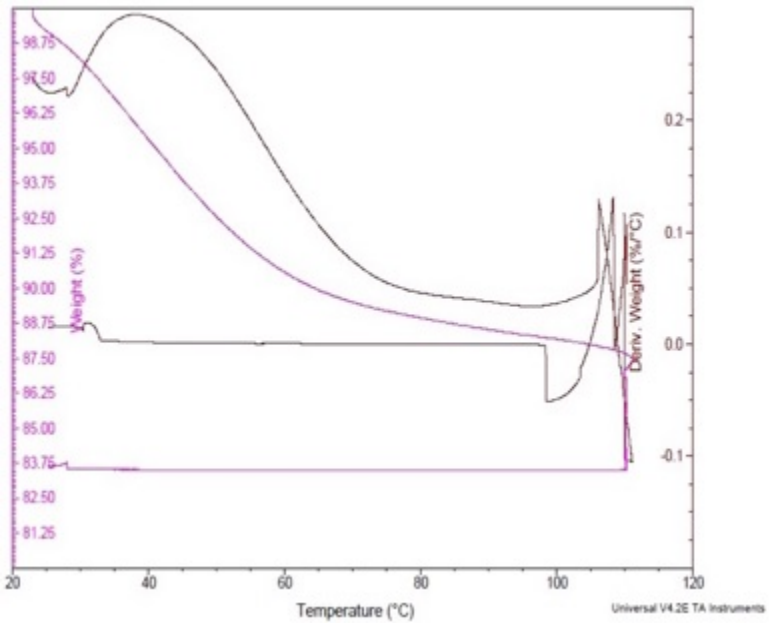

Cabot-C-M-PEI

B.5 Particle Size Distribution of powdered sample of SG Si 150M PEI (uncrushed).

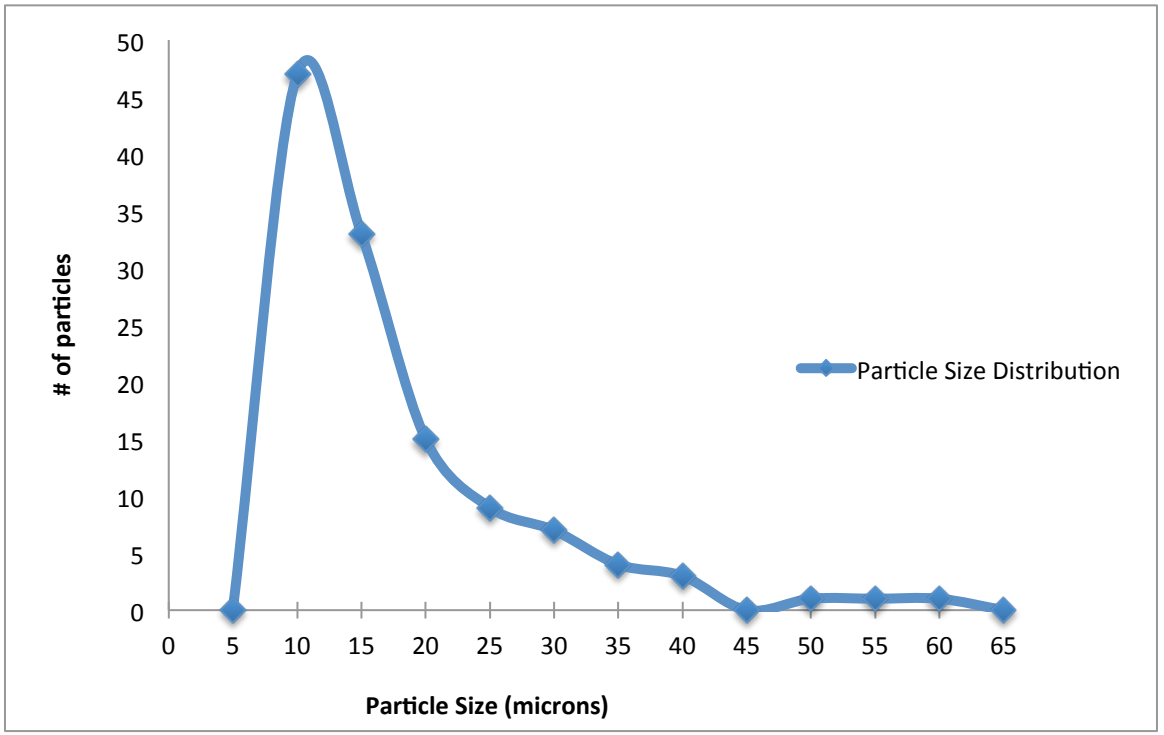

Average particle size = 13.78 microns

B.6 Adsorption curve of a single pellet removed from the adsorber system.